TECHNISCHE UNIVERSITÄT
BERGAKADEMIE FREIBERG
Die Ressourcenuniversität. Seit 1765.

IBF
Institut für Bohrtechnik
und Fluidbergbau

Development and Testing of Alternative Methods for Speeding up the Hydraulic Data Transmission in Deep Boreholes

To the Faculty of Geosciences, Geoengineering and Mining
of the Technical University Bergakademie Freiberg
approved

DOCTORAL THESIS

to attain the academic degree of

Doktor-Ingenieur

(Dr.-Ing.)

submitted

by Dipl.- Ing. Mouhammed Jandal Berro
born on 14 September 1982 in Homs, Syria

Reviewers: Prof. Dr.-Ing. Matthias Reich, TU Bergakademie Freiberg, Germany
Prof. Dr.-Ing. Catalin Teodoriu, University of Oklahoma, USA
Prof. Dr.-Ing. Gerhard Thonhauser, Montanuniversität Leoben, Austria

Date of the award: 24.01.2019

Declaration

I hereby declare that I completed this work without any improper help from a third party and without using any aids other than those cited. All ideas derived directly or indirectly from other sources are identified as such. In the selection and use of materials and in the writing of the manuscript I received support from the following persons:

- Prof. Dr.-Ing. Matthias Reich, TU Bergakademie Freiberg: Supervisor
- Justus Ehras: Student Master Thesis 2016 „Investigation of a Novel Signal Generator (Multi-Frequency Generator) to Speed up the Hydraulic Data Transmission in Borehole“, supervised by Dipl.-Ing. Mouhammed Jandal Berro
- Brigitte Hegenberg: Assistance with proofreading

Persons other than those above did not contribute to the writing of this thesis. I did not seek the help of a professional doctorate-consultant. Only those persons identified as having done so received any financial payment from me for any work done for me. This thesis has not previously been published in the same or a similar form in Germany or abroad.

Freiberg, 24.01.2019 Mouhammed Jandal Berro

Berro, Mouhammed Jandal

Development and Testing of Alternative Methods for Speeding up the Hydraulic Data Transmission in Deep Boreholes

Dissertation 2019; 147 Pages; 88 Figures; 12 Tables; 4 Appendices; 1 DVD

TU Bergakademie Freiberg, Faculty of Geosciences, Geoengineering and Mining, Institute of Drilling Engineering and Fluid Mining

Keywords: *MWD, LWD, drill string, drilling mud, mud pulse telemetry, hybrid mud pulse telemetry system, multi-frequency mud siren, multi-frequency generator, multi-sensor receiver, data transmission, data rate, pressure wave, measuring position*

Abstract

For developing the available hydrocarbon reserves and for exploring new reservoirs, deeper and more complex wells are drilled. Drilling such deeper and complex wells requires a constant monitoring and controlling of the well paths. Therefore, the bottom hole assembly, the lower section of the drill string above the drill bit, is equipped with numerous measuring sensors for collecting geological and directional data while drilling. The collected data have to be transmitted to the surface in real time.

Prior to transmit the data measured downhole to the surface, they are processed and translated into a binary code. Accordingly, the data will be represented as a series of zeroes and ones. The most common method for data transmission in boreholes is the so called mud pulse telemetry which sends the information through the drilling mud inside the drill string by means of coded pressure pulses. There are two types of devices available for downhole pressure pulses generation. The first type is the (positive or negative) pressure pulser which transmits the data by quasi-static variations of the pressure level inside the drill string. The second type is the (rotating or oscillating) mud siren which transmits the data by generating continuous pressure waves at specific frequencies.

The main disadvantage of the mud pulse telemetry is its low data transmission rate which is about 10 bps. This data rate is very low compared to the measured amount of raw data.

Therefore, the efficiency of the mud pulse telemetry must be improved, so that the data could be transmitted at higher rates. The present research work presents different developed and tested concepts for increasing the efficiency and the data transmission rate of the mud pulse telemetry. Both, the transmitter and the receiver end, were taken into consideration by developing the new concepts. Different hardware and software tools were used for performing the present research work. The available flow loop test facility and the experimental prototypes of the mud siren and positive pulser were used. The test facility was extended in order to enable the investigation of the new concepts. The available 3D numerical model (ANSYS CFX) was modified and extended in order to study the new concepts.

At the transmitter end, a novel concept for a hybrid mud pulse telemetry system was developed and successfully tested. Here, two different types of mud pulse telemetry could be used in a combination, such as a mud siren and a pressure pulser. The developed concept was registered at the German Patent and Trade Mark Office for a patent in 2018. Two concepts for a multi-frequency mud siren were developed for simultaneous generation of two frequencies. In the first approach, two sets of stator/rotor were installed in a row connection, while they were installed in a parallel connection in the second approach. The two concepts were registered at the German Patent and Trade Mark Office for patents in 2015. An experimental multi-frequency generator was built and used for testing of several new ideas, such as transmitting the data using several carrier frequencies at the same time, transmitting the data with different wave forms (sine, sawtooth, triangle and rectangle), or transmitting the data using the chirp modulation. The innovative design of the experimental multi-frequency generator was registered at the German Patent and Trade Mark Office for patents in 2016.

At the receiver end, two different methods for processing and analyzing the received multi-frequency signals using the Wavelet and Fourier analysis were drafted and tested. A novel concept for the use of a multi-sensor receiver was developed and successfully tested. The use of a multi-sensor receiver could strongly improve the detection of the received signals.

Acknowledgements

First of all, I would like to express my sincere gratitude to Prof. Dr.-Ing. Matthias Reich, my doctoral supervisor, for his support of my Ph.D. research work. In particular, I would like to thank him for his guidance, patience, encouragement throughout the whole research work. With his continuous support I could perform this research work, write the present thesis, register four patent applications at the German Trade and Mark Office and publish several scientific and technical papers. I was very lucky to have had the opportunity to work with such a professional advisor as Prof. Dr.-Ing. Matthias Reich.

I would like to thank Dr.-Ing. Silke Röntzsch, Dipl.-Ing. Erik Börner and Dipl.-Ing. Andreas Schramm for their technical support during the laboratory work. I also would like to thank Dr. Uwe Prüfert for his support regarding the MATLAB program. Many thanks to Mrs. Brigitte Hegenberg for her help with proofreading.

Furthermore, I would like to thank the members of the drilling engineering research group at the institute for the great cooperation. In particular, I would like to thank Dr.-Ing. Mohammed Ali Namuq for the useful discussions. I would like to thank the institute director, Prof. Dr.-Ing. Moh'd M. Amro, and all the colleagues of the Institute of Drilling Engineering and Fluid Mining of the TU Bergakademie Freiberg. Special thanks go to the two friendly and very helpful women at the institute, Mrs. Sabine Bayer and Miss Romy Hänsel.

Last but not the least, I have to thank my mother and my wife for their continuous support throughout performing this work and my life in general. I'm grateful for my three wonderful children: Razan, Iman and Abdullrahman, who shine brilliantly like the stars in the sky and give me unending inspiration. This thesis is dedicated to them and to my father in his different world.

****
I miss you so much, my father, you had too early seen me as a doctor. If you were still alive, you would have seen that the dream we shared becomes true. I did it, but unfortunately too late after your decease.

Table of Contents

List of Abbreviations

Abbreviation	Meaning
AT	Acoustic Telemetry
ASK	Amplitude Shift Keying
BHA	Bottom Hole Assembly
BOP	Blowout Preventer
CDR	Compensated Dual Resistivity tool
CFD	Computational Fluid Dynamics
CSS	Chirp Spread Spectrum
CWT	Continuous Wavelet Transformation
DFT	Discrete Fourier Transformation
DPPM	Differential Pulse Position Modulation
EMT	Electromagnetic Telemetry
FFT	Fast Fourier Transformation
FDM	Frequency division multiplexing
FE	Formation Evaluation
FSK	Frequency Shift Keying
HMPT	Hybrid Mud Pulse Telemetry
HSMPT	High-Speed Mud Pulse Telemetry
IBF	Institute of Drilling Engineering and Fluid Mining, Freiberg, Germany
IFFT	Inverse Fast Fourier Transformation
IUG	Interface User Guide
LCM	Lost Circulation Material
LWD	Logging While Drilling
MFSK	Multiple Frequency Shift Keying

MIMO	Multiple-Input, Multiple-Output
MISO	Multiple-Input, Single-Output
MPT	Mud Pulse Telemetry
MWD	Measuring While Drilling
NRZ	Non-Return-to-Zero
OOK	On-Off Keying
P1, P2, P3 and P4	Pressure sensors installed on the pipeline of the test facility
P1-1 till P1-14	Monitoring points installed between P1 and P2 in ANSYS CFX model
P2-1 till P2-18	Monitoring points installed between P2 and P3 in ANSYS CFX model
PAM	Pulse Amplitude Modulation
PCM	Pulse Code Modulation
PDM	Pulse Duration Modulation
PPM	Pulse Position Modulation
PSK	Phase Shift Keying
PVC	Polyvinyl Chloride
PWM	Pulse Width Modulation
QPSK	Quadrature Phase Shift Keying
RSS	Rotary Steerable System
RZ	Return-to-Zero
SIMO	Single-Input, Multiple-Output
SNR	Signal-to-Noise Ratio
STFT	Short-Time Fourier Transformation
TS	Training Sequence
WPT	Wired Drill Pipe Telemetry

List of Symbols

Symbol	Meaning	Unit
A	Amplitude	[bar]
AZI	Azimuth	[°]
c	Wave speed	[m/s]
CFA	Clearance flow area between the pipe and the outside of the stator/rotor	[m^2]
D	Modulation rate (symbols rate per second)	[Bd]
F	Carrier frequency	[Hz]
f(t)	Time signal	
$\mathbf{F_c}$	Center frequency of the used wavelet (= 0.8125 for a Morelet wavelet)	[Hz]
$\mathbf{F_s}$	Pseudo-frequency calculated corresponding to a certain scale (s)	[Hz]
i	Iteration time step	
ID	Internal diameter	[mm]
INC	Inclination	[°]
j	imaginary number $j^2 = -1$	
K	Temperature	[K]
L	The number of bits transmitted via each signal symbol	
M	Number of the representable signal symbols	
$\mathbf{P_a}$	Absolute pressure	[Pa]
$\mathbf{P_0}$	Reference pressure, absolute value is 10^5	[Pa]
Q	Flow rate	[m^3/h]
R	Data rate	[bit/s]
ROP	Rate of penetration	[m/s]

$\mathbf{R_{pipe}}$	Radius of the pipe (internal)	[mm]
$\mathbf{R_{rotor}}$	Radius of the rotor disc	[mm]
$\mathbf{R_{stator}}$	Radius of the stator disc	[mm]
$\mathbf{R_{space}}$	Radius of the space between the two stator/rotor sets	[mm]
s	Scale parameter of the Wavelet transformation	
S(t)	Time function of the sine wave	
SFA	Free flow area through the stator and rotor discs	[m^2]
SPFA	Space flow area between the two sirens in parallel connection	[m^2]
$\mathbf{S_M}$	Momentum source	[$kg/(m^2 s^2)$]
t	Time variable	[s]
T	Symbol (bit) duration	[s]
TFA	Total flow area	[m^2]
TFO	Tool face orientation	[°]
U	Vector of velocity $U_{x,y,z}$	[m/s]
v	Fluid (water) flow velocity	[m/s]
$\mathbf{WMP_y}$	Index for wave measuring position, y = 1, 3, 5, 7, 9, …	
WOB	Weight on bit	[N]
X	The number of bits transmitted via each signal symbol	
x(t)	Continuous-time signal	
$\boldsymbol{X(j\omega)}$	Spectrum of a continuous-time signal x(t)	
ΔP	Change in the pressure created by the moving of the rotor against the stator	[bar]
$\boldsymbol{\alpha}$	Circular angle	[°]
Φ	Initial phase of the carrier signal	[°]
θ(t)	Time dependent phase	[°]

$\boldsymbol{\omega}$	Angular frequency	[rad/s]
$\boldsymbol{W_{\psi}(s,\tau)}$	Wavelet-Coefficient of a time signal f(t)	
$\boldsymbol{\lambda}$	Length of the propagated wave	[m]
$\boldsymbol{\mu}$	Dynamic viscosity	[kg/(m s)]
$\boldsymbol{\rho}$	Density	[kg/m3]
$\boldsymbol{\rho_0}$	Reference density = 998	[kg/m3]
$\boldsymbol{\tau}$	Stress tensor	[Pa]
$\boldsymbol{\tau_{Tr}}$	Translation parameter of the Wavelet transformation	
$\boldsymbol{\delta}$	Identity matrix or Kronecker Delta function	
$\boldsymbol{\psi_0}$	Wavelet function	
Δ	Sampling period	
$\boldsymbol{\nabla}$	$\left[\frac{\partial}{\partial x}, \frac{\partial}{\partial y}, \frac{\partial}{\partial z}\right]$, x, y, z are Cartesian coordinates	

Conversion factors:

1 Pa = 10^{-5} bar

1 K = -272.15 celsius (°C)

1 ft = 0.3048 m

CHAPTER 1 Introduction

Production of oil and gas from its underground reservoirs requires the construction of deep wells which act as a path between the reservoirs underground and the production stations above ground. Some reservoirs are located deep, may be several kilometers under the seafloor, others could be reached through deep wells of 4-6 kilometers, which, however, have to be extended horizontally along the reservoir for many kilometers in order to increase the contact area between the production well and the reservoir, raising the produced amount of oil and gas.

Drilling of such extreme deep wells and precisely reaching the target area can only be performed using the best available high-tech equipment, where for example several measuring sensors are integrated in the lower part of the drill string above the drill bit. Some measuring sensors allow a constant control of the drill path. For example, the inclination and azimuth of the drill path are continuously measured during drilling. If the current well path deviates from the planned one, directional corrections can be initiated by the drilling team at the surface. Other sensors are used for monitoring the drilling process. For this purpose they continuously measure, for example, the bending moment in the drill string, weight and torque on bit, vibrations and shocks on bit, well temperature, drilling mud pressure, etc. The measuring tool including these sensors is known as MWD (Measuring While Drilling) system. There is another measuring tool, called LWD (Logging While Drilling) system. During the drilling process, LWD sensors measure the rock properties, which are the most decisive and interesting for reservoir engineers, such as porosity and permeability.

The sensors perform their measurements at the bottom of a several thousand metres deep borehole. Thus, the measured data have to be transmitted for several kilometres from the bottom of the borehole to the surface. The data could be transmitted using a cable, a wired drill pipe (cable inserted in the drill pipe wall), or electromagnetic or acoustic waves. However, because of various reasons (higher cost, short reach, etc.) the methods mentioned last are still not the first option to be used for data transmission in deep boreholes. The most commonly used telemetry system for data transmission in boreholes

is the so-called mud pulse telemetry (MPT), see Figure 1.1. In order to remove the drill cuttings from the bottom of the borehole, drilling mud is pumped through the drill string towards the bottom hole. The drilling mud carrying the drill cuttings flows again to the surface in the outer annular space between the drill string and the borehole wall. The drilling mud inside the drill string will be used as a transmitting channel for the mud pulse telemetry. Therefore, the mud pulse telemetry can be considered and called as a hydraulic data transmission system.

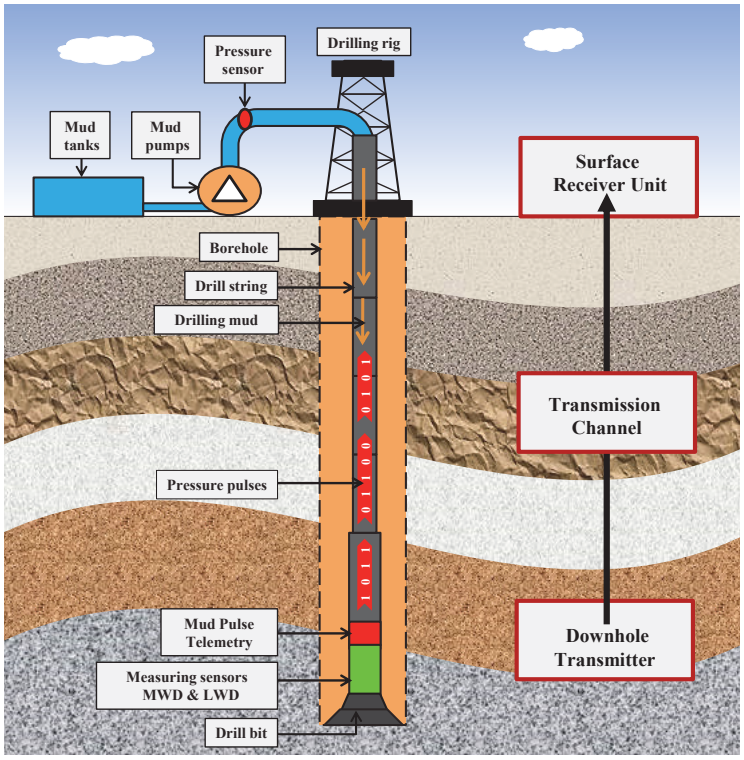

Figure 1.1: Principle of mud pulse telemetry system

Before transmitting the measured data to the surface they are processed and transformed into a binary code, which is consisting only of zeros and ones by an underground computer. Thereafter, the mud pulse telemetry sends the information by means of coded pressure pulses (or fluctuations) via the mud channel. For downhole pressure pulses generation, the conventional mud pulse telemetry utilizes one type of four devices available: positive pulser, negative pulser, mud siren or oscillating shear valve. The pulsers are transmitting the data by quasi-static variations of the pressure level over a fixed duration (time slot) inside the drill string. In contrast, the mud siren and oscillating

shear valve are generating continuous pressure waves at specific frequencies. At the surface, the receiver (pressure sensor) is fixed to the standpipe which connects the mud pumps and the drill string. The resulting pressure variations in the drill string can be detected through this pressure sensor and forwarded to a surface computer which again translates the recorded pressure variations back into measured values which are shown at the work platform.

In spite of the fact that the mud pulse telemetry is still the most frequently used telemetry system in the field, it still has a main problem represented in its low data transmission rate. The achieved data rate is usually less than 10 bit/s, which is very low compared to the amount of raw data measured downhole. This limited data rate is the main reason for the need for intense raw data processing in the bottom hole assembly before the compressed signal can be transmitted. Thus, the capacity of the downhole data transmission system must be improved so that the data can be transmitted at higher transmission rates. The present work is primarily concerned with developing and testing new approaches to increase the data transmission rate of the mud pulse telemetry system. Based on the standard design of the common digital communication system, Figure 1.2 illustrates the basic elements of MPT as a hydraulic data transmission system.

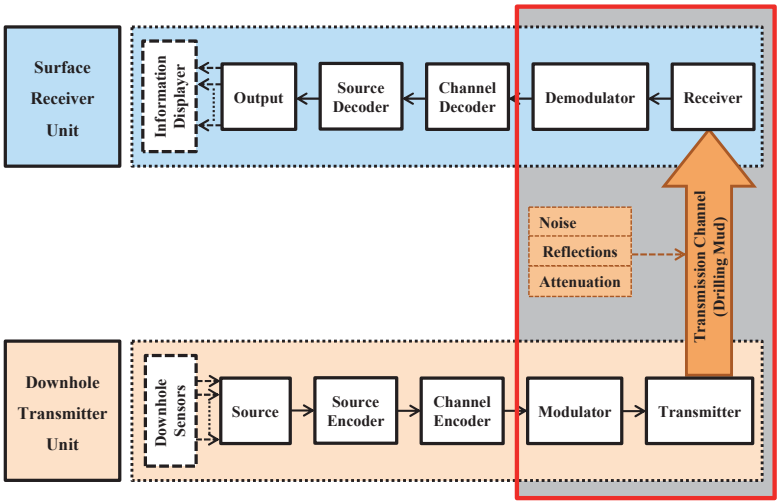

Figure 1.2: The basic elements of a hydraulic data transmission system

All the developed concepts and the executed investigations focus only on the transmitter device, receiver device, transmitting channel, and, finally, signal modulation and

demodulation methods. The rectangle with a grey background in Figure 1.2 shows the work area in the present research work. All the other elements of the transmission system were not taken into consideration.

An essential part of this work is to develop new transmitter devices for hydraulic data transmission that are able to transmit the data at rates higher than those of conventional MPT systems. One concept is based on combining of two conventional types of MPT devices, such as a combination of a positive pulser and a mud siren. In this case, the system is called a hybrid mud pulse telemetry (HMPT) system. In a second concept, two approaches were developed for a multi-frequency mud siren. In order to investigate the data transmission in boreholes using several frequencies, an innovative experimental multi-frequency generator was built and tested. On the other hand, two concepts were developed regarding the receiver end. In the first concept, the Wavelet analysis will be applied to processing the received multi-frequency signal. The second one is represented by the use of a flexible placement of a multi-sensor receiver for a better detection of the transmitted signal.

After introducing the main goal of the present work in Chapter 1, an introduction to the modern drilling technology and to the low data rate of the mud pulse telemetry system as a problem with respect to the whole drilling operation is given in Chapter 2. Chapter 3 presents the fundamentals of modulation techniques and digital signal processing tools for the data transmission in boreholes. The state of the art for mud pulse telemetry systems and the transmission limitations are presented in Chapter 4. A brief description of the developed concepts and approaches during this research work is given in Chapter 5. Chapter 6 presents the laboratory test facility with its experimental prototypes and numerical model. The investigation results of the transmission tests using the hybrid mud pulse telemetry are presented in Chapter 7. Chapter 8 presents the mathematical and numerical study of the multi-frequency mud siren. Chapter 9 presents the investigation results of the data transmission tests using several carrier frequencies and the analysis using Fourier and Wavelet tools. The investigation results of the use of a multi-sensor receiver are presented in Chapter 10. The last Chapter, Chapter 11, concludes the research results and gives an outlook for future work.

CHAPTER 2 Modern Drilling Technology and Low Data Transmission Rate as a Limitation

2.1 Introduction to the modern drilling technology

2.1.1 Directional drilling technology

Due to environmental and technical reasons and economic issues the oil or gas wells are usually not drilled vertically but directionally to the target area. Drilling directional oil wells was first done in the California Huntington Beach field in 1933 (Warren, 2006). Directional drilling became more familiar as a drilling technology over the years, so that today an approximate estimation could be given, that more than 60 % of the deep wells are drilled directionally (Reich, 2012).

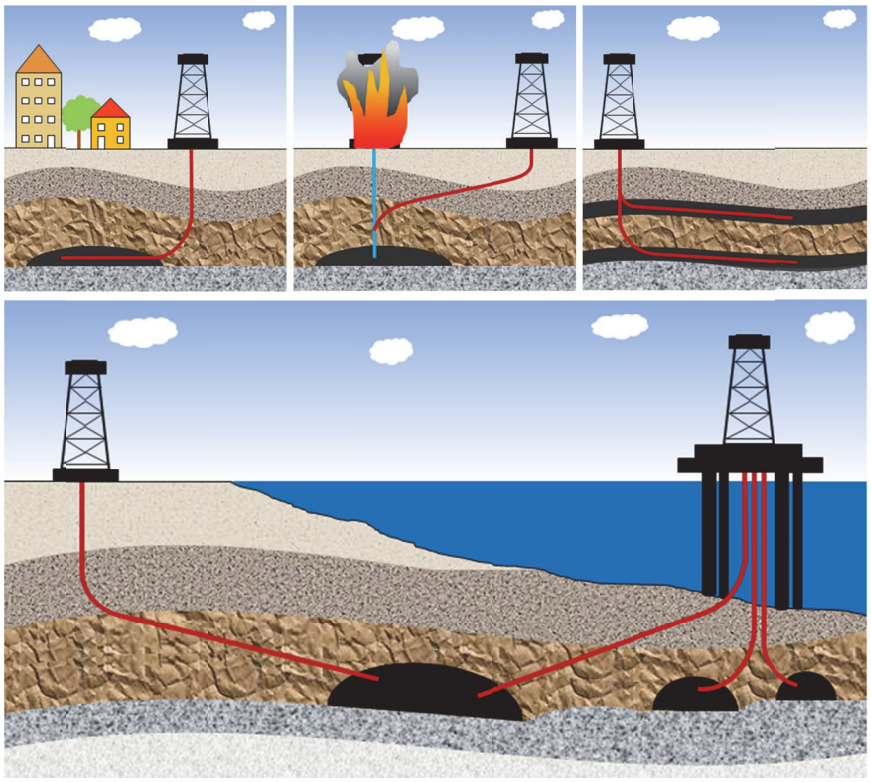

Figure 2.1: Application examples of directional drilling technology

Figure 2.1 presents some application examples of directional drilling technology. In some locations the drilling costs are very high and/or the environmental working conditions are

very hard. Therefore, multiple wells are created from the same surface location. This case is widely applied on offshore drilling platforms. The Hydrocarbon reservoir can exist underneath populated cities or areas, where the drilling rigs cannot be operated. Directional drilling technology enables to drill a deviated well from a location existing in a few kilometers outside of the populated city into the hydrocarbon reservoir under this city. When a wellbore is suffering a blowout, another well called relief well can be drilled deviated towards the blowing well creating an injection path, through which an extreme heavy drilling mud will be pumped down into the bottom hole of blowing well in order to kill it and stop the blow out (Reich, 2012). As an example, the blowing out of the deep water well in the Gulf of Mexico in April 2010, where two relief wells had to be drilled to depth of 5,486 m in order to kill the blowing well (Devereux, 2012). Directional drilling is a very important technique not only regarding the drilling costs and challenges but also regarding the well productivity after the drilling phase. Today it is common practice, that in order to increase the produced amount of hydrocarbons the wellbore must be horizontally as long as possible placed along the hydrocarbon–bearing layer. The wellbore, whose horizontal section is at least two or three times longer than its vertical section, is called an extended reach well. The record breaking wellbore has a vertical section of about 3,048 m and a horizontal section of about 9,144 m (Reich, 2012). Drilling such wellbores, as in examples mentioned above, and successfully placing it according to a certain path into the target area can only be performed using the best available high-tech equipment, in the first instance steering head, measuring while drilling and logging while drilling systems. The steering head is used in order to deviate the well path as needed.

2.1.2 Steering technology

In the early 1980s, steerable motor technology was introduced making a change in directional drilling capability. Prior to the use of steerable motor, a combination of turbine/bent-sub assemblies and conventional rotary assemblies was used in order to perform directional drilling operations. Changing the well trajectory was made by using turbine/bent-sub assembly only in the sliding mode, building/dropping inclination or turning the well. After the desired azimuth/inclination and trajectory were achieved, a

roundtrip was made to replace the turbine/bent-sub assembly with a conventional rotary bottom hole assembly (BHA) and continue the drilling operation. Each time an unacceptable change or tendency in the well path occurred, two roundtrips would be made. One roundtrip would be made to run a turbine/bent-sub BHA to get the well path back on track. The second one would be made to run the conventional rotary BHA again and continue the drilling. Steerable downhole motor BHA is typically composed of a mud motor section and a bent housing device. Such assembly can be used for drilling in a combination of both sliding and rotary drilling modes (Berger et al., 1999). In case of rotary drilling mode, the drill string rotates, usually at 60 to 100 rpm (revolution per minute). The bent in the downhole motor rotates in turn with the same rotational speed. The directional behavior of the BHA assembly will not be affected and a straight section will be drilled. In case of drilling with a sliding mode, the drill string rotation is stopped and the drilling operation is continued only by the power of the downhole motor directly above the drill bit. In this case, the bent in the motor is constantly pointing in the same direction. The motor follows the bent and a curved well section is created (Reich, 2012).

However, using drilling motors without drill string rotation became more challenging as the engineers continuously tried to extend the length of the horizontal sections of the wells, for instance in case of offshore drilling rigs. Since the mostly offshore drilling rigs are associated with expensive investments and must be located at the same location and cannot be moved to another one, many wells as possible should be drilled down into all possible directions so that the production of oil and gas can be maximized. Drilling such long horizontal well sections requires steering with downhole motor, which in turn requires stopping the drill string rotation. But on other side, the static friction effect increases during drilling without string rotation and consequently makes drill string pushing forward in the borehole very difficult. The problem described above can be overcome by rotating the drill string during drilling. However, steering the well path by using steerable downhole motors in rotary drilling mode is not possible. Therefore, a new steerable system was developed, whereby the steering can be done with continuous drill string rotation. The new developed drilling system, the so called rotary steerable system (RSS), was commercially used in the 1990s. It could be considered as the dominant

drilling system in the field of horizontal drilling and extended-reach wells. The modern steerable system is very complex and equipped with several sensors in order to monitor the drilling path and correct it as needed even without the influence of the driller at the surface (Reich, 2012; Berger et al., 1999).

2.1.3 Measuring technology

It should be taken into consideration that the successful steering of the well path is done depending on directional data and geological information collected in real time while drilling. Therefore, the lower section of the drill string above the drill bit, called bottom hole assembly (BHA), is equipped with sophisticated sensors to determine the directional and formational parameters (Berro[a] and Reich, 2015). The typical bottom hole assembly (BHA) contains two main measuring systems, measuring while drilling system (MWD) and logging while drilling system (LWD), (Taylor et al., 2010). The introduction of measuring while drilling (MWD) in the late 1980s successfully improved the navigation of the drill string (Berro[b] and Reich, 2015). The MWD system usually consists of three subsystems: the downhole sensor unit, the telemetry unit to transmit the measured data to the surface in real time and the surface receiver unit, where the transmitted data are received, processed and finally displayed in the useful format (Gravley, 1983). MWD systems measure the directional parameters such the inclination (INC), azimuth (AZI) and tool face orientation (TFO) at the drill bit. Depending on the directional data, an approximate path of the wellbore can be computed (Reich, 2012). Due to the importance of the directional drilling data they are constantly represented (digitally) on a screen on the rig floor (Reich, 2012; Gravley, 1983). Further information such as weight on bit (WOB), temperature, mud pressure, torque, bending moments and dynamic effects on the BHA may also be provided by the MWD (Berro[b] and Reich, 2015).

In the 1990s, Logging While Drilling (LWD) tools were added to the bottom hole assembly (BHA) to complement the directional data with formation data. The real time LWD systems provide reliable information about the porosity, permeability, hardness and the pore content of the drilled formation. Moreover, it is possible to determine the pore pressure and to take samples from the formation (Berro[b] and Reich, 2015). LWD systems

can also provide primary evaluation of the formation being drilled. LWD systems contain Compensated Dual Resistivity tool (CDR), which in turn measures the resistivity and spectral gamma ray of the rocks being drilled (Hansen and White, 1991). Depending on the rock specifications resulting from the formation evaluation while drilling, the well path can be precisely steered into the target area. Such steering based on real time measured formation parameters is called in real time geo-steering (or geological steering) (Hansen and White, 1991; Reich, 2012). Recent image logs have become state of the art, as they create an azimuthal image of the collected data from the wellbore (Tollefsen et al., 2007).

2.1.4 Technology of data transmission in boreholes

As previously explained the bottom hole assemblies are equipped with a wide variety of measuring sensors, which collect geological and directional data while drilling. The collected data are analyzed and processed downhole. In order to enable the driller to correctly make decision, the information must be transmitted to the surface in real time. Any system for transmission of data or information consists of three main parts: the transmitter unit, the transmission channel and the receiver unit. In the transmitter unit the measured data will be analyzed and processed. Thereafter the transmitter sends the data in the form of specific waves over a specific channel. Depending on the kind of the carrier waves generated by the transmitter as well as on the kind of the used transmission channel, there are four main systems commercially available for data transmission in boreholes. These are: mud pulse telemetry, electromagnetic telemetry, acoustic telemetry and wired pipe telemetry. The so-called mud pulse telemetry (MPT) system was introduced into the oil and gas industry began in the late 1970's (Schnitger and Macpherson, 2009). MPT system uses the drilling mud inside the drill string as a transmitting channel, therefore it is considered as a hydraulic transmission system. Before transmitting the measured data to the surface they must be translated into a binary code, thus the data will be represented as a series of zeroes and ones by an underground computer. MPT system sends the information by means of coded pressure pulses (or fluctuations) via the mud channel. By means of a pressure sensor, attached to the standpipe which connects the mud pumps and the drill string, the resulting pressure

variations in the drill string can be measured and forwarded to a surface computer which detects and translates the recorded pressure variations back into values which are displayed on a display at the work platform (Reich, 2012). Electromagnetic telemetry (EMT) was commercially introduced into the oil and gas drilling operations first in 1987. The downhole measured data will be coded and transmitted in the form of electromagnetic waves. The electromagnetic waves propagate from the bottom hole assembly to the surface through the formation surrounding the wellbore. At the surface the electromagnetic waves will be received and processed in order to extract the decoded transmitted data (Rodriguez et al., 2013). The downhole measured data can be transmitted by acoustic waves propagated up the drill string wall. Such a transmission system is known as acoustic telemetry system (AT). The first commercial introduction of the acoustic telemetry system into drilling operations was in 2000 (Shah et al., 2004). The measured data can be transmitted by using a cable as a transmission channel as in the case of the wired drill pipe telemetry (WPT). The commercial introduction of the wired drill pipe telemetry (WPT) into the drilling operations was early in 2006 (Ali et al., 2008). Special drill pipes are developed and manufactured, so that a high speed data cable (coaxial cable) is mounted along the drill pipe within its wall. Retransmitting the data from a pipe to the adjacent pipe is done by using inductive coils integrated in the connection tool joint between each two drill pipes (Nygaard et al., 2008).

An optimal telemetry is that one which can transmit the downhole information at high data rates over a long distance with a high reliability. Such telemetry must be cost effective and workable with all drill rigs as well with all standard drill pipes used by the drilling operations. Several scientific and technical papers have described the efficiency of the available transmission systems regarding their achieved data transmission rates and operation depths. Figure 2.2 presents the mean or maximum data rates and transmission reaches achieved by the available telemetries. Besides its low data rates, another disadvantage of EMT is its limited operation depths because of the high formation resistivity and signal attenuation. Despite its operations in a combination with a casing antenna system the achieved transmitting reach was limited up to 3,840 m and the data rate up to or more than 6 bit/s (Rodriguez et al., 2013). A maximum data rate up to 12

bit/s and a record operation depth of 4,267 m were mentioned by (Janwadkar et al., 2010). However, the achieved depth is still less than the usual operation depths of wellbore nowadays.

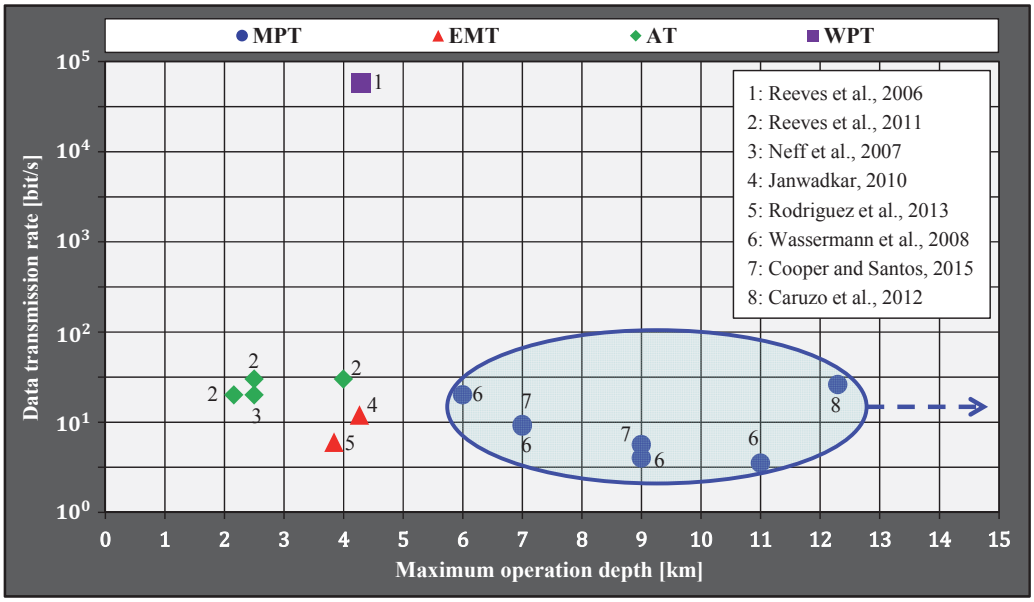

Figure 2.2: Highlights of the transmission telemetries with respect to their data transmission rates and operation depths

Similarly to EMT, AT has low data rates and limited operation depths. It could be operated in vertical and directional land wells with operation depths of less than 2,500 m. This is because of the significant attenuation encountered by the acoustic waves. The attenuation in the signal strength becomes greater in the horizontal applications, so that the transmitting reach of AT is reduced to just about 800 m. Extension of the operation depths of AT up to 4,000 m can be achieved by installing acoustic repeaters with certain distances between each other along the drill string. The new AT system, containing repeater stations along the drill string, is known as acoustic telemetry network. The acoustic telemetry network can allow data transmission at rates more than 30 bit/s (Reeves et al., 2011). WPT is the most rapid telemetry, it can transmit the downhole data at higher rates up to 57,000 bit/s over a transmission distance of approximately 4,287 m (Reeves et al., 2006). However, WPT can be considered as the most expensive telemetry, because it cannot be used with the standard drill pipes which are utilized by all the drilling rigs worldwide. Its applications demand the use of very special drill pipes in

addition to extensive modifications to the rig equipment, such as the top drive (Edwards et al., 2013). Moreover, in order to compensate the signal attenuation downhole amplification joints must be integrated into the drill string spaced with intervals of about 366 - 457 m (Reeves et al., 2006; Edwards et al., 2013). The transmission reach of 4,287 m mentioned above was achieved by using 12 amplification joints (Reeves et al., 2006). Thus, the transmission process is highly depending on the inductive coils between the drill pipes as well as on the amplification joints along the drill string. Accordingly, the reliability of the WPT could not be considered highly sufficient. Once just an inductive coil is damaged and not more workable, the whole transmission process can be failed. Similarly, a non-workable connection between the inductive coil and the coaxial cable can interrupt the data transmission too (Edwards et al., 2013). Another reliability issue is the used amplification joints which can make the WPT out of service, when one or many elements of them are damaged (Reich, 2012). Although it is the oldest system for data transmission in boreholes, nowadays MPT is still the most commonly used real time telemetry in drilling operations. In contrast to the other telemetry systems, the MPT system can reliably be used in ultra-deep drilling operations, enabling drilling achievements of more than 15 km. The main disadvantage of MPT system is its low data rates. For instance, a data rate less than 10 bit/s could be achieved over a distance of 7,000 m (Cooper and Santos). Moreover, it should be taken into consideration that the data rates decrease with the increased operation depths, as shown for example in Figure 2.3.

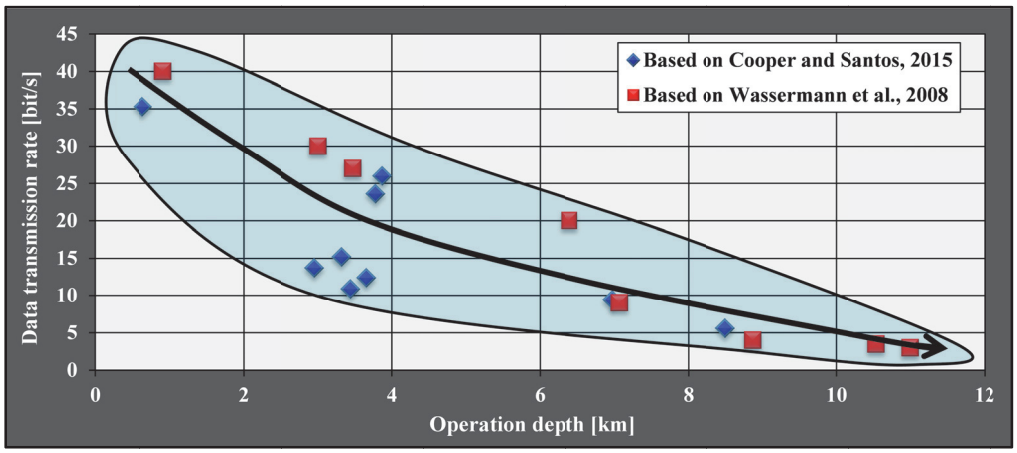

Figure 2.3: Decreased data rates with increased operation depths (the figure is created based on the data given by Cooper and Santos, 2015 and Wassermann et al., 2008)

Due to its high reliable, cost effective operations, long reaches, MPT is still the most frequently used telemetry as well as in the foreseeable future. However, its data transmission rates are still low and cannot keep up with the amount of data collected downhole. This problem will be described in the following section with respect to the whole drilling operation.

2.2 Low data transmission rate as a problem with respect to the whole drilling process

Recent drilling activities have widely been expanded, so that the drilling operations nowadays cover different environments and more challenging oil and gas reservoirs, such as deepwater and ultra-deepwater reservoirs in the Gulf of Mexico or those found in arctic areas. The drilling activities become more and more challenging. High-tech BHAs with MWD and LWD tools are developed to be continuously used and operated in harsh environments with temperatures up to 175°C and pressures up to 620 bars. They are able to withstand shocks of approximately 4,903 m/s^2 (Rodriguez et al., 2013). For successful drilling applications, especially in challenging environments, many issues such as optimizing the drilling operations, increasing their reliability and cost efficiency, maximizing the reservoir productivity through an enhanced well placement, and increasing capability for real-time decisions during the drilling operation become more essential. Consequently, the amount of the required downhole information measured and logged while drilling must widely be increased (Cooper and Santos, 2015; and Emmerich[a] et al., 2016).

For optimizing the drill process, which in turn allows faster drilling and costs saving, data about the drilling dynamics are needed. Collecting data about the wellbore stability and pressure will allow a drilling process with more safety and reliability. Maximizing reservoir productivity in the subsequent phase (production phase) requires precise wellbore placement within the reservoir. For this purpose, formation evaluation data are needed (Cooper and Santos, 2015). Reservoir navigation is based on a combination of many measured data, such as deep azimuthal propagation resistivity imaging, improved resistivity imaging, density and gamma imaging, fluid analysis, sampling and magnetic resonance measurements (Emmerich[b] et al., 2016).

The increasing amount of the required downhole data is reflected as a raise in the number of the downhole measuring and logging tools integrated into the bottom hole assemblies. Thus, the development works of new high-tech BHAs not only refer to the quality of the downhole tools (such as workability in extreme hard operation conditions), but also to their quantity. The number of the downhole tools, which can be integrated into the BHAs, has been several times multiplicated during the past thirty years, see Figure 2.4 (Cooper and Santos 2015). For example, many new measurements for formation evaluation (FE) are educed and utilized in modern BHAs. Several conventional FE measurements are not more executed in form of wireline, they are nowadays included in the downhole MWD tool (Emmerich[a] et al., 2016).

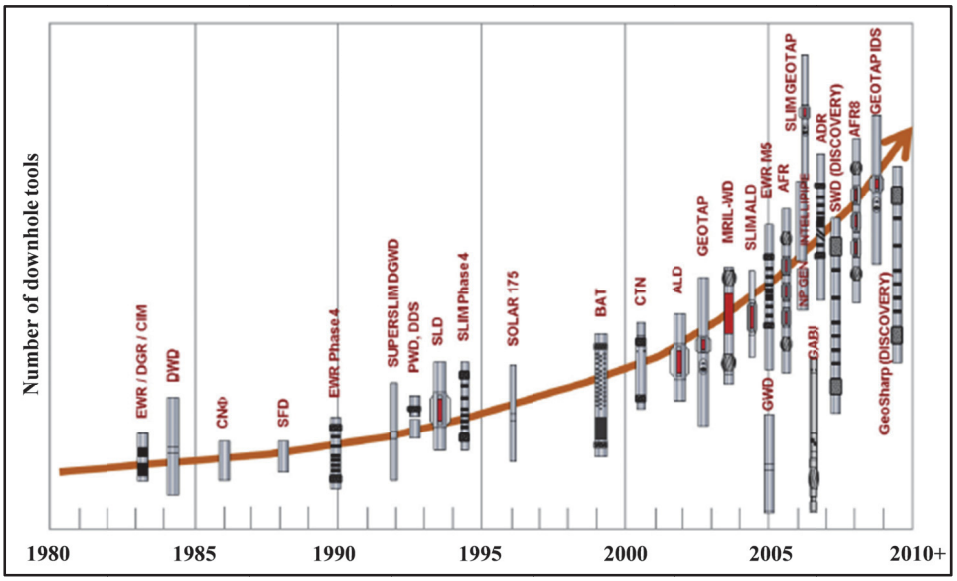

Figure 2.4: Increasing number of downhole tools available to be used in the BHAs over the last thirty years (modified), (Cooper and Santos, 2015)

The effective use of the large amount of the downhole measured data can be achieved, if the measured data can be available in real time to the operator. Moreover, the real time data density will be affected through the increasing number of the downhole measurements. Data density is identified as the number of the measuring points existing in one foot (0.3048 m) on a real time log (Wassermann et al., 2008). Data density represents the log quality (Martin et al., 1994). By the same rate of penetration (ROP), the date density for each log will be decreased due to the increased number of downhole

measuring and logging while drilling tools. Consequently, the log quality will be reduced, making the log interpretation and data extraction at the surface very difficult. Avoiding the decrease in the data density can be achieved by speeding up the data rate of the transmission telemetries or by slowing down the rate of penetration. However, slowing down the ROP leads to extra costs which must be avoided. In contrast, increasing the data transmission rate does not have such negative effects and can enable the operator to effectively use the downhole measured data in real time (Wassermann et al., 2008). Furthermore, the current advances in drill bits technology can lead to a high rate of penetration (ROP). High ROP in turn is another challenge, where keeping the data density at the same level demands also the data transmission rate to be increased (Emmerich[a] et al., 2016).

Due to its high reliable, cost effective operations, long reaches, mud pulse telemetry is still the most common used telemetry for data transmission in boreholes. In order to keep up with the other advances in the modern drilling technology, such as the increased amount of the data collected downhole, high rate of penetration (ROP) and high data density or log quality, the data transmission rates of the mud pulse telemetry must be increased.

Within the scope of the present work innovative concepts for speeding up the mud pulse telemetry system are developed and investigated. Before presenting the developed concepts and the achieved results, it is necessary to give an overview of some basic fundamentals of communication technology, code modulation techniques and signal processing that are related to the present work. In addition, state of the art a brief description of the transmission process using mud pulse telemetry and the challenging coming from the transmission channel (drilling mud column) and other limitations as well will be presented.

CHAPTER 3 Fundamentals of Communication Technology

3.1 Modulation techniques for data transmission in baseband

Mud pulser telemetry is used to transmit downhole data to the surface in real time. By baseband transmission, the data are transmitted in a sequence of discrete pressure pulses which propagate via the drilling mud to the surface carrying the encoded information. For generating such discrete pressure pulses, negative or positive pulsers can be used. Before transmitting the measured data to the surface they need to be translated into a binary code using code modulation techniques. There are many different modulation codes for baseband transmission. According to Ulrich (2009) and Das (2010), Figure 3.1 shows how to modulate a bit stream using three common modulation techniques for transmitting the data via the mud pulse telemetry. They are return-to-zero (RZ), non-return-to-zero (NRZ) and Manchester (or split-phase) modulation.

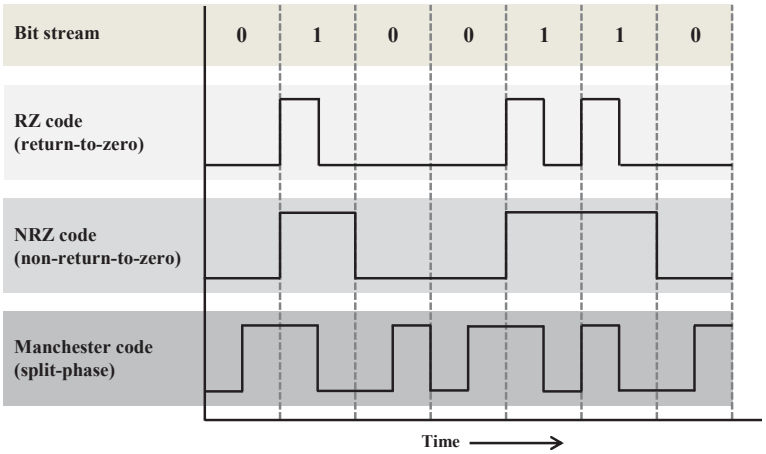

Figure 3.1: Examples for modulation techniques used for baseband transmission

With return-to-zero (RZ) modulation, a binary ‘one’ is represented by the presence of a pulse within the bit interval (or time slot). The presence of the pulse must take place just in the first half of the bit interval. The absence of the pulse within the bit interval represents a binary ‘zero’, see Figure 3.1. With non-return-to-zero (RZ) modulation, each binary digit is represented by a certain pulse level within the bit interval. For instance, the high level (pulse presence) represents the binary ‘one’, while the binary ‘zero’ is

represented by the lower level (pulse absence), see Figure 3.1. With the Manchester code modulation (split-phase), there is always a change in the level in the midpoint of each bit interval. A binary ‘one’ is represented by a level increase taking place in the middle of the bit interval, while the level decrease in the middle of the bit interval represents a binary ‘zero’, see Figure 3.1. With all the above mentioned modulation techniques, opposite representing of the binary digits (ones and zeros) is also possible.

Each code modulation technique has its specific advantages and disadvantages. For instance, detecting pulses modulated with RZ or Manchester code modulation is more difficult than those modulated with NRZ, since the pulses modulated with NRZ modulation are wider than the pulses modulated with RZ or Manchester code modulation (1/2 time slot). But by using NRZ modulation, a long sequence of ones or zeros for example will lead to the risk of losing the synchronization and bit error, correspondingly. This problem can be overcome by using the Manchester code modulation. However, this code modulation requires more movements of the pulser valve because the level must be changed in the midpoint of each bit interval. The last described code modulations encode the information depending on the presence and absence of pulses. These techniques are known as pulse code modulations (PCM).

However, there are further modulations used for baseband transmission, where the information is encoded by varying one of the pulse specifications such as its amplitude, duration or width. Once the encoding is carried out by varying the pulse amplitudes, the applied modulation is called pulse amplitude modulation (PAM). In pulse duration modulation (PDM) all the pulses have the same amplitude but they differ from each other in their adjusted durations. By using PDM, one of the pulse edges is fixed in time sequence while the other one varies according to the value of the information to be transmitted. In another encoding type, called pulse width modulation (PWM), both pulse edges are varied with time. Compared to PDM, in pulse position modulation (PPM) a short pulse is used instead of a variable pulse width or duration (Foster, 1965).

3.2 Modulation techniques for data transmission in passband

The mathematical function of a sine wave can be described as:

$$S(t) = A * sin(F * t + \Phi) \quad (1)$$

Equation (1) presents the three fundamental parameters of any carrier signal, which are: the amplitude (A), frequency (F) and phase (θ(t) = (F * t + Φ)), where (Φ) is the initial phase of the carrier signal. Thus, signal modulation can be achieved by modification of either or all the three parameters (Das, 2012). Mud sirens or oscillating shear valves are used for transmitting the date in passband. They transmit the data by generating pressure waves with specific carrier frequencies. Before transmitting the downhole data, they need to be modulated. Depending on the three basic parameters of any carrier wave, there are three main modulation techniques. These are frequency shift keying (FSK), amplitude shift keying (ASK) and phase shift keying (PSK). Figure 3.2 shows examples for such modulation techniques created in MATLAB. In FSK modulation two different carrier frequencies are used. For instance, a binary 'one' is transmitted by generating a specific frequency for a fixed period (bit interval), while another frequency represents the binary 'zero'.

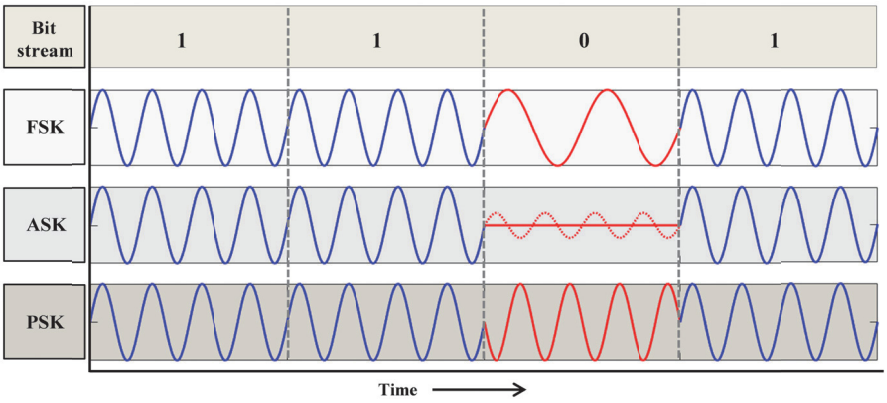

Figure 3.2: Examples for modulation techniques used for passband transmission

In ASK modulation, the two binary digits (one and zero) are represented by two different amplitudes of the carrier frequency. For instance, the higher amplitude can be used to represent a binary 'one', while the lower amplitude represents a binary 'zero'. A special case of ASK modulation is when no signal is transmitted to indicate a binary 'zero'. Thus, the amplitude modulation in this case is 100 %, this is achieved by switching the carrier wave on and off. Therefore this modulation is called as on-off keying (OOK). With PSK modulation two different phases of the same carrier wave represent the two

binary digits (one and zero). For instance, the binary ‘one’ can be represented by the same carrier wave in phase (no phase change), while the carrier wave at a phase shift of 180° represents a binary ‘zero’ (Das, 2010). By all the above mentioned modulation techniques, opposite representing of the binary digits (ones and zeros) is also possible.

3.3 Multiple frequency and chirp spread spectrum modulation techniques

In wireless communication and networks the data rate (R) is defined as the rate in bit per second at which the data are transmitted. The time in second needed by the transmitter to emit the bit is known as bit duration. Another term should be taken into consideration is the modulation rate. Modulation rate (D) is the rate at which the signal is changed to represent a defined number of signal elements or symbols per second. Consequently, it can be simply defined as symbol rate per second and expressed in baud. The data rate can be calculated in relationship with the modulation rate from the following Equation:

$$R = D * \log_2 M \qquad (2)$$

where (M) is the number of the signal symbols that can be represented and used for transmitting the data. It can be calculated using Equation 3:

$$M = 2^L \qquad (3)$$

where (L) is the number of bits transmitted per each signal symbol. Representing a signal with its components in the frequency range is called the signal spectrum. The width of the signal spectrum is known as bandwidth. Each medium has in turn a transmission bandwidth which is mostly wider than the required bandwidth for transmitting a certain signal. Therefore, multi-signals can be transmitted simultaneously by modulating each signal onto a different carrier frequency. When more than two carrier frequencies can be used for signal encoding and transmitting, multiple frequency shift keying (MFSK) can be applied. Each signal element or symbol (M) is transmitted onto a constant carrier frequency and encodes L bits. It should be noticed that in this case more than one bit will be transmitted in each signal symbol. For instance, by using four carrier frequencies for encoding a signal, four possible signal symbols can be represented (M = 4) and each one

represents two bits (L = 2) as shown in Figure 3.3. The shaded rectangle by each symbol refers to which frequency is transmitted in order to represent this symbol at this time step (Stallings, 2005).

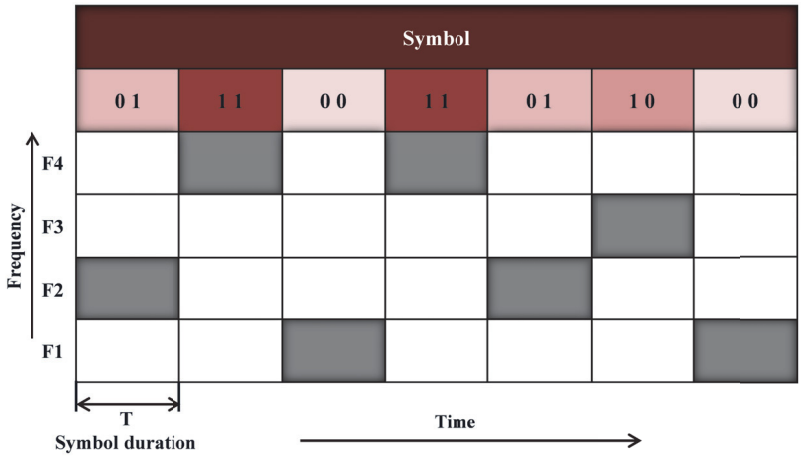

Figure 3.3: Signal transmitting using MFSK, in this case 4-FSK (M = 4) (modified and redrawn), (Stallings, 2005)

One of the latest radio technologies for using the total available bandwidth of the channel for signal transmitting over a predefined duration is the Chirp Spread Spectrum (CSS). Each generated chirp is a frequency modulated signal. Once the chirp signal is changed from a low frequency to a high one, then it is an upchirp, while with a downchirp the signal changes from a high to a low frequency, see Figure 3.4.

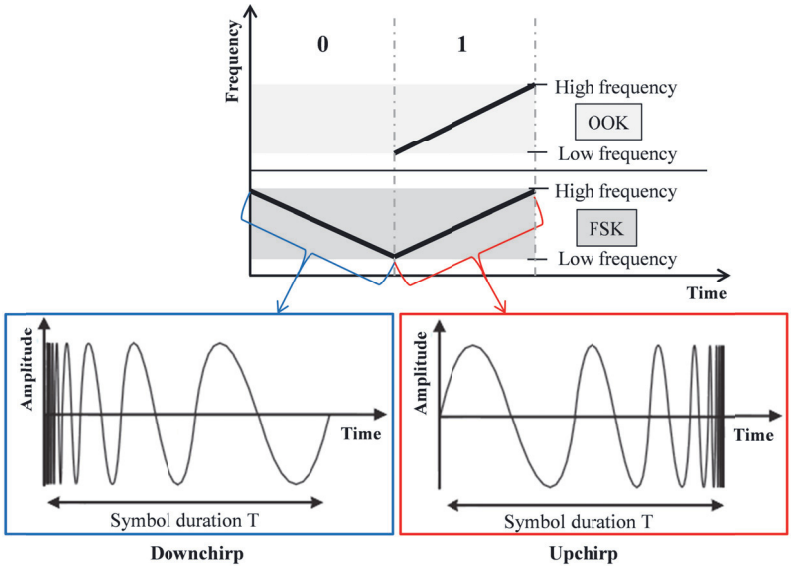

Figure 3.4: Upchirp and downchirp signals with encoding example (modified and redrawn), (Yoon, 2011)

Both chirp signals are linearly frequency modulated with a constant amplitude. Figure 3.4 shows an example of encoding the chirp signals with ASK and OOK. One of the greatest advantages of transmission with CSS is its robustness against noise and interferences coming from the transmission environment (Yoon, 2011).

3.4 Digital signal processing

3.4.1 Fourier transformation

In many cases it is very difficult to identify the signal characteristics by only looking at the raw data. Therefore, in order to make the desired information available, different analysis methods must be used and applied to the data. One of the most commonly used methods is the so-called Fourier Transformation. Hereby, the data signal will be decomposed into its underlying frequencies. By applying the Fourier transformation the output data signal will be transformed from the time domain into the frequency domain (or spectrum) providing information on the contained frequency components as well as the associated amplitudes. After processing the data signal in the frequency domain, it can be retransformed again into the time domain using the Inverse Fourier Transformation (Thuselt and Gennrich, 2013). According to Werner (2010), both Fourier transformations can be expressed mathematically using the following Equations (4) and (5), correspondingly:

$$X(j\omega) = \int_{-\infty}^{\infty} x(t) * e^{-j\omega t}\, dt \tag{4}$$

$$x(t) = \frac{1}{2\pi} \int_{-\infty}^{\infty} X(j\omega) * e^{j\omega t}\, d\omega \tag{5}$$

Normally, in practice the values of a time-based signal are available only at discrete time points and in a finite number. An example in practice is when the value to be measured is sampled in certain time intervals during a measurement. In this case Discrete Fourier Transformation (DFT) must be applied for analyzing the data signal. However, analyzing the signal according to this scheme requires a large number of computational steps,

especially in the case of a large number of data points. A more efficient calculation of the discrete Fourier transformation can be achieved by applying the Fast Fourier Transformation (FFT) algorithm. Thus, the above described Fourier transformation is able to determine and visualize the frequency components contained in a time-sampled signal and their amplitudes as well. But it cannot provide information regarding the frequencies change over the time, also when they have occurred. For instance, Figure 3.5 shows an example of an information pressure signal. The upper part shows in its left section the signal in the time domain, whereas the right section presents the power spectrum of the signal, which is calculated by applying the Fourier analysis.

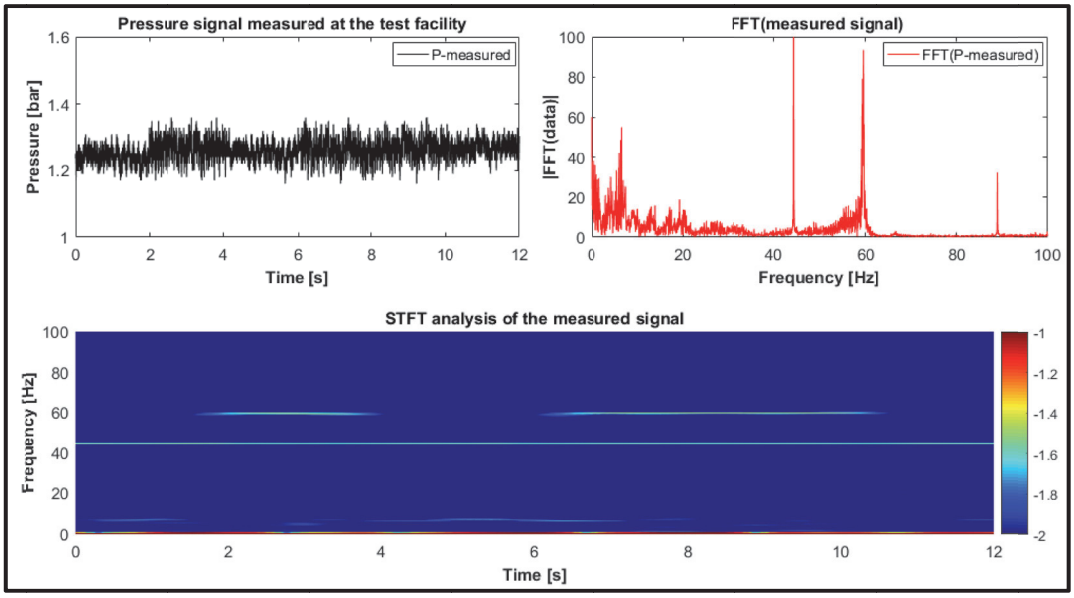

Figure 3.5: An example of a signal in time and frequency domain (top part) and its STFT analysis (lower part)

The frequency spectrum shows the frequency components contained in the time signal (e.g. 44.5 and 59.7 Hz) and their amplitudes. But it does not give any information if the frequency components have changed over the time in the signal. For an effective signal analysis, both the frequency components and the associated time interval equally must be determined and identified. This can be achieved by applying Short-Time Fourier transformation (STFT). STFT enables an observation of the signal frequency components in the frequency domain over the time (Thuselt and Gennrich, 2013). The STFT analysis of the signal example mentioned above is presented in the lower part of Figure 3.5.

3.4.2 Continuous wavelet transformation

Continuous wavelet transformation (CWT) can be considered as a developed ST-Fourier transformation. It is more flexible and able to make an "adaptive" time-frequency analysis. CWT enables the recognizing and the visualization of the frequencies contained in a signal with their corresponding time ranges. Thus, it could be effectively used for processing the received information signals transmitted via the mud pulse telemetry. The wavelet is shifted stepwise over the signal and a Wavelet-Coefficient is calculated. The Wavelet-Coefficient of a time signal f(t) can be mathematically calculated using the following Equation:

$$W_{\psi}(s,\ \tau_{Tr}) = \frac{1}{\sqrt{s}} \int_{-\infty}^{\infty} f(t)\ *\ \psi_0 \left(\frac{t - \tau_{Tr}}{s} \right) dt \qquad (6)$$

where (ψ_0) is the wavelet function, (τ_{Tr}) is the translation parameter and (s) is the scale parameter. Using CWT, the signal to be analyzed is compared at a certain position given by (τ_{Tr}) with the shape of the selected wavelet (e.g. Morelet wavelet) at a certain scale (s). Greater value of the wavelet coefficient indicates a high similarity between the investigated signal and the used wavelet (Thuselt and Gennrich, 2013). At low scale values, the wavelet is compressed and refers to rapidly changing details. Thus, it indicates a high frequency, whereas at high scales the wavelet is stretched referring to slowly changing features. Thus, it indicates a low frequency (Misiti et al., 2009), see Figure 3.6.

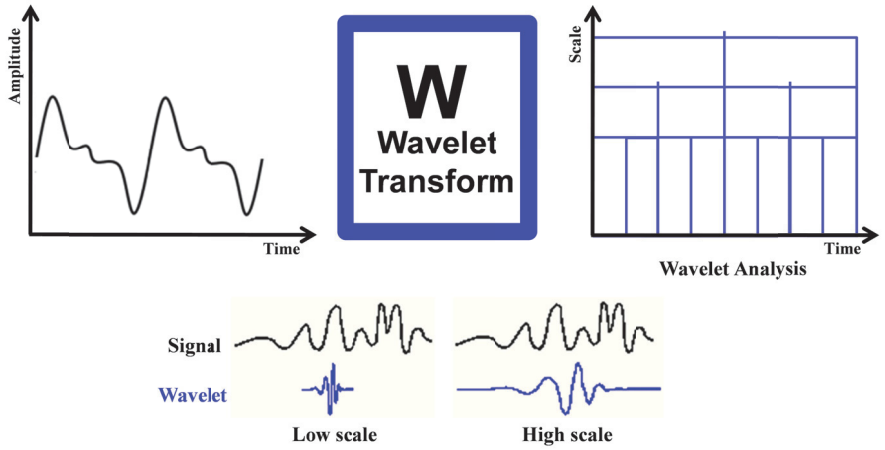

Figure 3.6: The principle of Wavelet Transformation (top part), and relationship between scale and frequency (lower part) (redrawn), (Misiti et al., 2009)

The wavelet coefficients are not calculated at different frequencies (F), but for different scales (s). The relationship between the scale and the corresponding frequency is given by the Equation (7), and the calculated frequency corresponding to a certain scale (s) is called pseudo-frequency (F_s).

$$F_s = \frac{F_c}{s * \Delta} \tag{7}$$

where (F_c) is the center frequency of the used wavelet (= 0.8125 for Morelet wavelet) and (Δ) is the sampling period (Misiti et al., 2009). The information pressure signal presented in (3.4.1) is measured with a sampling rate of 1000 Hz. It will be analyzed using Continuous Wavelet Transformation, whereby the used wavelet is the Morelet wave. Thus, the resulting scales corresponding to the frequencies 44.5 and 59.7 Hz are 18.3 and 13.6, respectively. The wavelet analysis is presented in Figure 3.7 and shows that the frequency 44.5 Hz continues over the entire signal, while the frequency 59.7 Hz is changed over the time.

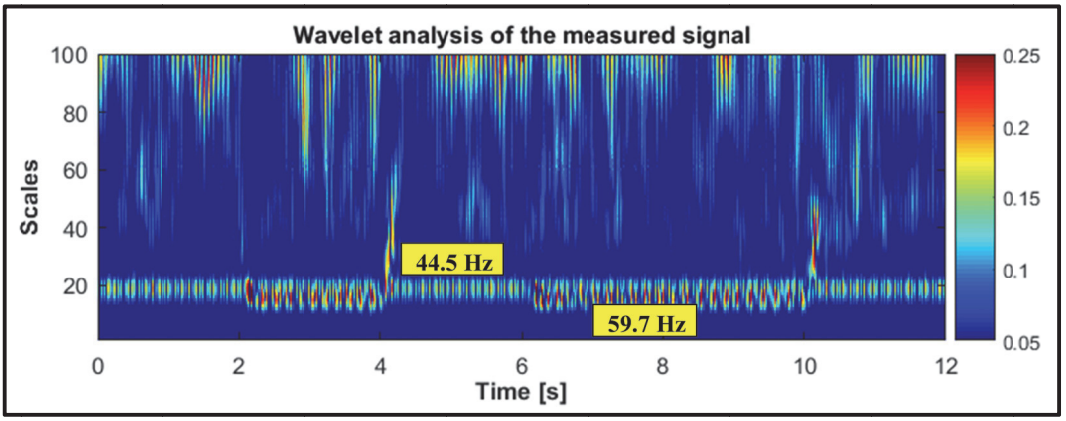

Figure 3.7: Wavelet analysis of the signal example presented in (3.4.1)

3.4.3 Filtering

One of the mostly used functions in signal processing is the filtering function, because not all of the frequency components of a signal refer to valid data. Filtering is applied to reject the unwanted frequencies of the signal and thus to pass only the usable part of the signal to the next processing stage (Das, 2012). For instance, the pressure signal (presented in 3.4.1) is an information signal sent at a carrier frequency of 59.7 Hz and

modulated with OOK code modulation. But as represented in Figure 3.5 and Figure 3.7, the received signal contains other frequency components, such as 20, 44.5 and 89 Hz. All these frequencies, except for 59.7 Hz, are considered as an unwanted part of the signal. Filtering these components before analyzing the signal using Fourier and Wavelet Transformation will lead to better signal evaluation and, consequently, to a more successful detection of the information sent via this signal, see Figure 3.8. Filtering can be achieved using FFT and IFFT. The signal is translated firstly to the frequency domain using FFT and then all the unwanted frequencies are set to zero. After that, the signal is translated again to time domain using IFFT. Finally, the resulting signal can be better evaluated in time domain or by Wavelet analysis.

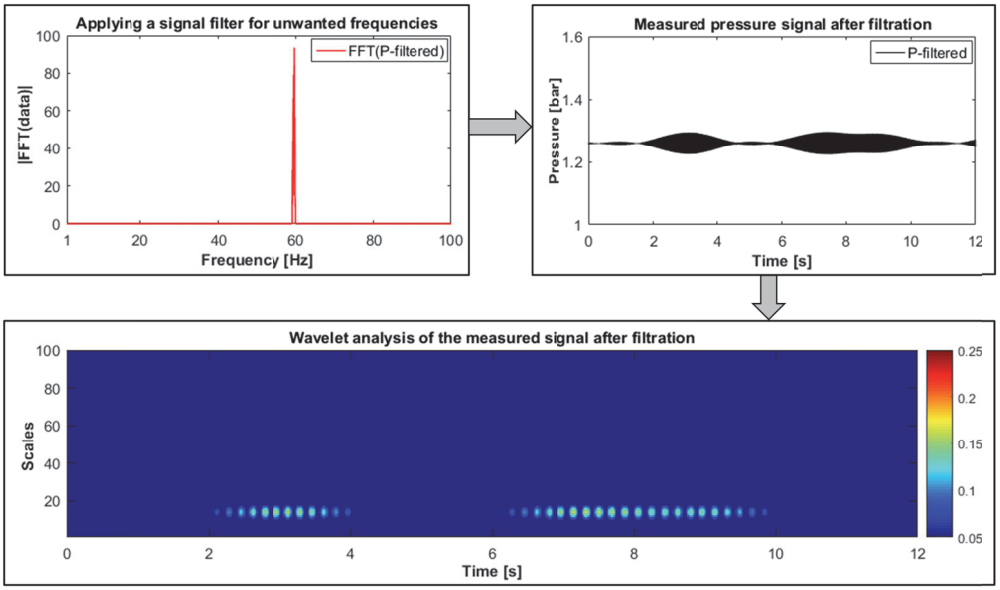

Figure 3.8: Filtering the unwanted frequency components and evaluating the filtered signal in time domain and by Wavelet analysis

CHAPTER 4 State of the Art for Mud Pulse Telemetry Systems

4.1 Historical development of mud pulse telemetry including latest improvements applied for increasing its data transmission rate

The first description of the current mud pulse telemetry system was published by Arps in 1964. The described MWD system transmitted downhole data by generating discrete pressure pulses using a plunger valve. The achieved data rate was extreme low, less than 1 bit/s, (Hutin[a] et al., 2001). An LWD system using a rotary valve to transmit data to the surface was patented by Mobil Oil in the early 1960s. The downhole data were transmitted by generating a continuous pressure wave up to 24 Hz and using phase shift keying as a code modulation. The developed system could generate a pressure signal with a source amplitude of 6.9 bars and achieve data rates up to 3 bit/s. Based on this concept, the currently used mud siren was developed by Schlumberger. The first commercial MWD mud pulse telemetry system was introduced by Teleco in 1978. The Teleco telemetry used a poppet valve that could generate discrete pressure pulses. In comparison to the rotary valve signals, the created pressure pulses had higher amplitudes, so that their detection at the surface could be successfully executed even in hard environments such as deep wellbores and loud hydraulic pump noise. Transmission rates up to 2 bit/s could be achieved. The power supply by this telemetry is provided by a powerful multistage turbine and oil pump. In order to reduce the electrical power consumption, new mud pulse telemetry was developed by Dresser. The main valve of mud pulse telemetry is driven by a pilot valve which in turn is operated by an electrical drive.

Until the 1990s, the achieved data rates were up to 3 bit/s and enough for transmission of downhole data. Due to the introduction of new LWD tools and rotary steerable drilling systems and many other real-time drilling dynamic tools in the 1990s, the achieved data rate at that time was no more sufficient. Drilling operations with such very low data rates will demand decreasing either the ROP or the data density. To avoid that, the transmission rate of the mud pulse telemetry system had to be increased (Wassermann et al., 2008). On the other hand, during its propagation towards the surface the generated

mud pulse telemetry signal encounters many challenges, such as signal attenuation, surface and drilling noise, signal reflection inside the pipe system, in addition to the maximum downhole signal strength. These factors limit the telemetry transmission rates. In most cases, prediction or adjusting of those factors is not possible. Furthermore, their properties can change during the transmission process. A highly flexible telemetry system had to be developed in order to transmit the downhole data at maximum possible rates under those limiting boundary conditions. Adaption of the downhole and surface operating settings had to be achievable during the drilling process. Taking into consideration all the last mentioned challenges, in 2001 Baker Huges INTEQ developed a novel mud pulse telemetry system, known as oscillating shear valve pulser (Klotz[a] et al., 2008). The shear valve pulser was used in deep water off Norway (at operation depths up to 6,706 m) by Norsk Hydro ASA in 2006. In 2007, the shear valve system was used off Brazil by Petrobars (Wassermann et al., 2008). In addition to the North Sea and South America, the new system was successfully run in field-trials in the United States and the Middle East (Klotz[b] et al., 2008).

The Oscillating shear valve was the newest mud pulse telemetry system. The developments are not related only to the downhole unit, such as using a precise motor controller, but also to the surface unit. The developed telemetry system uses a new surface data acquisition unit with sophisticated signal processing algorithms to maximize the data rates. The surface unit utilizes two pressure transducers, one at the standpipe and the other at a certain distance on the same line. By using two pressure sensors instead of just one, a diversity of signal processing algorithms can be applied in order to clean the telemetry signal of noise signals coming from surface equipment such as pressure fluctuations caused by mud pumps. In order to perform digital signal processing, the two measured pressure signals must be converted from analog into digital format. For this purpose, the two signals are passed through a data acquisition system. Pump noise cancellation, diversity processing and band filtering are executed in the data acquisition and signal processing unit in order to achieve a maximum Signal-to-Noise Ratio (SNR). Inter-Symbol Interferences caused by reflections of the telemetry signal on the pulsation dampener and diameter changes in the surface pipe system can be reduced by applying an

equalization filter (Klotz[a] et al., 2008). According to Emmerich[c] et al., 2016, developing and introducing the oscillating high-speed shear valve pulser to the drilling operation, 10 years ago, can be considered as the start of the next age of mud pulse telemetry, known as High-Speed Mud Pulse Telemetry (HSMPT). Due to the introduction of the new drilling optimization, new MWD and LWD tools, reliable high data rates were more challenging. This was an important reason to improve the reliability of HSMPT to cover the market demands. Increasing the reliability can be achieved by improving the surface signal processing algorithms and the decoding quality. For this purpose, an initial calibration for the algorithms must be executed. Due to the changes in drilling conditions and environment, the transmission channel will be dynamically changed. Therefore, the calibration must be updated during the drilling process. For the calibration a special transmitting control sequence, known as training sequence (TS), is sent by the oscillating shear valve. The TS is detected by the surface controls to be used after that for automatically calibrating adjustable filters at the receiver. Because of many reasons such as high signal attenuation in very deep wells and signal distortion, detecting of TS becomes more challenging. In order to increase the reliability in TS detection and, consequently, the reliability of the HSMPT, Baker Hughes has improved the detection method by using an adjusted training sequence and applying new noise reduction algorithms. The improved system is used in more than 300 field runs in deep boreholes up to 8,000 m and it has achieved a success rate of 100% in decoding (Emmerich[c] et al., 2016).

However, developing the oscillating shear valve and its use as high speed mud pulse telemetry do not mean that the other types of mud pulsers are not used anymore. In the meantime innovative improvements are applied to the other pulser types in order to increase their capability to be used in ultra-deep drilling operations. For instance, Schlumberger has further improved its mud siren system to be used with a high data rate in an ultra-deep environment, more than 15 Km. Enhancements are integrated into the software and hardware of the telemetry system leading to duplicate the data transmission rate. A key element was the use of advanced modulation techniques such as quadrature phase shift keying (QPSK). In comparison with discrete modulation techniques a higher

data transmission rate can be achieved by applying QPSK, because multiple bits can be transmitted on a single pressure symbol, see Figure 4.1 (Caruzo et al., 2012). Schlumberger claimed in a new patent that three digital bits in each symbol can be transmitted by using eight phase shift keying (8-PSK). Such a modulation requires a smooth phase transition between successive symbols (Reyes et al., 2010).

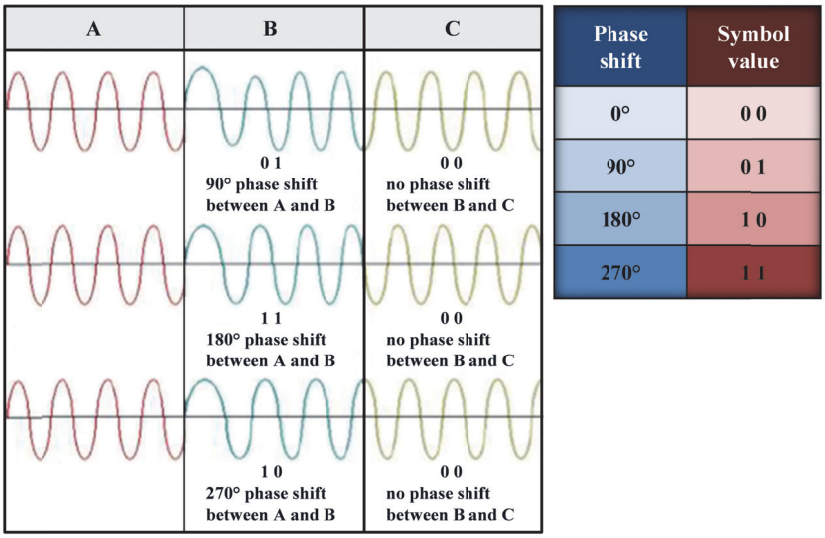

Figure 4.1: Used QPSK for higher data transmission rate (redrawn and modified), (Caruzo et al., 2012)

Another key element for developing the mud siren system was the application of new compression schemes leading to increase the system transmission speed up to seven times. A time based message is encoded by downhole compression algorithm, so that the bit stream is represented through pre-defined words. After transmitting the words to the surface a compatible de-compression algorithm is used in order to decode them and represent the real time data. An essential pre-work to the operation is the risk managed planning stage. Schlumberger uses its own signal prediction software whereby quantification of signal attenuation for particular drilling conditions can be pre-defended and, accordingly, the best suitable bandwidth can be selected to be used for transmitting the data. The developed mud siren system can thus transmit data with rates up to 26 bit/s over a distance of 12,300 m (Caruzo et al., 2012). Halliburton in turn has introduced an improved negative mud pulser system. Physical hardware and software improvements were undertaken in order to increase the date rate achieved by the new mud pulser system. For encoding the generated negative pressure pulses, differential pulse position

modulation (DPPM) is used. Utilizing DPPM does not require maintaining the synchronization between downhole and surface. In addition, it can be used more effectively with error-correction techniques (Cooper and Santos, 2015). Moreover, Halliburton described in a new patent another encoding technique for discrete pressure pulses. In this patent it is claimed, that combination of pulse position modulation (PPM) and pulse width modulation (PWM) can be used for increasing the data transmission rates (Shearer, 2013). In many patents it was claimed that the data rate can be increased by utilizing a plurality of rotors and stators (Chin, 1996; Chin and Ritter, 1998; Lehr, 2005 and Hutin et al., 2010). However, based on the research review efforts done during this work it can be said that there are no real investigation results or field applications to date.

4.2 Available types of mud pulse telemetry devices

The downhole measured variables (data) are translated into a binary code of ones and zeros, and then they are transmitted to the surface as packet of bits which is known as a telemetry data frame. The bits are transmitted over fixed time intervals, called time slots, and all the time slots have the same width, see Figure 4.2. Several encoded measured variables, for instance inclination, tool face orientation, azimuth, gamma ray, resistivity, downhole torque, downhole weight on bit (WOB), etc., are transmitted in a one data frame. The measured data is transmitted in a fixed sequence, one by one, to the surface.

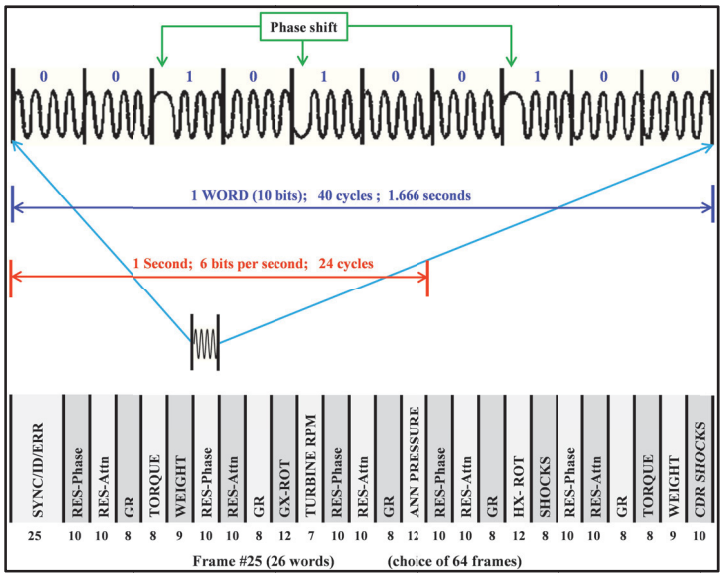

Figure 4.2: An example of telemetry data frame (redrawn and modified), (Martin et al., 1994)

In addition to encoded variables, a telemetry frame contains synchronization or control bits in order to detect and correct transmission errors. Figure 4.2 shows an example of a telemetry data frame consisting of 26 words (25 variables plus synchronization). Moreover, it shows that the variable (resistivity) is represented with a word consisting of 10 bits and was transmitted be means of a mud siren using phase shift keying modulation (Martin et al., 1994). For transmitting the data frames, mud pulse telemetry uses one type of four available devices: negative pulser, positive pulser, mud siren or oscillating shear valve.

4.2.1 Negative pulser

Negative pulser is used in order to generate discrete pressure reductions within the drilling mud in the drill string to carry encoded binary information to the surface. For this purpose, a dump valve is deployed in order to vent a certain amount of drilling mud from inside the drill string to the annulus, creating a pressure drop inside the drill string. As the valve is closed, the pressure inside the drill string will go back to its original level. Opening and closing the venting valve according to a certain modulation technique will generate encoded pressure variations in the drilling mud which propagate as negative pulses via the drilling mud inside the drill string towards the surface, as shown in Figure 4.3. For instance, a binary one can be represented by reduced pressure (negative pulse) while the original pressure level can represent a binary zero (Hutin et al., 2001).

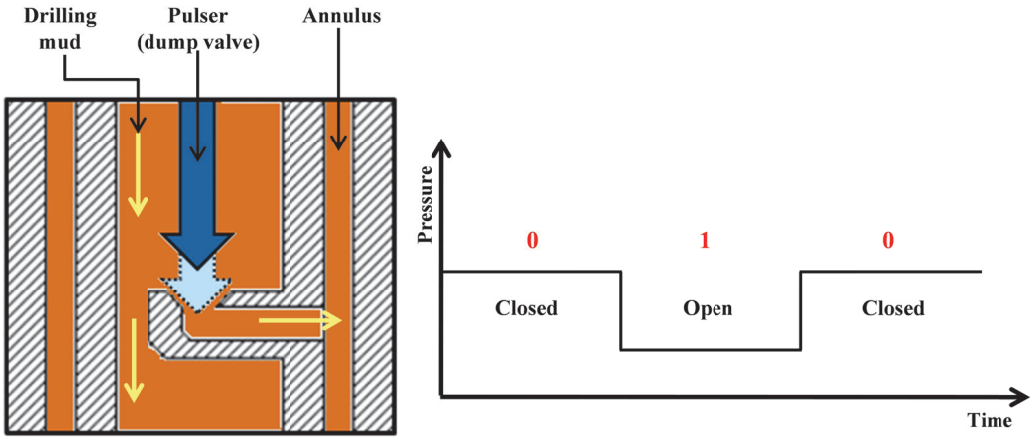

Figure 4.3: Negative pulser for generating discrete pressure variations within the drill string carrying encoded binary information (redrawn and modified), (Caruzo et al., 2012)

4.2.2 Positive pulser

In contrast to negative pulser, positive pulser uses a valve in order to partially restrict the cross-sectional area of the mud flow inside the drill string, leading to a pressure increase inside the drill string ahead the pulser valve. Once the pulser valve goes back, the cross-sectional area will be opened again and the pressure returns back to its original level. Thus, discrete pressure variations can be generated to be used for transmitting encoded data to the surface, see Figure 4.4. A binary one can be represented by the presence of a positive pulse, while its absence can represent a binary zero (Hutin et al., 2001).

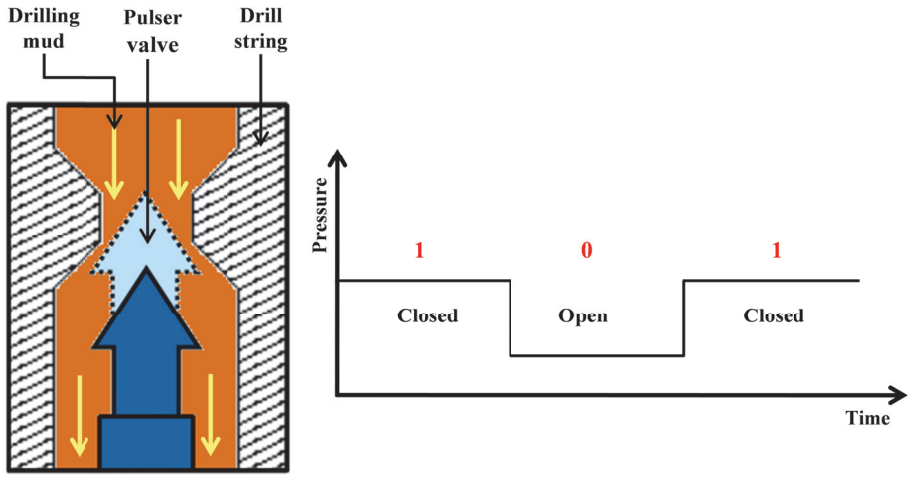

Figure 4.4: Positive pulser for generating discrete pressure variations within the drill string carrying encoded binary information (redrawn and modified), (Caruzo et al., 2012)

4.2.3 Mud siren

A mud siren is used to generate a continuous pressure wave which travels up hole via the drilling mud inside the drill string to the surface. The two main elements of the mud siren are a slotted stator and a slotted rotor disc. The rotor can be rotated against the stator making continuous changing in the open flow area, and accordingly generating continuous pressure waves which travel up the mud channel with a specific frequency, see Figure 4.5. The frequency of the generated pressure waves is dependent on the number of the lobes in the used stator/rotor arrangement as well as on the rotational speed of the rotor disc (Caruzo et al., 2012). In order to represent the binary ones and zeroes many code modulation can be applied. For instance, the resistivity value in the example

presented in Figure 4.2 was transmitted with a mud siren and modulated using phase shift keying, where the binary one was represented by phase shifting.

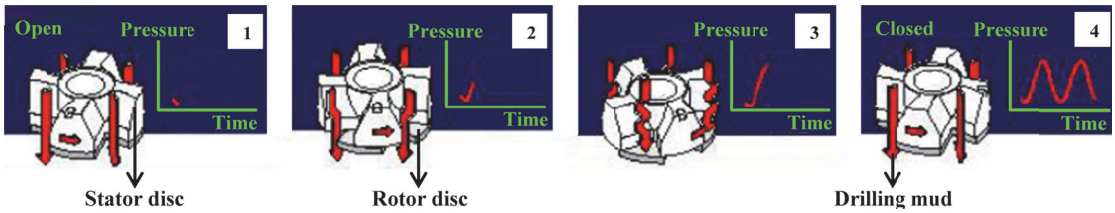

Figure 4.5: Mud siren pulser for generating continuous pressure waves (redrawn and modified), (Caruzo et al., 2012)

4.2.4 Oscillating shear valve

The oscillating shear valve pulser uses a slotted stator and a slotted rotor disc. Instead of rotation, the rotor disc is oscillated around its middle position into the flow area and out creating pressure fluctuations that travel up the mud channel with a specific carrier frequency (Klotz[a] et al., 2008), see Figure 4.6.

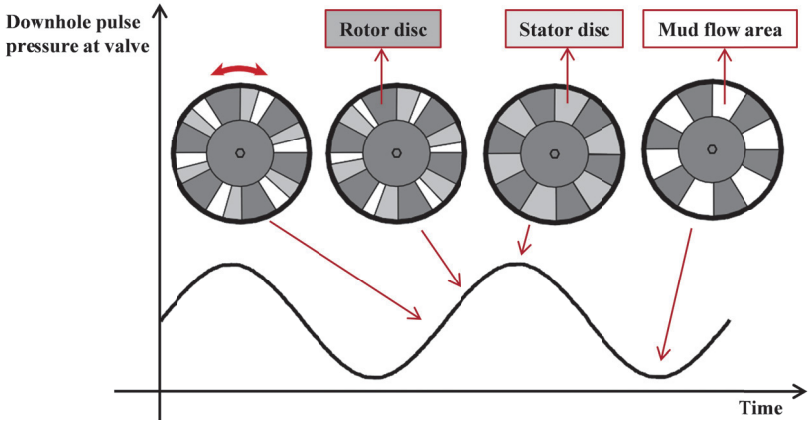

Figure 4.6: Oscillating shear valve for generating discrete or continuous pressure waves (redrawn and modified), (Klotz[a] et al., 2008)

Positive and negative pulsers transmit the data in baseband while the mud siren is used for data transmission in passband. Oscillating shear valve can be adapted to be used for baseband or passband transmission according to the variable drilling conditions. Oscillating shear valve is driven by a precise motor controller and can generate discrete pressure pulses or continuous pressure waves (Wassermann et al., 2008). For data transmission in baseband, the rotor disc is oscillated at a low speed, while oscillating the

disc with a higher frequency will generate passband pressure signals. A further advantage of the oscillating shear valve is its increased tolerance against lost circulation material (LCM). The angle of the oscillating rotor can be adjusted by means of downlinking or prior programming of the tool. The angle can be reduced in order to increase the flow area enabling LCM materials to pass through the downhole BHA (Klotz[b] et al., 2008).

4.3 Limitations of data transmission via mud pulse telemetry

The drilling mud inside the drill pipe is used as a channel for transmitting MWD/LWD data. Mud sirens or mud pulsers are used as a transmitter. They transmit the data by means of pressure waves or pulses. Pressure waves are created by transforming the kinetic energy of the mud siren (or pulser) into potential energy (into pressure in this case). The created pressure wave travels in the mud channel towards the surface at the speed of sound in the mud, which ranges from 1,000 to 1,600 m/s depending on the mud properties (Martin et al., 1994). It should be taken into the consideration that the drilling mud inside the drill string is a very complex transmission channel. Several parameters affect the telemetry pressure wave during its propagation via the mud channel. Beside the effect of the transmission channel, the data transmission via mud pulse telemetry is limited to a minimum transmission time slot, at which the transmitted information bits can be successfully detected and decoded at the surface unit.

4.3.1 Effect of noise sources in the mud channel on the transmission signal

Due to the very complex drilling dynamics in the borehole, there are several sources of noise that affect the telemetry pressure wave in the mud channel. Mud pumps are one of the loudest sources of hydraulic noise encountered by the telemetry pressure waves. Operating the mud pumps at specific stroke rates causes a harmonic movement of the pump pistons. Due to this harmonic pistons movement, pressure variations are induced and travel downward in the mud channel (Hutin[a] et al., 2001). By means of a pressure sensor mounted at the top of the drill string, also very close to the pumps, the pressure inside the drill string is measured (Reich, 2012). Thus, the measured pressure signal contains the pressure waves created downhole by the MWD telemetry system and the pressure noise coming from the surface pumps. The telemetry pressure wave must travel

for many kilometers from the bottom of the borehole towards the surface before it can reach the pressure sensor, whereas the mud pumps are much close to the pressure sensor. Thus, the pump noise has a higher energy than the telemetry pressure wave, and therefore it can be considered as dominant in the measured pressure signal. This makes the detection of the received pressure pulses very difficult, especially when the telemetry pulser is operated at the same frequency of the pump pistons. For instance, Figure 4.7 shows the frequency spectrum of a single action triplex mud pump with its dominant frequencies. In order to increase the reliability of the pressure pulses detection at the surface, the MWD telemetry system must transmit its signal within frequency bands, where the noise amplitudes (amplitudes of mud pumps harmonic frequencies) are very low. Thus, mud pulse telemetry can be operated to transmit its signal in the frequency band above the dominant frequency components of the mud pump noise. In the signal example shown in Figure 4.7, the mud pulse telemetry is operated at a carrier frequency of 12 Hz. Mud pulse telemetry signal can also be transmitted in the frequency band below the dominant pump noise frequencies. In this frequency range other noise sources, known as drilling noise, must be taken into consideration.

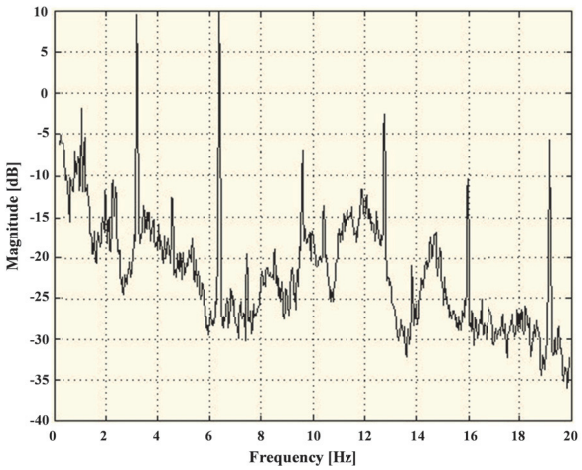

Figure 4.7: Frequency spectrum of the hydraulic noise coming from mud pumps (redrawn), (Hutin[a] et al., 2001)

Such sources include, for example, the mechanical interaction of the drill bit with the formation and the drill string with the borehole walls, mud motor stalling and stick/slip phenomena. The amplitudes of the drilling noise in the frequency domain of the measured pressure signal drilling noise can be very large, whereas their frequencies are

very low, lower than 0.5 Hz (Hutin[a] et al., 2001). Since discrete mud pulsers (positive and negative pulsers) are operated at low frequencies (1 Hz), their transmitted signals measured at the surface will be strongly affected by the mud pumps noise and drilling noise. In contrast, the transmission frequencies used by mud sirens or shear valves can be flexibly shifted to be out of the noise frequency range, for example between 10 and 20 Hz (Martin et al., 1994).

4.3.2 Effect of attenuation in the mud channel on the transmission signal

Attenuation is the biggest challenge facing the transmission signal during its propagation through the mud channel (Caruzo et al., 2012). The maximum transmission reach of the pressure signal is strongly affected by its attenuation within the mud channel (Gravley, 1983). The main contributors to the signal attenuation are high plastic viscosity mud, small channel diameters and the carrier frequency of the signal itself. The smaller the channel diameter, the grater the carrier frequency of the transmission signal and the greater the mud viscosity, the greater the signal attenuation will be. Figure 4.8 shows the attenuation of a signal transmitted at a carrier frequency of 12 Hz (left) and of 1 Hz (right) by different mud density cases. At a constant mud density for both transmission carrier frequencies it can be seen, that the signal attenuation at higher frequency (12 Hz) is greater than at lower frequency (1 Hz). For a reliable transmission, telemetry system must therefore be operated at low frequencies (Caruzo et al., 2012). However, transmitting the data at low frequencies will limit the achievable data rate.

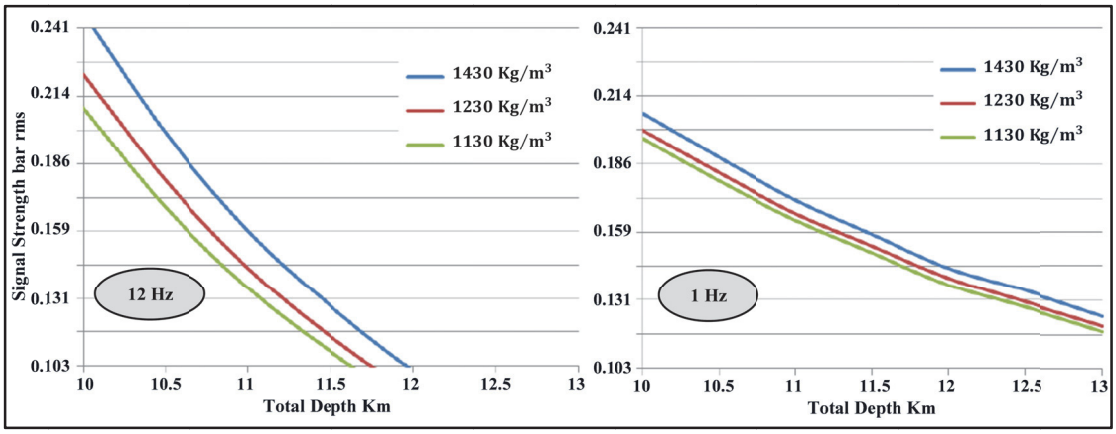

Figure 4.8: Attenuation of signal transmitted at carrier frequency of 12 Hz (left) and 1 Hz (right), (redrawn and modified), (Caruzo et al., 2012)

4.3.3 Effect of reflections and their interference with the main transmission signal

A drill string consists of different types of drill string elements, including drill pipes, heavy weight drill pipes and drill collars. Thus, the cross sectional area for the flow in the drill pipe will change frequently, each change of the cross sectional area generating a reflection of the main propagated wave as shown in the left part of Figure 4.9. In addition to the change in pipe cross-sectional area, there are other acoustic reflectors such as mud pumps, pulsation dampeners (desurgers), rotary hose, swivel and drill bit. The reflections of a main wave, coming from pulsation dampeners, bottom hole assembly and from the change in cross sectional area in the drill string, are called echoes.

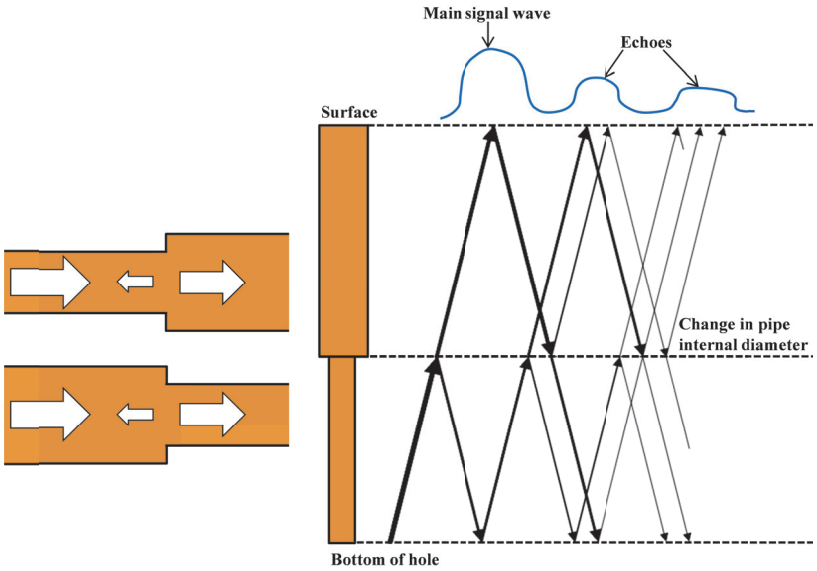

Figure 4.9: The change in cross sectional area as a reflector (left), main signal wave and its reflections coming from the change in cross sectional area of the drill string (right), (redrawn and modified), (Hutin[a] et al., 2001)

For instance, the right part of the Figure 4.9 shows a main signal wave and its echoes received at the surface, the echoes arrive at the surface with a time delay related to the main wave. It means the echoes from a previous pressure pulse or wave will interfere with the subsequent pressure pulses increasing the difficulty of correct detection of such pressure pulses. Additional issue, represented in overlapping, must be taken into consideration. The drilling mud channel will contain the main wave generated by the MWD system plus all of its reflections which will overlap with each other at certain locations. When the generated wave and its reflections have the same or similar phase, then constructive overlapping will occur, otherwise it is destructive (Hutina et al., 2001).

Figure 4.10 shows an illustration of the resulting overlapping wave inside a pipe in both destructive and constructive cases.

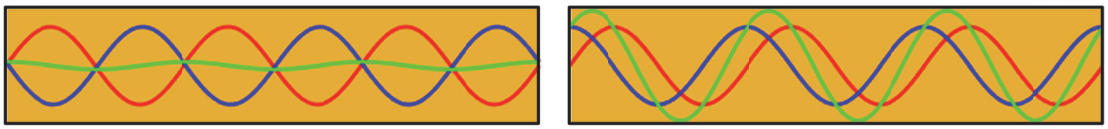

Figure 4.10: Illustration of destructive (left) and constructive overlapping (right) of a main pressure wave and its reflection inside a pipe. The red one is the main wave while the blue one is the reflected wave and the overlapping wave is in green.

4.3.4 Pass and stop bands

Due to the effects of reflections, overlapping and attenuation, the transmission channel shows passbands, where the signal amplitudes at the receiver are large enough to be recognized and used for data transmission, and stopbands, where the signal amplitudes at the receiver are too small and unsuitable to be used for data transmission. This will reduce the capacity of the transmission channel, since data transmission should be executed just in the passbands, where transmission frequencies have large amplitudes. Moreover, the characteristics of the pass and stop bands vary with each change in the drill string configuration. The induced pressure waves may be significantly changed during their propagation from the bottom of the hole to the surface. In the worst case, due to the strong hydraulic noise, the signal cannot, or at least not easily be identified at surface without special data or signal processing (Berro[a] and Reich, 2015).

4.4.5 Minimum transmission time slot

Physically, the frequency (F [Hz]) can be identified by its number of cycles in one second or by the duration required to complete one cycle:

$$F\ [Hz] = Number\ of\ cycles\ in\ one\ second = \frac{1}{Cycle\ duration\ [s]} \qquad (8)$$

The shorter the used time slot, the higher the data transmission rate. Taking the Equation (8) into consideration, the theoretical shortest time slot for transmitting the data at a certain carrier frequency could be equal to the duration of one complete cycle. For instance, by transmission at a carrier frequency of 24 Hz the shortest possible

transmission time slot could be 0.0417 s (duration of one cycle). However, the used transmission time slot in practice is wider than the theoretical slot. The transmission example presented in Figure 4.2 was executed using a carrier frequency of 24 Hz and the used time slot was 0.167 s which is four times greater than the duration of one cycle. Another transmission example executed using the oscillating shear valve is given by Wassermann et al., 2008, see Figure 4.11. The data was transmitted at 30 Hz as a carrier frequency using a transmission time slot of 0.1 s which is three times wider than the shortest possible time slot in this case (0.033 s).

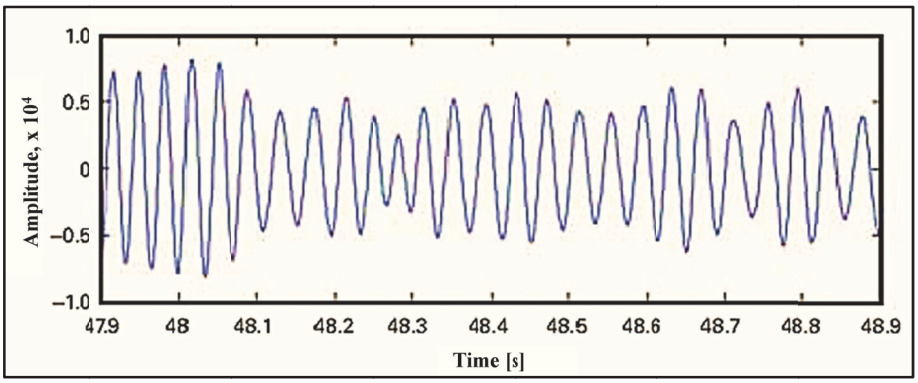

Figure 4.11: An example of data transmission using oscillating shear valve at a carrier frequency of 30 Hz and time slot of 0.1 s (redrawn), (Wassermann et al., 2008)

These two transmission examples from practice show that the transmission time slot could not be shortened to the smallest possible width without any limitation. Shortening the time slot can make signal detection and decoding at the surface more difficult. This is because the transmission signal encounters attenuation during its long propagation way from the downhole to the surface. In addition, the signal receiver (pressure sensor) is located at the upper end of the drill string very close to the mud pumps. Here, the hydraulic noise is the most intensive and the quality of the transmission signal coming from downhole is the lowest (Reich et al, 2012). Therefore, mud pulse telemetry is not operated at the smallest possible time slot. But it should be operated at a time slot, at which pressure pulses can be detected and decoded at the surface.

CHAPTER 5 Novel Concepts and Tools for Increased Data Transmission Rates of Mud Pulse Telemetry

This chapter presents the concepts developed and to be investigated within the frame of the present research work. In the case of transmitting by means of mud pulse telemetry there are only two representable symbols available to be used for data transmission, and in each symbol just one bit to be transmitted, as shown in Table 5.1 and Table 5.2.

Table 5.1: Representable symbols by transmitting in baseband

Transmitting in baseband using positive pulser or negative pulser				
Positive pulser	Symbol		Negative pulser	Symbol
Valve open	0		Valve closed	0
Valve restricted	1		Valve open	1

Table 5.2: Representable symbols by transmitting in passband

Transmitting in passband using mud siren or oscillating shear valve							
ASK	Symbol		PSK	Symbol		FSK	Symbol
Frequency off	0		Without phase shifting	0		Frequency 1 on	0
Frequency on	1		With phase shifting	1		Frequency 2 on	1

Depending on the Equation (2) the data rate can be raised by increasing the symbol rate or the number of the representable symbols or both of them. The symbol rate can be increased by shortening the symbol duration, known also in hydraulic transmission as “time slot”. However, shortening the time slot can make signal detection and decoding at the surface more difficult. Service engineers already operate mud pulse telemetry at the smallest time slot at which pressure pulses can be detected and decoded at the surface. Thus, the other option for increasing the data rate is the increasing of the number of the representable symbols. This will lead to an automatical increase in the number of bits transmitted via each symbol. Within the scope of the present work three concepts are developed and investigated for speeding up the data rate by increasing the number of the

representable symbols. These are parallel transmission in baseband and in passband, multi-frequency mud siren (or multi-frequency generator). However, development and investigation works are related not only to the transmitter end but also to the receiver end. Developments and improvements must be made on the receiver end to keep up with the new capacity of the developed transmitter, especially the high ability to detect different simultaneous frequencies. On the other side, increasing the date rate of hydraulic data transmission system could be achieved by increasing the potential of successful signal detection depending on the variable receiver position. Thus, the works undertaken on receiver end include investigation of the detection of a multi-frequency signal with Wavelet algorithms, investigation into the effect of the receiver position on the measured signal and investigation into the effect of different wave forms on the transmission quality.

5.1 Transmitter end

5.1.1 Hybrid mud pulse telemetry (HMPT)

The mud pulse telemetry uses the drilling mud inside the drilling string as a channel for transmitting the downhole date to the surface. To date, the conventional mud pulse telemetry transmits the downhole data either in baseband using pressure pulser (positive or negative) or in passband using rotating or oscillating mud siren, see Figure 5.1 (left part). Physically, there is only one transmitting channel available to be used, which is the drilling mud. But from a technical side, the transmitting channel can be used twice, where the date can be transmitted in base- and passband at the same time. Parallel transmitting in base- and passband can enable a more effective use of the only one available transmitting channel. This is the main idea of the developed concept hybrid mud pulse telemetry (HMPT). HMPT uses mud siren in a combination with a pressure pulser to transmit the downhole date parallel in base- and passband, see Figure 5.1 (right part).

An increase in the data transmission rate is expected using HMPT. The question is how much could be the data rate increased with this new telemetry compared to the transmission rate achieved by the conventional mud pulse telemetry.

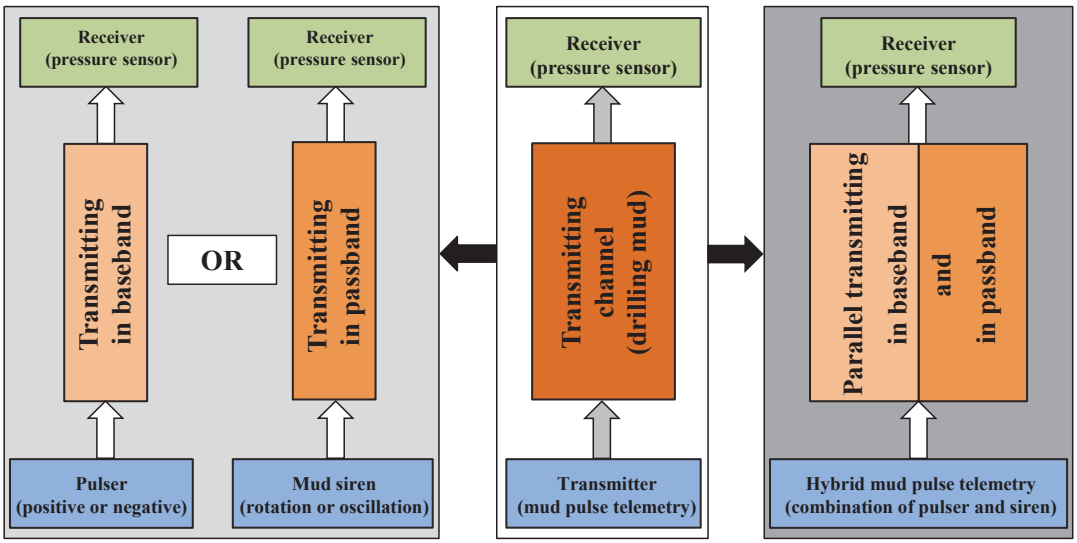

Figure 5.1: Transmitting either in baseband or in passband by conventional mud pulse telemetry (links), parallel transmitting in base- and passband using hybrid mud pulse telemetry HMPT (right)

The data transmission rate could be duplicated, if the pressure pulser and mud siren are operated in practice using the same transmission time slot. In this case two bits, one bit via the siren and one bit via the pulser, could to be transmitted in each time slot. However, the mud siren and pressure pulser do not work at the same time slot in the practice. The mud siren has a higher transmission speed than the pressure pulser, because it works at a time slot smaller than that used by pressure pulser. As shown in the transmission examples presented in Figure 4.11, the mud siren can transmit the data at a smaller time slot (0.167 - 0.1 s). The pressure pulser works at a time slot which is relative larger than 0.1 s. Depending on the experience of the scientific researchers of the Institute of Drilling Engineering and Fluid Mining, which is gained thorough different cooperation projects with oil and gas companies, a time slot of up 0.5 s is used by the pressure pulser. This must be taken into the consideration by developing the concept of HMPT. In order to make the hybrid mud pulse telemetry (HMPT) implementable in the practice, it must work at two different time slots. Each component of the HMPT system (mud siren and pressure pulser) must work at its own workable transmission time slot. By using HMPT, two individual (different) information signals can be transmitted at the same time, one via the mud siren and the other one via the pressure pulser. The approach of the hybrid mud pulse telemetry (HMPT) is widely investigated during this work and the results are presented and discussed in Chapter 7.

5.1.2 Multi-frequency generator

For utilizing the available bandwidth more effectively, multi-carrier transmission methods have been used in the field of electromagnetic data transmission, whereby several carrier frequencies are simultaneously used. The used conventional mud siren is similar to a trumpet player and can induce only a single frequency at any time. This frequency occupies only a small part of the available bandwidth (frequency spectrum), although on the receiver end capacities would be available for the reception of an entire orchestra.

Based on the multi-carrier transmission method, a second approach for increasing the data rate of the hydraulic transmission system is developed. Here, a multi-frequency mud siren was developed to be used as a multi-frequency generator for hydraulic transmission. It can generate several frequencies at once compared to a conventional mud siren. In such a way, several bits, depending on the number of the different frequencies generated, can be transmitted simultaneously. For example, Table 5.3 demonstrates this effect of a mud siren with three individually adjustable frequencies. It is evident that in this case, three bits per time slot (also per symbol) could be transmitted simultaneously.

Table 5.3: Transmission options by a multi-frequency siren with three frequencies

First frequency	Second frequency	Third frequency	Symbol
off	off	off	0 0 0
off	off	on	0 0 1
off	on	off	0 1 0
off	on	on	0 1 1
on	off	off	1 0 0
on	off	on	1 0 1
on	on	off	1 1 0
on	on	on	1 1 1

Two concepts for multi-frequency mud siren were developed. These are row connection of two mud sirens and parallel connection of two mud sirens within the drill string. The

two concepts have been intensively investigated through mathematical and numerical models. The developed models and the results will be represented in Chapter 8.

The investigations described in Chapter 8 show that the generation of several frequencies based on the multi-frequency siren concept is very difficult. For instance, interference frequencies are generated and they considerably complicate the data transmission. On the other side, multi-frequency transmission seems to be a very promising concept to increase the hydraulic data transmission rates. Therefore, a basic research is required in order to investigate the whole process of multi-frequency transmission with its potential to be used in hydraulic data transmission. Such a basic research includes the investigation of multi-carrier signal generation and its propagation in the pipe system as well as its receiving at the receiver side. In order to study the behavior of several frequencies travelling simultaneously through the drill string, an experimental multi-frequency generator using a unique setup of special loudspeakers was designed and built (Chapter 9). The speaker assembly works like a conventional loudspeaker, allowing the user to create several clear frequencies at the same time. The speaker unit allows a much easier generation of independent frequencies than the multi-frequency siren, thus providing an ideal environment for initial basic research. The use of such a multi-frequency generator makes it possible to investigate and evaluate the application of new multi-frequency transmission techniques such as the chirp spread spectrum in the hydraulic data transmission area, see Chapter 9.

Moreover, using the developed experimental multi-frequency generator different wave forms (sinus, rectangular, saw etc.) can be generated. Within the frame of the improvement work, it will be investigated if the measured pressure signal at a certain wave form has a better quality or amplitude in comparison with other wave forms. Furthermore, the developed experimental multi-frequency generator has enabled performing data transmission tests using one of the latest radio technologies, chirp modulation or chirp spread spectrum (CSS). The CSS allows transmitting the data with a high robustness against noise and interferences coming from the transmission environment. The investigation results are represented in Chapter 9.

5.2 Receiver end

5.2.1 Investigation of the Wavelet analysis suitability for multi-frequency signal detection

To date the receiving unit has to deal with a single frequency signal. During this work, concepts for generating multi-frequency signals are to be developed and tested. Consequently, the receiving unit must be able to detect and identify such signals generated by multi-frequency siren or generator. It is expected that the Wavelet analysis could be a suitable method to be used for signal processing at the receiver end. During a previous research work at the IBF, a novel method for extracting and detecting the transmitted signals at the receiver end of the flow loop was developed. The new method is based on the Wavelet algorithm. The Wavelet analysis is recognized through its ability to extract weak signals coming from the downhole mud siren from the dominant noise in the standpipe. Moreover, it enables the identification of the used carrier frequency, its period and its discontinuity positions in the signal.

For instance, a synthetic time signal containing four carrier frequencies (11, 17, 35 and 67 Hz) is created. As shown in Figure 5.2, the four carrier frequencies are switched on and off independently from each other. In its upper part Figure 5.3 shows the created signal in time domain. The corresponding Wavelet analysis in the lower part clearly shows the different frequencies as colored bands. On the time axis on the bottom of the chart the start and the end point as well as the duration of each individual frequency can clearly be assigned.

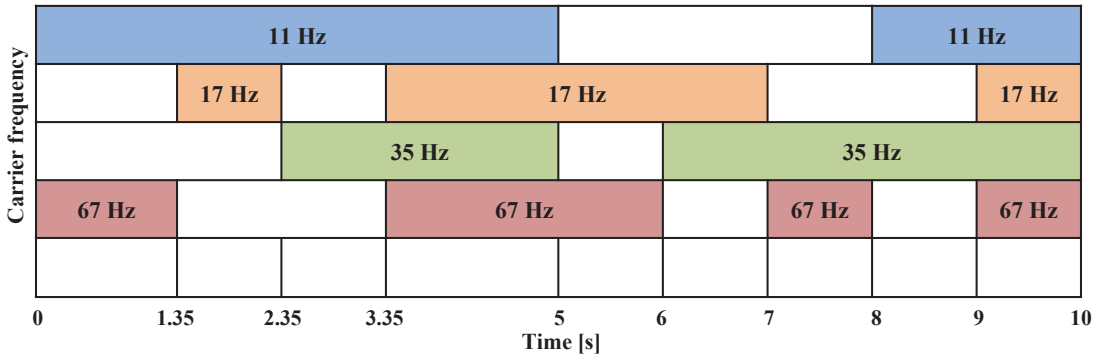

Figure 5.2: Creating a synthetic time signal containing four carrier frequencies with different time discontinuities

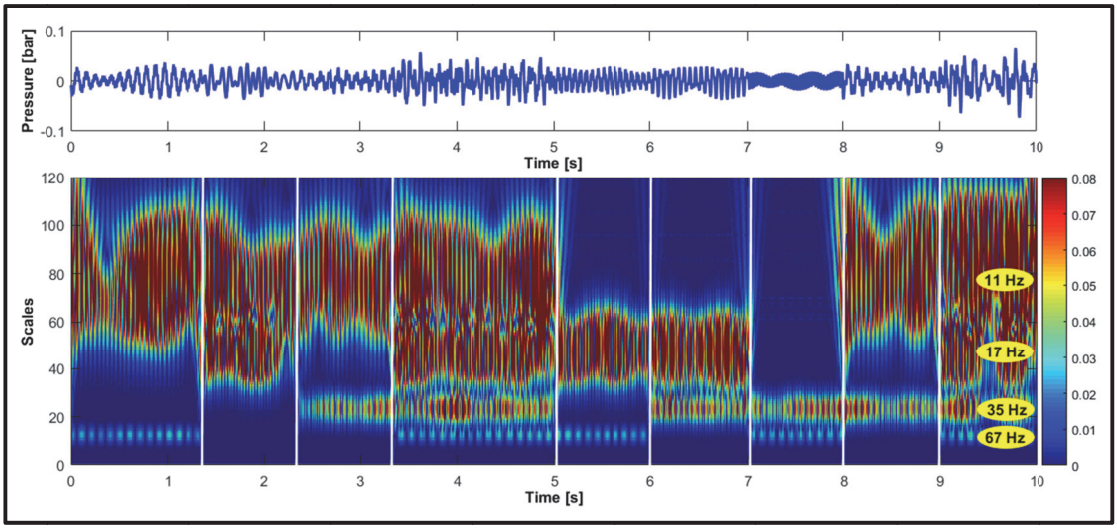

Figure 5.3: Application of the Wavelet analysis on a synthetic time signal containing four frequencies

However, the suitability of the Wavelet analysis for the identification of several frequencies in real measured signals will be investigated and evaluated during the present work. All the multi-frequency signals generated during this work are evaluated using The Wavelet analysis as shown in Chapter 9.

5.2.2 Flexible placement of multi-sensor receiver

The propagation of an acoustic wave inside a pipe with closed end (reflector) is described by Ehrenfried (2004). The pressure fluctuates between solid and dashed lines as shown in Figure 5.4. The wave shows different pressure amplitudes along its propagation way. At certain positions the pressure fluctuates are maximum, while they are minimum at other certain positions. The positions of the maximum and minimum pressure fluctuations are related to the length of the propagated wave. The term (WMP_y) will be used as an index for wave measuring position. To find out the positions, where the pressure fluctuations are maximum, the Equation (9) can be used:

$$WMP_y = y * \frac{\lambda}{4} \; ; \; where \; y = 1, 3, 5, 7, 9, \ldots. \tag{9}$$

The positions, where the pressure fluctuations are minimum, can be identified by using the Equation (10):

$$WMP_y = y * \frac{\lambda}{2} \; ; \; where \; y = 1, 2, 3, 4, 5, ... \qquad (10)$$

The positions, where the pressure fluctuates are minimum, are known as pressure nodes. While pressure antinodes refer to the positions of the maximum pressure fluctuations.

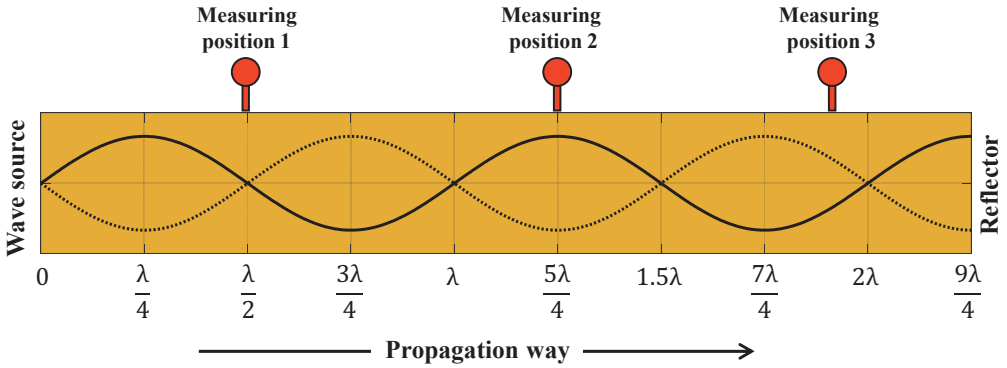

Figure 5.4: Pressure nodes and antinodes for a carrier wave propagated inside a pipe and the use of multiple measuring sensors

As mentioned in (4.4.4), the capacity of the transmission channel is reduced, since transmitting the data should be executed just in the passbands, where transmission frequencies have large amplitudes. The passband and thus the useful transmission frequencies are changing depending on the drill string dimensions, the specific mud parameters and the position of the receiver. At the same mud properties and drill string dimensions, the resulting pass- and stopbands at a certain time are related to the considered measuring position, also to the pressure sensor position.

To date, just one measuring sensor is used at the receiver end in the field. But as described above, the generated wave shows different pressure amplitudes, also pressure nodes and antinodes, along its propagation way inside the drill string towards the surface. The position, where the pressure sensor is located at the drill string, has therefore a great influence on the received signal. As shown in Figure 5.4, if the carrier wave is measured just at the measuring position 1, the carrier wave will be measured at its minimum pressure amplitude and the corresponding carrier frequency will be located in a stopband. Consequently, it cannot be used for transmitting the data. While measuring the same carrier wave at the same time at other locations, such as at the measuring positions 2 or 3,

will enable to record the carrier wave with a large amplitude or even with its maximum pressure amplitude. Accordingly, the same carrier frequency will not be located in a stopband but in a passband and can be used for transmitting the data at the same boundary conditions.

Therefore, further improvements in the detection of the carrier pressure signals can be achieved by using a receiver unit consisting of multiple measuring pressure sensors. The use of such multiple measuring sensors will help to overcome the transmission limitation of stopbands and improve the detection of pressure carrier waves at the surface. Consequently, the capacity of the transmission channel will be increased.

According to Garg (2007), the use of multiple receiver elements in a combination with one single or multiple transmitter elements is one of the smart wireless communication antenna techniques. The transmission case, where multiple receiver elements used in a combination with one transmitter element, is called SIMO (Single-Input, Multiple-Output). When multiple receiver elements and multiple transmitter elements are simultaneously used, the transmission case is called MIMO (Multiple-Input, Multiple-Output).

The effect of the pressure sensor position on the measured signal and the use of multiple measuring sensors will be investigated numerically and laboratively in the context of the present work. The both transmission cases, the use of multiple receiver elements with one single transmitter (SIMO) and the simultaneous use of multiple receiver and transmitter elements (MIMO) are investigated. The investigation results are represented in Chapter 10.

CHAPTER 6 Laboratory Test Facility and Used Hard and Soft Tools

6.1 Laboratory test facility for hydraulic data transmission in boreholes

In order to investigate the data transmission in boreholes, a test facility (flow loop) was built during a previous research work at the Institute of Drilling Engineering and Fluid Mining (IBF) of the TU Bergakademie Freiberg. The data transmission test facility can be considered as a unique device in the academic sector. The wellbore is represented by a 40 m long test pipe. The used pipes are made of PVC (Polyvinyl Chloride) and have a maximum operating pressure of 10 bars. At one end mud pulser modules (MPT unit) can be installed as transmitters, and at the other end a centrifugal pump connected to a 1 m^3 water tank is used to supply the water circulation in the pipeline with an adjustable flow rate. The maximum flow rate is 40 m^3/h. In addition, an actuator system is incorporated to generate an interfering noise signal with a defined frequency and amplitude, thus simulating real wellbore conditions. The main signal receiver (pressure sensor P1) is fixed close to the pump. To gain a better understanding of the pressure wave propagation behavior, three other sensors (P2, P3 and P4) are installed along the pipeline at specific distances between each other. The used pressure sensors have a measuring range between 0 and 6 bars. The measured signals are shown on a computer display inside a measuring cabin using a LabVIEW program. Here, the time signal and its frequency spectrum can be displayed in real time. The LabVIEW program enables recording of the measured signal and saving it on the computer desktop. In this way, the signal can be later processed in other programs such as MATLAB. With the existing test facility only one pulser module can be installed and operated, and the length of the usable experimental pulser is limited to 60 cm. Also the available LabVIEW program is able to operate and control the transmission test with only one pulser module. However, during the present research work a hybrid mud pulse telemetry must be tested, where two pulser modules, for example positive pulser and mud siren, must be installed and operated simultaneously. A multi-frequency generator should be developed and used to generate multi-frequency signals from different transmitting positions. Moreover, another research project is executed parallel to the present work with different concepts and, consequently,

with other modification requirements. Therefore, the pipeline is extended at the pulser module end so that the transmitter section is currently 4 m long, and up to four pressure pulser modules can be installed and used simultaneously. Figure 6.1 gives an overview of the extended test facility with its most important components.

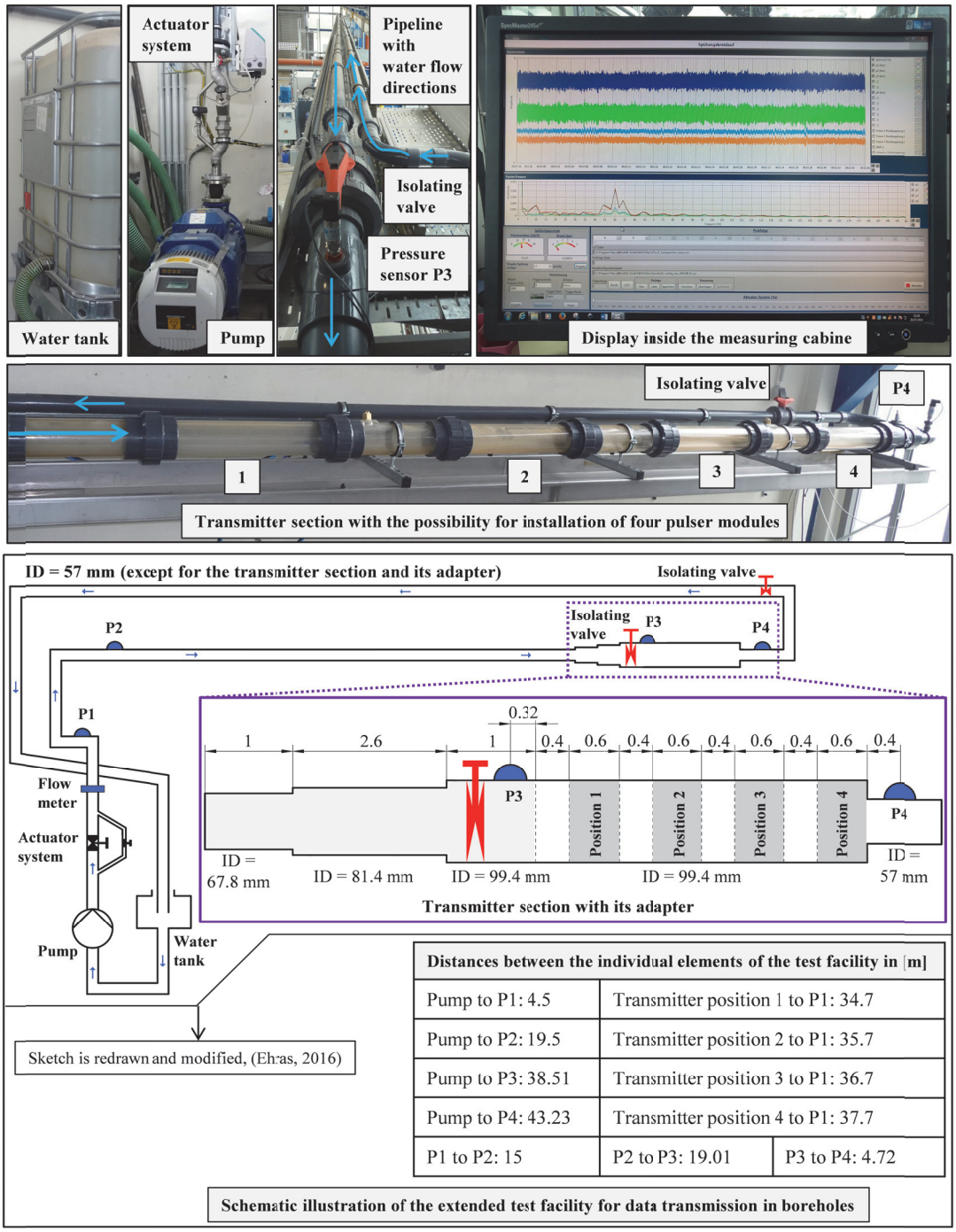

Distances between the individual elements of the test facility in [m]		
Pump to P1: 4.5	Transmitter position 1 to P1: 34.7	
Pump to P2: 19.5	Transmitter position 2 to P1: 35.7	
Pump to P3: 38.51	Transmitter position 3 to P1: 36.7	
Pump to P4: 43.23	Transmitter position 4 to P1: 37.7	
P1 to P2: 15	P2 to P3: 19.01	P3 to P4: 4.72

Schematic illustration of the extended test facility for data transmission in boreholes

Figure 6.1: Overview of the extended test facility with its most important components

The whole transmitter section is made of transparent plastic pipes, so that the interesting flow process during and shortly after the signal generation can be visually investigated. Furthermore, the length of the single pulser module to be used is any longer limited to 60 cm, but it can be longer as the construction designs demand. As the schematic illustration of the test facility (Figure 6.1) shows, two isolating valves are installed before and after the transmitter section. The two valves are used to isolate the transmitter section during integration or removal of a pulser reducing the amount of lost water.

The pipeline, except for the transmitter section, has an internal diameter of 57 mm. In contrast, the internal diameter of the transmitter section is 99.4 mm. For smooth water flow from pipeline into transmitter section as well as for smooth signal propagation from transmitter section into the pipeline an adapter was built between the pipeline and the transmitter section. The adapter, as shown in Figure 6.1, consists of three pipes with different lengths and internal diameters and has a total length of 4.6 m. The whole pipeline system of the test facility after extension, inclusive of the transmitter section and its adapter, has a total length of 90.5 m. According to the hardware changes and updates of the test facility, the operating software must be changed. Therefore, a new operating software using a LabVIEW software was programed and installed, whereby the transmission process with up to four pulser or transmitter modules can be set up and regulated at once.

The interface user guide (IUG) of the new software is shown in Figure 6.2. In the new software, the actuator system can be operated in a frequency range of 0 – 10 Hz and in steps of 0.2 Hz, while the operating frequency range in the old software was 0 – 5 Hz and in steps of 0.5 Hz. The induced pressure signals can be measured, displayed and saved with a high resolution, also with a sampling rate up to 5,000 Hz. With the new software, audio signals which are prepared prior to the test can be sent and recorded. The multi-frequency generator is used as a transmitter for such signals. Moreover, it is now possible to adjust the frequency, the phase, the offset, the wave form as well as the source amplitude of a single frequency signal prior to its generating by means of the multi-frequency generator.

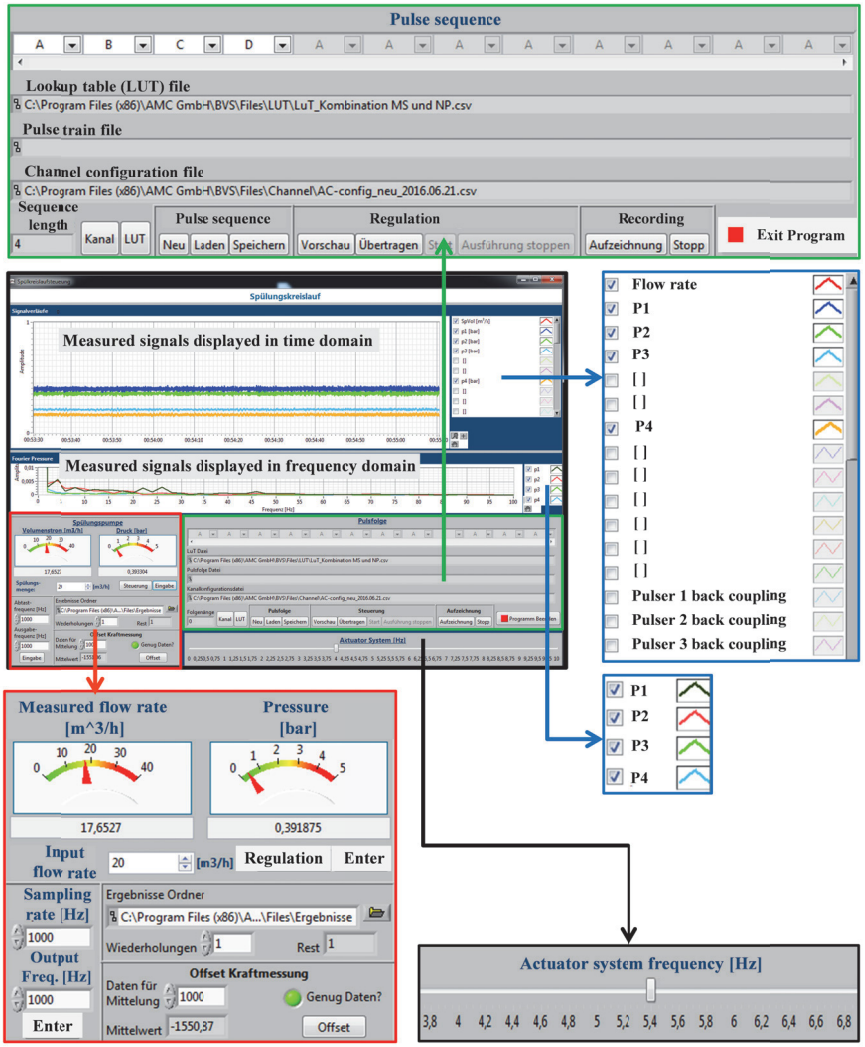

Figure 6.2: Interface user guide (IUG) of the new operating software

A new control box is built and works as a transition stage between the transmitting orders sent by the operating software and the transmitter section, as shown in Figure 6.3. The control box enables adjusting the single carrier frequency (in case of OOK) or the two carrier frequencies (in case of FSK) of the mud siren to be operated. The carrier frequencies of up to three mud sirens can be set simultaneously. In addition, the control box contains an audio amplifier for audio signals sent or generated via the multi-frequency generator. The audio amplifier can be adjusted in order to generate signals with certain source amplitudes. Each transmitter has a connection cable. Once a transmitter must be used and operated, its cable must be connected to the control box. Moreover, the control box has many keys or buttons in order to manually operate the transmitter, for

instance during executing practical works or lab experiments by the students of the institute.

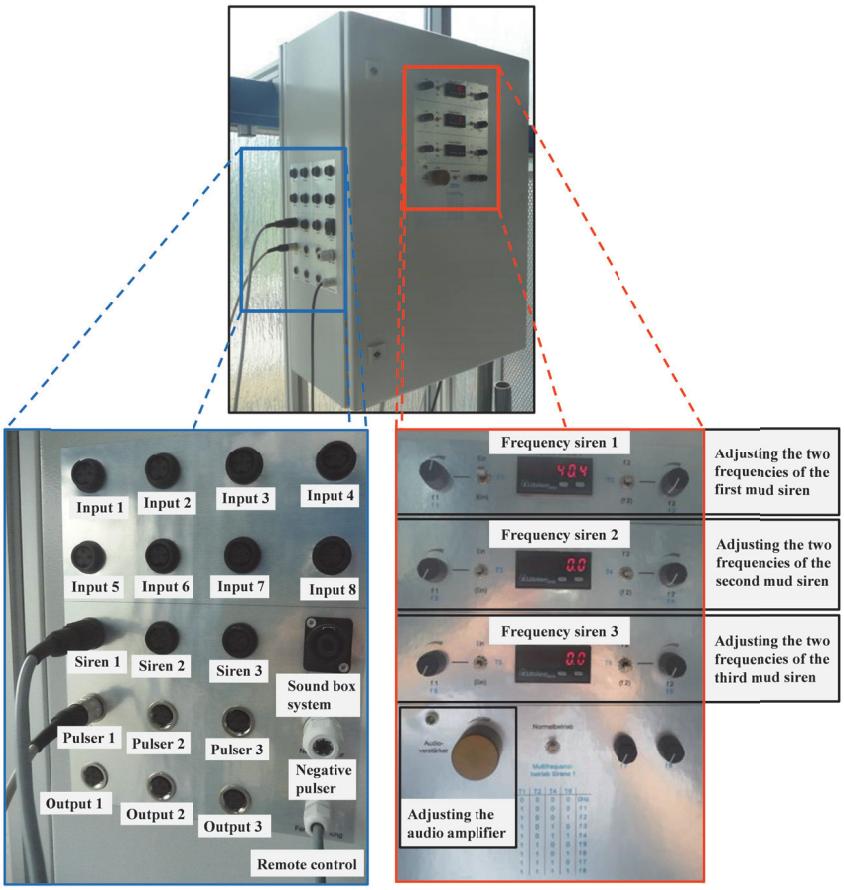

Figure 6.3: Control box

6.2 Experimental prototypes of the pressure pulsers and mud siren

The experimental prototypes of the positive pulser and mud siren were built together with the test facility during a previous research work at the institute. Each one of them has a length of 60 cm and is installed inside a double transparent pipe which has an ID of 93 mm. Both prototypes can be regulated and operated by hand via prompts or automatically via a computer. The positive pulser is composed of a double acting pneumatic cylinder with a continuous piston rod. The piston rod is actuated by air pressure and connected at one of its ends to the moving part of the pulser which has a diameter of 80 mm. Ahead of the moving part a transparent restriction ring with an ID of 81 mm is built as a part of the inner transparent pipe. The flow area can be partially restricted once the moving part is

moved into the restriction ring and again released when the moving part is moved back to its original position, see Figure 6.4.

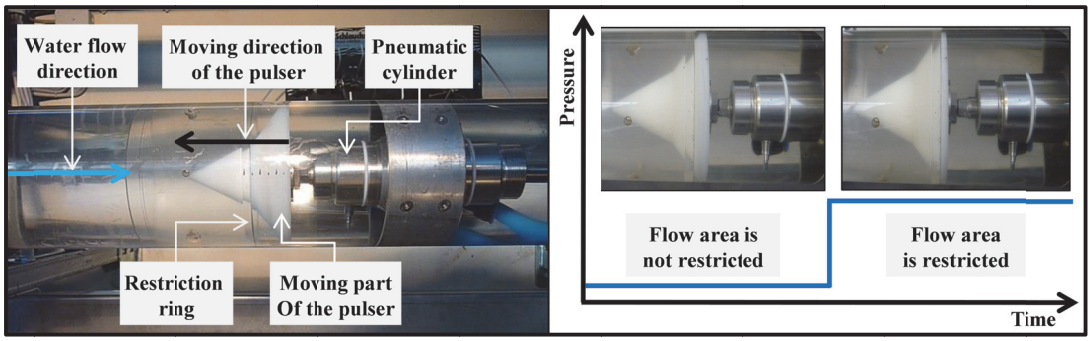

Figure 6.4: Experimental prototype of positive pulser (redrawn and modified), (Namuq and Reich, 2010)

In contrast, the main parts of the mud siren prototype are stator disc and rotor disc with four lobes for each one, and an electrical motor. The electrical motor is used to rotate the rotor disc against the stator disc. A small distance of 1 mm is adjusted between the two discs to avoid friction. By closing and opening the open flow spaces in the stator disc by the rotor disc lobes, continuous positive pressure pulses or waves will be generated, see Figure 6.5. Using a regulator system, two carrier frequencies can be adjusted for operating the mud siren using FSK modulation or ASK (OOK) modulation. The regulator system uses an inductive proximity sensor in order to measure the position of the rotor. Once the rotor lobes pass by the inductive sensor the value of 1 is represented while the value of zero indicates that the rotor open spaces pass by the inductive sensor. The regulator system has a small screen where the induced carrier frequency is digitally displayed.

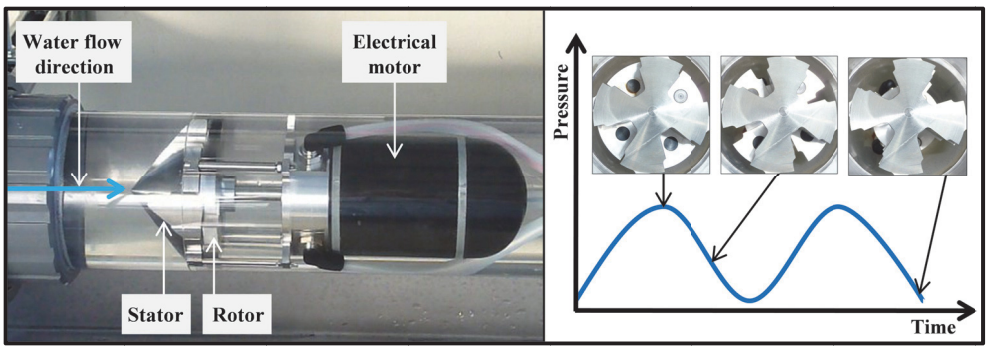

Figure 6.5: Experimental prototype of mud siren (redrawn and modified), (Namuq and Reich, 2010)

The laboratory investigations of the HMPT concept include testing of two different combinations. These are the combination of mud siren with positive pulser and the combination of mud siren with negative pulser. Therefore, a negative pulser has to be built. A Servo-assisted 2/2 way diaphragm valve is selected to be used as a negative pulser. The negative pulser valve is built as shown in Figure 6.6. It is installed between the first transmitter position and the pressure sensor P3. Within response times of 0.1 - 0.4 seconds it can vent a small section (3.6 m^3/h) of the water circulated inside the pipeline to the outside, and thus create negative pressure pulses that propagate ahead towards the pump side

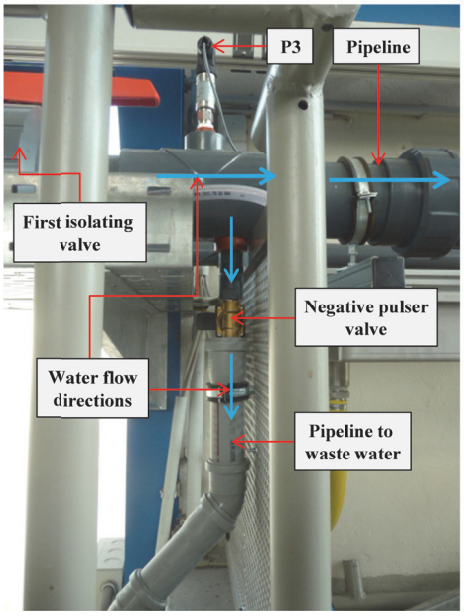

Distances between negative pulser valve and some other elements of the test facility in [m]
Negative pulser to pump: 38.61
Negative pulser to P1: 34.11
Negative pulser to P2: 19.11
Negative pulser to P3: 0.10
Negative pulser to P4: 4.62

Figure 6.6: Laboratory negative pressure pulser

6.3 3D numerical simulation model for the test facility and mud siren

Nowadays, numerical simulations play an important role in new system developments or in specific problem investigations and solutions. For such purposes, engineers and scientists from different fields use Computational Fluid Dynamics (CFD) which is a computer-based tool for simulating the behavior of systems involving fluid flow, heat transfer, and other related physical processes. The processes of momentum, heat and mass transfer are described by a set of equations known as the Navier-Stokes equations. These are partial differential equations and can be discretized and solved numerically.

Different solution methods are used in CFD codes. However, the most commonly used one is known as the finite volume technique. This finite volume technique is the base of the ANSYS CFX which is one of the CFD products. Depending on this technique, the region of interest is divided into many small sub-regions, called control volumes. The equations are discretized and solved iteratively for each control volume. Consequently, the result obtained is an approximation of the value of each variable at specific points throughout the domain. By this means, a full picture of the behavior of the flow can be derived (Manual ANSYS CFX Introduction, 2006).

A basic numerical simulation model for the test facility and its laboratory mud siren was created in ANSYS CFX during a previous research work. Figure 6.7 shows the geometry model of the laboratory mud siren that used in ANSYS simulation. This model will be updated, changed and extended according to the aims and requirements of the present research works as presented in Chapters 8 and 10.

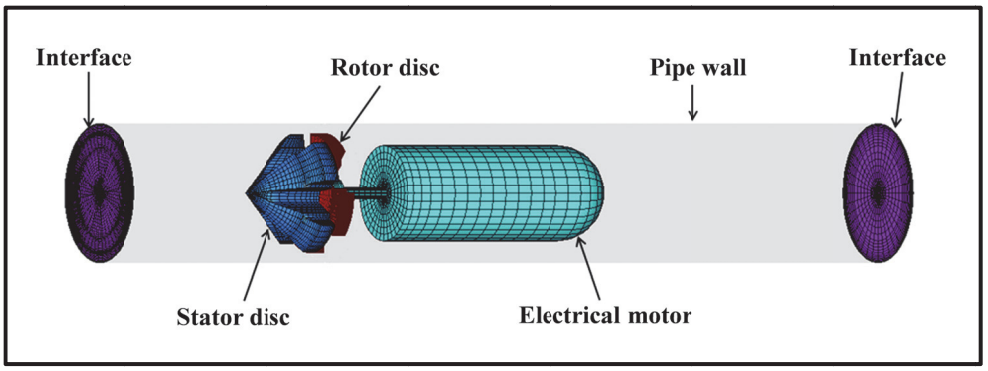

Figure 6.7: Modeled mud siren pulser section domain in 3D for ANSYS simulation (Namuq et al., 2012)

According to Manual ANSYS CFX-Solver Theory Guide (2006), the instantaneous equations of mass, momentum and energy conservation used and solved by ANSYS CFX can be written as follows in a stationary frame:

The Continuity Equation:

$$\frac{\partial \rho}{\partial t} + \nabla * (\rho U) = 0 \qquad (11)$$

The Momentum Equations:

$$\frac{\partial(\rho U)}{\partial t} + \nabla * (\rho U \otimes U) = -\nabla p + \nabla * \tau + S_M \qquad (12)$$

where the stress tensor, τ, is related to the strain rate by

$$\tau = \mu\left(\nabla U + (\nabla U)^K - \frac{2}{3}\delta\nabla * U\right) \qquad (13)$$

In all simulation cases (steady and unsteady state simulations), the shear stress transport turbulence model and the high resolution advection scheme were applied. The whole research work was executed under room temperature, and the modeled system, therefore, was considered as an isothermal one. Accordingly, there is no need for solving the energy equation. The required information to perform a CFD analysis is passed through five software modules which are the main components of ANSYS CFX structure, see Figure 6.8.

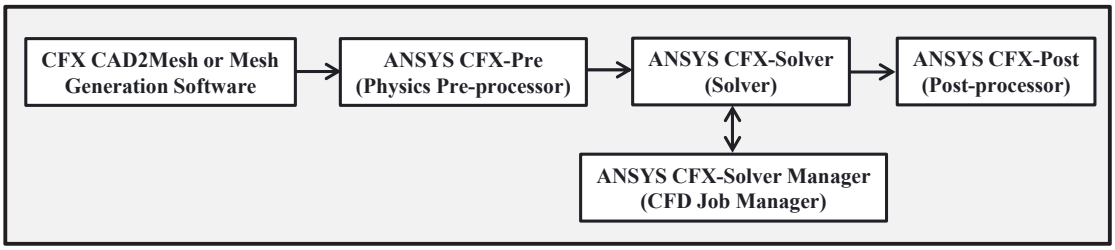

Figure 6.8: The structure of ANSYS CFX (redrawn), (Manual ANSYS CFX Introduction, 2006)

Firstly, a mesh of the system to be investigated must be generated. In ANSYS CFX-Pre the generated system mesh or meshes, in case the system consists of many different parts, should be imported. After that the flow physics, boundary conditions, initial values and solver parameters must be specified. In the next step, all the solution variables for the simulation for the problem specification generated in ANSYS CFX-Pre are solved using the ANSYS CFX-Solver. The ANSYS CFX-Solver Manager enables the user to:

- Specify the input files to the ANSYS CFX-Solver.
- Start/stop the ANSYS CFX-Solver.
- Monitor the progress of the solution.

- Set up the ANSYS CFX-Solver for a parallel calculation.

Moreover, it enables the exporting of the solver results (as an output.csv or output.dat file) giving the possibility to process the simulation results. Interactive analyzing and presenting the ANSYS CFX simulation results can be performed using ANSYS CFX-Post which provides state-of-the-art interactive post-processing graphics tools (Manual ANSYS CFX Introduction, 2006).

6.4 MATLAB software

All the measured signals are processed using the MATLAB software and its available functions for Fourier, Inverse Fourier, Wavelet Transformation and Filtration.

CHAPTER 7 Hybrid Mud Pulse Telemetry (HMPT) System

The developed concept of HMPT was intensively investigated at the laboratory test facility. The tow combinations (mud siren with negative pulser, and mud siren with positive pulser) were tested at different operation conditions and parameters, see Figure 7.1 and Figure 7.2.

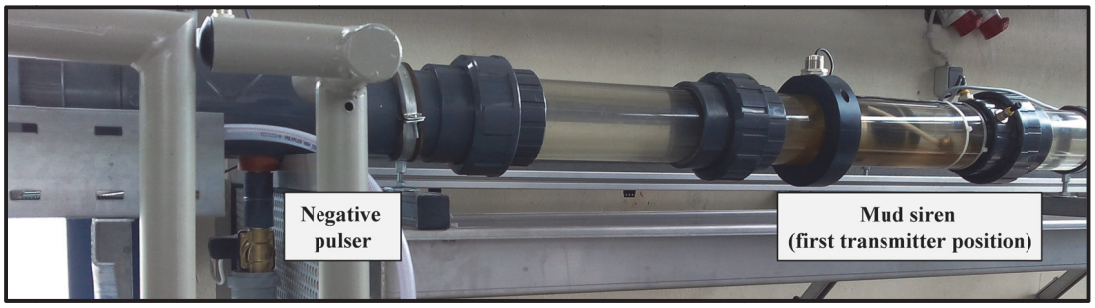

Figure 7.1: Combination of the mud siren and negative pressure pulser

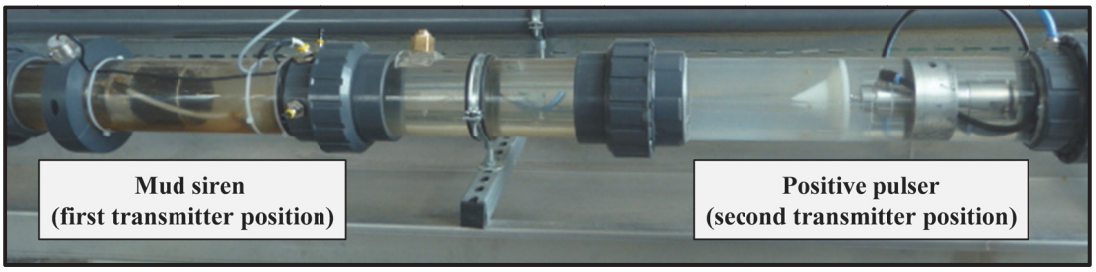

Figure 7.2: Combination of the mud siren and positive pressure pulser

Three transmission test examples were selected and presented in the next section. All the transmission tests were executed using a sampling rate of 1000 Hz. In each transmission test, two individual sets of information were simultaneously transmitted, one via the mud siren and the other one via the pulser (negative or positive). In order to successfully receive the bits transmitted via the mud siren or the pressure pulser, the time slot should be equal to or larger than 0.5 s. Transmission tests were executed using different time slots and at different flow rates. Depending on the measured signal spectrum at the receiver end, suitable carrier frequencies were selected for transmitting the data.

7.1 Combination of mud siren and negative pressure pulser

Transmission test (1): Two different data strings were transmitted see Table 7.1. The first data string consisted of 11 bits and was transmitted via the mud siren using a transmission time slot of 0.8 s. The information bits were modulated using frequency shift keying (FSK) and transmitted using carrier frequencies of 44.5 and 61 Hz. The second data string consisted of 9 bits and is transmitted via the negative pulser using a time slot of 1 s and non-return to zero (NRZ) as a code modulation. The transmission test was executed at a flow rate of 30.6 m^3/h.

Table 7.1: Data strings transmitted via the mud siren and negative pulser in the transmission test (1)

First data string transmitted via the mud siren	**0**	**1**	**0**	**1**	**1**	**0**	**0**	**1**	**0**	**1**	**1**
Second data string transmitted via the negative pulser	**0**	**0**	**1**	**0**	**1**	**1**	**0**	**0**	**1**		

The two generated signals propagated in the drilling mud (water) channel and were received at the receiver (P1) as a single pressure signal. Therefore, a special processing of the received pressure signal was required to extract the two transmitted data strings. For this purpose, an available MATLAB code was updated and further extended. The developed MATLAB code consisted of two main parts, see Figure 7.3 and Figure 7.4.

The first part is for processing the measured pressure signal and to extract and evaluate the data string transmitted in passband via the mud siren, as shown in Figure 7.3. The measured pressure signal (Figure 7.3.A) is transformed to the frequency domain (Figure 7.3.B), where a passband filter, called mud siren filter, is applied to cancel all the signal frequency components which are not generated by the mud siren. The remaining signal after the filtration contains only the frequency components generated by the mud siren, in this case 44.5 and 61 Hz (Figure 7.3.C). The filtered signal is transformed again to the time domain (Figure 7.3.D), and is used as a basis input signal to be analyzed and evaluated using the Wavelet method (Figure 7.3.E). The corresponding Wavelet scales to the frequencies of 44.5 and 61 Hz are 18.3 and 13.3, respectively. The colored bands (red and yellow) show the switching between the two frequencies along the time axis. The

presence of the frequency of 44.5 Hz within the time slot represents the binary bit ‘zero’, while the presence of the frequency of 61 Hz represents the binary bit ‘one’.

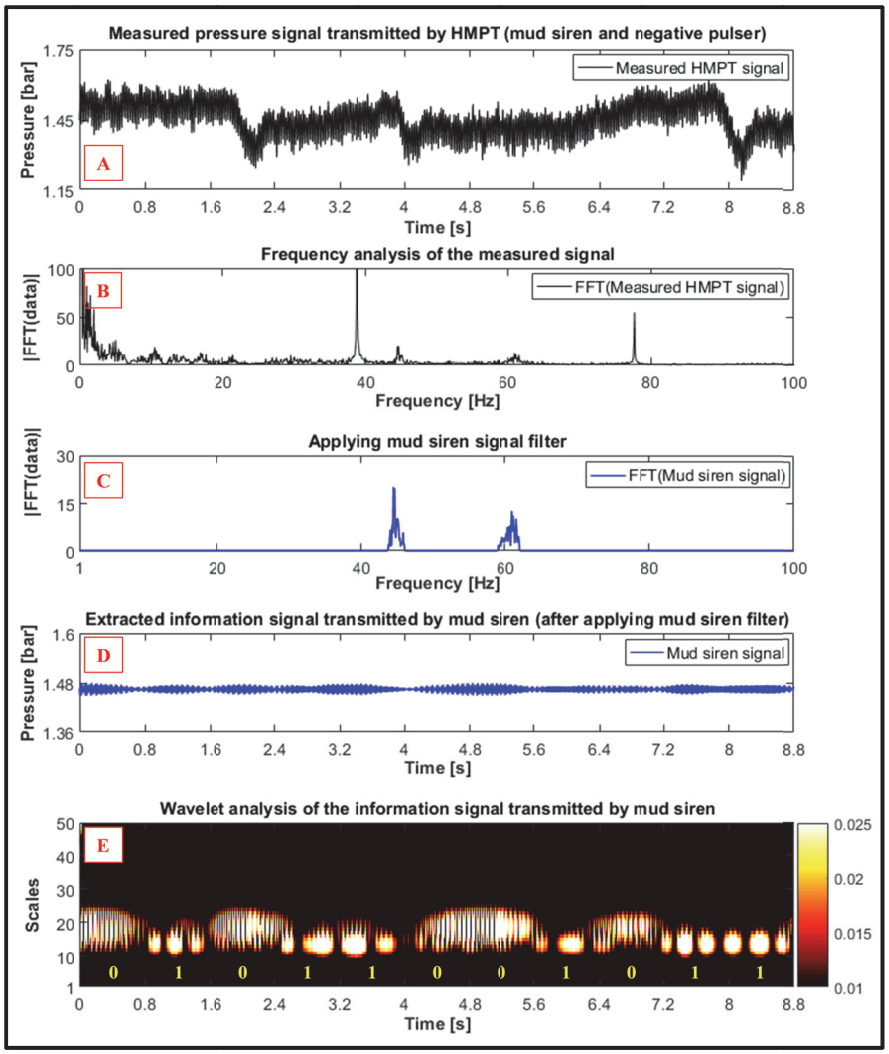

Figure 7.3: Extraction of the first data string (11-bits signal) transmitted in passband via the mud siren from the pressure signal received at the pressure sensor P1 and its evaluation using frequency and Wavelet analysis (time slot = 0.8 s, code modulation = FSK, carrier frequencies = 44.5 and 61 Hz, sampling rate = 1000 Hz, average flow rate = 30.6 m^3/h)

The second part of the MATLAB code is programmed to process the measured pressure signal and to extract and evaluate the data string transmitted in baseband via the negative (or positive) pressure pulser, Figure 7.4. As a first processing step, a baseband filter, called negative (or positive) pulser filter, is applied to the measured pressure signal (Figure 7.4.A) in order to cancel all the signal frequency components which are not generated by the negative (or positive) pulser. The remaining signal after the filtration

contains only the pressure pulses generated by the negative (or positive) pulser, see Figure 7.4.B. In the next step, the length of the filtered pressure signal is divided into time slots of a fixed length, in this example 1 s, see Figure 7.4.C.

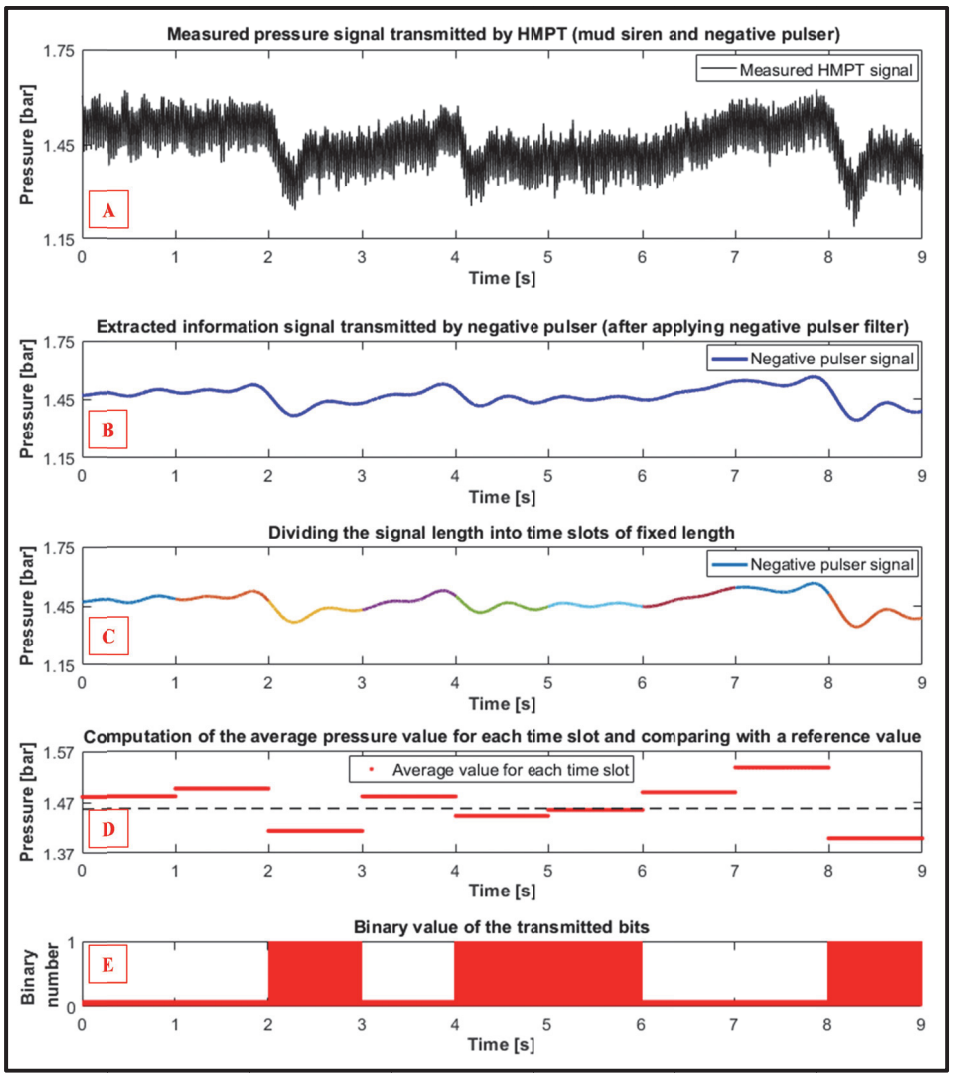

Figure 7.4: Extraction of the second data string (9-bits signal) transmitted in baseband via the positive pulser from the pressure signal received at the pressure sensor P1 and its evaluation using MATLAB (time slot = 1 s, code modulation = NRZ, sampling rate = 1000 Hz, average flow rate = 30.6 m^3/h, reference pressure value = 1.457 bars)

In order to differentiate between the presence and the absence of the pressure pulses, and, consequently, between the binary ones and zeros, a suitable reference pressure value should be selected and set in the program. Pressure pulses generated by positive pulser could be detected if the pressure value within each time slot is higher than the reference value. In case of the negative pulser, pressure pulses could be detected if the pressure

value within each time slot is lower than the reference pressure value. The average pressure value is computed for each time slot and is compared with a reference pressure value. For this transmission test, the reference pressure value was set for 1.457 bars, see Figure 7.4.D. As shown in Figure 7.4.E, a binary bit 'one' is represented each time the average pressure value within a time slot is lower than the reference pressure value, otherwise the transmitted bit is 'zero'.

Transmission test (2): The transmission test was executed at a flow rate of 25.6 m^3/h. Here, two different data strings were transmitted, see Table 7.2. The first data string consisted of 10 bits and is transmitted via the mud siren using a transmission time slot of 0.65 s. The information bits were modulated using on/off keying (OOK) and transmitted using a carrier frequency of 43 Hz. The corresponding Wavelet scale to the frequency of 43 Hz is 18.9. The second data string consisted of 7 bits and is transmitted via the negative pressure pulser using a transmission time slot of 0.9 s and modulated using non-return to zero (NRZ). For evaluation the signal transmitted via the negative pulser, a reference pressure value of 0.956 bars was used. Both information signals could be successfully received and processed. The evaluation and analysis of the two data strings transmitted and received during this test are presented in Appendix (Figure 7.8 and Figure 7.9, respectively).

Table 7.2: Data strings transmitted via the mud siren and negative pulser in the transmission test (2)

First data string transmitted via the mud siren	**1**	**1**	**0**	**1**	**1**	**0**	**0**	**1**	**0**	**0**
Second data string transmitted via the negative pulser	**0**	**0**	**1**	**0**	**1**	**1**	**0**			

7.2 Combination of mud siren and positive pressure pulser

Transmission test (3): The transmission test was executed at a flow rate of 20.2 m^3/h. Two different data strings were transmitted, see Table 7.3. The first data string consisted of 8 bits and is transmitted via the mud siren using a transmission time slot of 0.5 s. The information bits were modulated using on/off keying (OOK) and transmitted using a

carrier frequency of 40 Hz. The corresponding Wavelet scale to the frequency of 40 Hz is 20.3. Figure 7.5 presents the processing and evaluation of the data string transmitted in passband via the mud siren.

Table 7.3: Data strings transmitted via the mud siren and positive pulser in the transmission test (3)

First data string transmitted via the mud siren	**1**	**0**	**1**	**1**	**0**	**0**	**1**	**0**
Second data string transmitted via the positive pulser	**0**		**1**		**0**		**1**	**1**

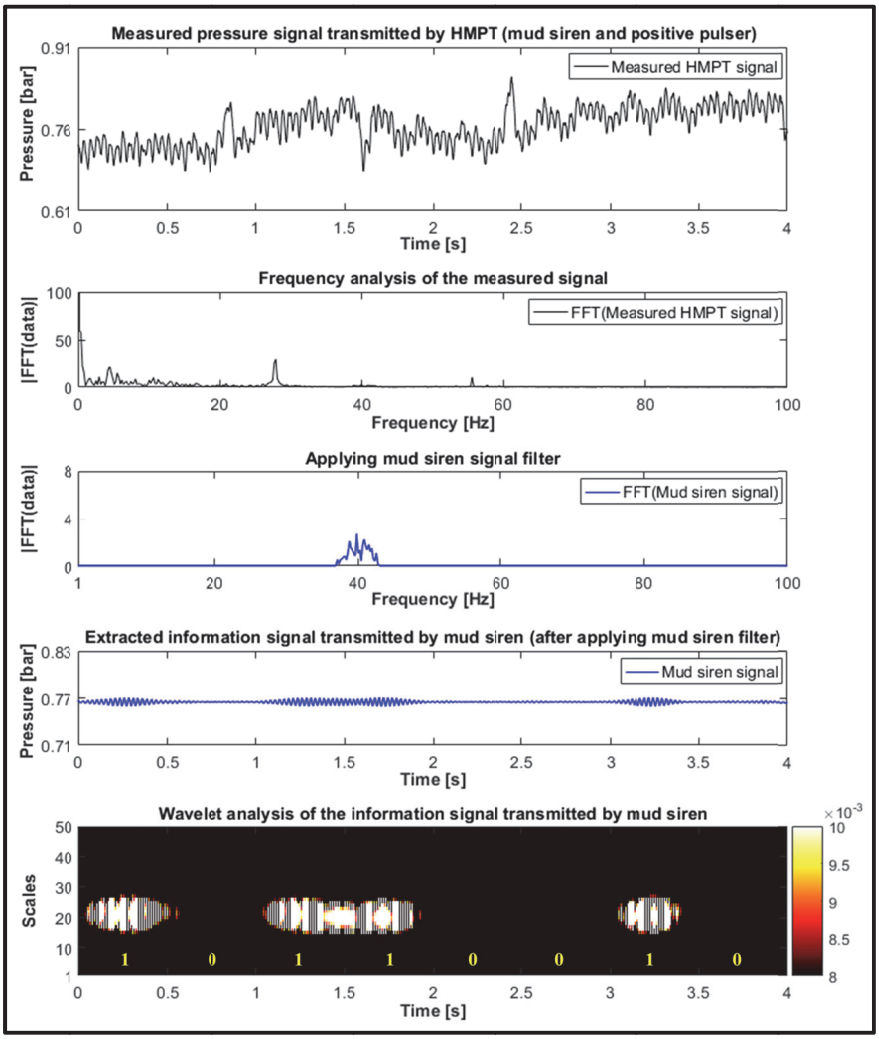

Figure 7.5: Extraction of the first data string (8-bits signal) transmitted in passband via the mud siren from the pressure signal received at the pressure sensor P1 and its evaluation using frequency and Wavelet analysis (time slot = 0.5 s, code modulation = OOK, carrier frequency = 40 Hz, sampling rate = 1000 Hz, average flow rate = 20.2 m^3/h)

The second data string consisted of 5 bits and is transmitted via the positive pressure pulser using a transmission time slot of 0.8 s and is modulated using non-return to zero (NRZ). Thus, a higher pressure level (pressure increase) within the time slot represents the binary bit 'one', while the binary bit 'zero' is represented by the original pressure level (without pressure increase). The processing and evaluation of the data string transmitted in baseband via the positive pressure pulser are presented in Figure 7.6. For evaluation the measured signal, a reference pressure value of 0.768 bars was used.

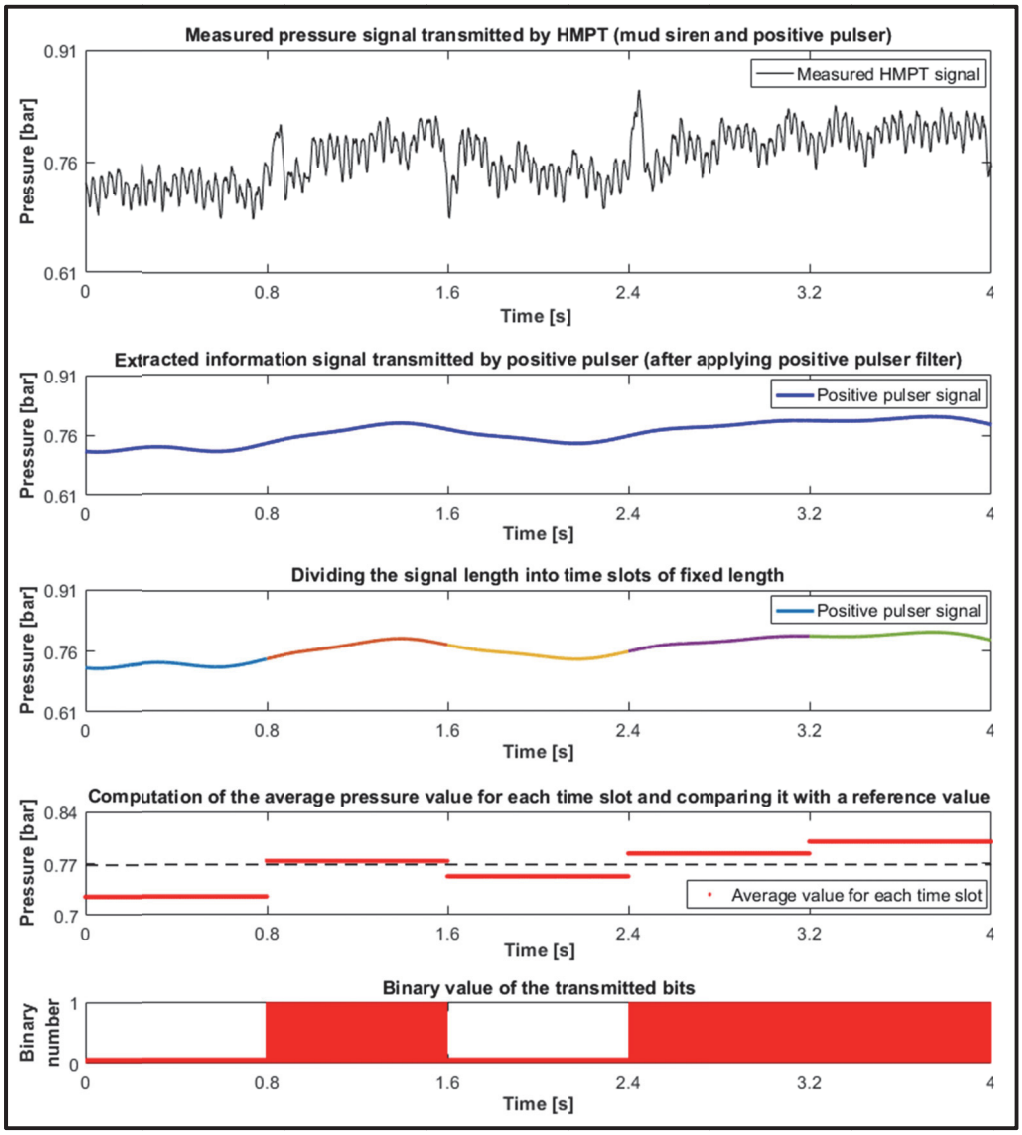

Figure 7.6: Extraction of the second data string (5-bits signal) transmitted in baseband via the positive pulser from the pressure signal received at the pressure sensor P1 and its evaluation using MATLAB (time slot = 0.8 s, code modulation = NRZ, sampling rate = 1000 Hz, average flow rate = 20.2 m^3/h, reference pressure value = 0.768 bars)

7.3 Evaluating the laboratory investigations of the hybrid mud pulse telemetry (HMPT) system

Several transmission tests were executed to investigate the hybrid mud pulse telemetry system. The HMPT system was investigated using different types of combinations. The mud siren was combined with the negative pressure pulser. In other tests, the mud siren was also combined with the positive pressure pulser. The HMPT system was tested at different operation parameters, also at different flow rates and thus at different pressures inside the mud channel, different bit stream lengths, different bit durations or time slots.

Moreover, the HMPT system was investigated using combinations of different code modulations. Some transmission tests were made using the combination of on/off keying (OOK) with non-return to zero (NRZ), and other tests using the combination of frequency shift keying (FSK) with non-return to zero (NRZ). All the transmission tests were effectively executed. All the bit strings were successfully transmitted, received and decoded. The data string transmitted in the baseband via the pressure pulser (positive or negative) could be successfully extracted and decoded from the pressure signal measured at the main receiver (pressure sensor P1). Likewise the data string transmitted in the passband via the mud siren could be extracted and decoded. Thus, the results of the laboratory investigations mentioned above confirmed the functionality of the hybrid mud pulse telemetry system.

Assuming that the HMPT system is operated at the same time slots used in practice (0.1 s for mud siren and 0.5 s for pulser), an increase in the data transmission rate of 20% can be achieved compared to the data rate achieved by mud siren alone using a time slot of 0.1 s. As mentioned in (4.2), the downhole data are sent in a fixed sequence within a telemetry data frame to the surface. For example, it could have been determined that the inclination of the borehole, then the azimuth, then the rock hardness, then the porosity of the rock, etc., is to be transmitted. When all the data have been transmitted, the process would be repeated again from the beginning. In practice, this means that each individual measured value is only updated at relatively long intervals. Due to each drilling process stage or conditions, some measured values are more important and more urgently to be transmitted to the surface than the others. For instance, resistivity and gamma ray values

are more important than azimuth or other variables during the reservoir navigation. In contrast, the resistivity and gamma ray are less important than inclination and azimuth during drilling an inclined well section outside of the reservoir. This can be taken into the consideration in order to use the HMPT system in a beneficial way. For instance, the most particularly interesting data during the drilling process can be selected and transmitted to the surface in a faster sequence than the less important ones. The master in the HMPT system sends the less important data via the slower pressure pulser to the surface, while the more important or critical data, at the moment, are sent via the faster mud siren. The distribution of the data on the two transmission components is variable and can be changed during the drilling process. Figure 7.7 gives an illustration of such an approach for a practical use of the HMPT system for the data transmission in boreholes.

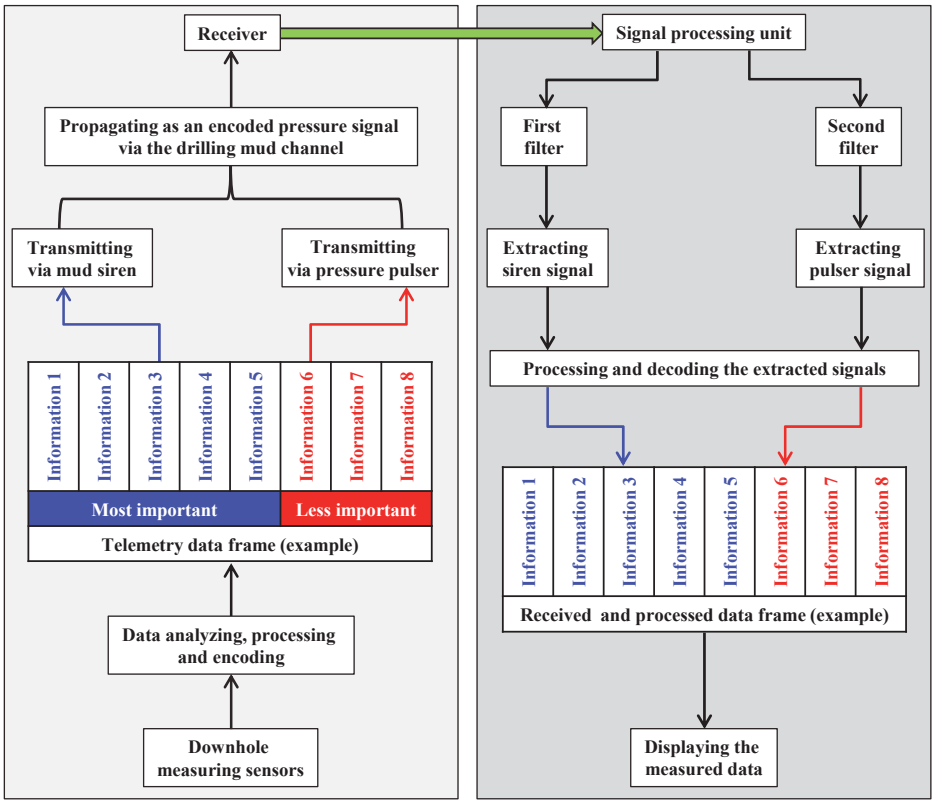

Figure 7.7: Illustration of a practical approach for using the HMPT system for data transmission in boreholes

The developed approach is very new and has not been mentioned in the literature. The new approach was registered at the German Patent and Trade Mark Office for a patent in 2018.

CHAPTER 8 Mathematical and Numerical Investigation of the Concept of the Multi-Frequency Mud Siren

As described, the mud siren can achieve a higher data rate than the pressure pulser, it transmits the data using one carrier frequency each time. This high data rate of the mud siren could be further increased, if the mud siren could generate and use many carrier frequencies at the same time for transmitting the data.

By multi-carrier data transmission, it is necessary as a first step to identify the best passbands for transmitting the data using a channel with a certain configuration. Therefore, the available one frequency mud siren at the institute was used to transmit several pressure signals; each signal was generated at a single specific frequency. Frequencies between 10 and 70 Hz were investigated. The signal amplitude was measured at the main receiver P1. Figure 8.1 shows the best suitable bands for data transmission at the IBF test facility. There are several bands with high amplitudes (marked in green) which can serve as potential transmission frequencies on the current flow loop setup (before extension). They lie between 10 and 18 Hz, 35 and 48 Hz and 54 and 66 Hz.

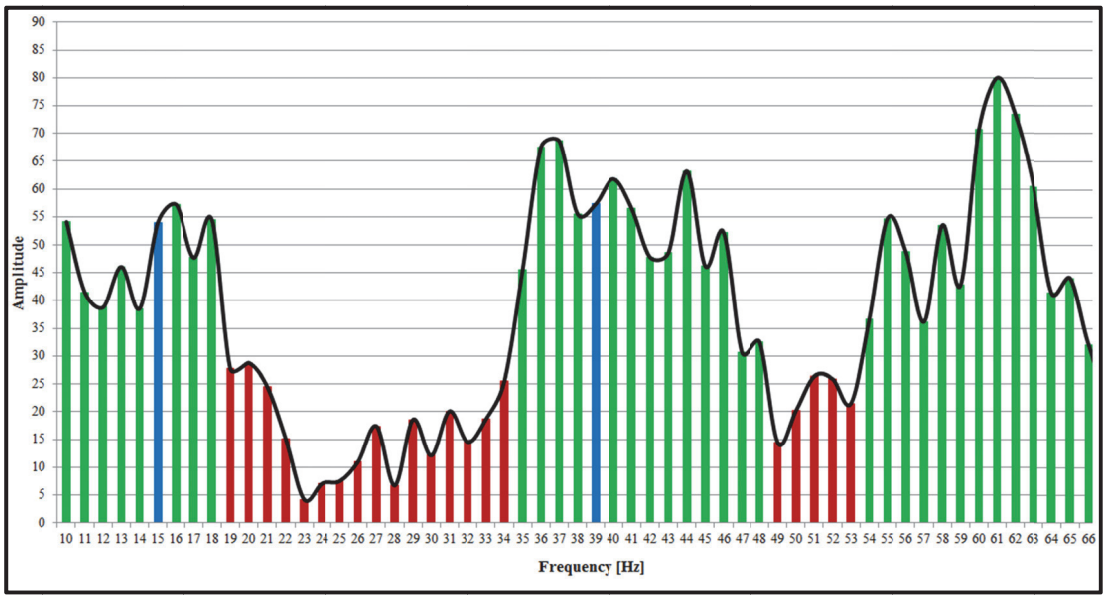

Figure 8.1: Passbands for data transmission at the IBF test facility (amplitude measured at P1)

In this Chapter a multi-frequency mud siren will be investigated and studied in detail using mathematical and numerical models. Here, the capability of the multi-frequency mud siren to generate at least two frequencies simultaneously will be investigated. In all the following calculation examples, the two carrier frequencies to be generated are 15 Hz (selected from the middle of the first passband) and 39 Hz (selected from the middle of the second passband).

8.1 Preliminary considerations for the concept of the multi-frequency mud siren

In order to simultaneously generate two carrier frequencies, two sets of stator/rotor are required. It was assumed, that each rotor disc has only one lobe (half circle). The two rotors should be rotated with two different rotational speeds in order to generate two different carrier frequencies, F1 and F2. According to the rotational speed, both rotors will rotate at different angular velocities, see Figure 8.2. Here, α is the circular angle created by the rotor during its rotation.

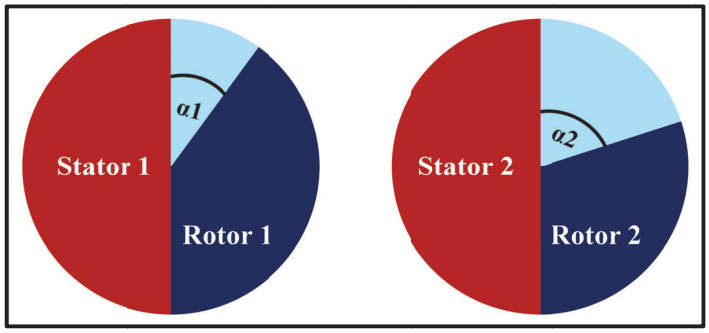

Figure 8.2: Two rotor discs operated with two different frequencies (two different rotational speeds)

Two configurations for installing the two stator/rotor sets inside a pipe could be taken into consideration. The two stator/rotor sets could be operated in a row or in a parallel connection. In case of the row connection, the second stator/rotor set is installed behind the first stator/rotor set. In case of the parallel connection, one stator/rotor set is installed in the center of the pipe, while the second stator/rotor set is installed around the first stator/rotor set. Each rotor can be operated with a specific rotational speed to generate a specific carrier frequency. In case of a row connection, for instance, a first frequency (F1) will be generated by the first stator/rotor set and a second frequency (F2) will be

generated by the second stator/rotor set. Figure 8.3 presents the created free flow area (marked with light blue color) through each stator/rotor set for F1 and F2 within one circulation. For instance, it was assumed that F1 = 2 Hz and F2 = 5 Hz.

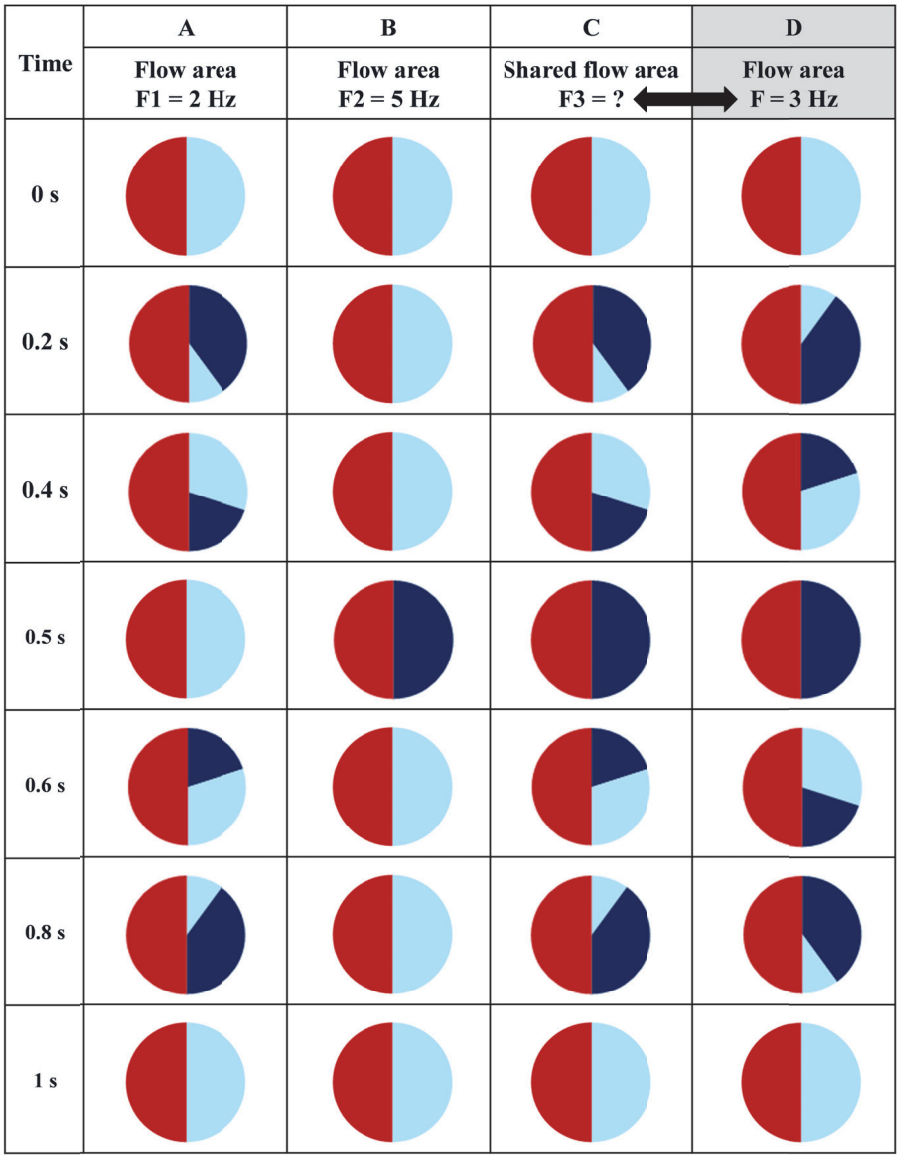

Figure 8.3: Free flow area created through each stator/rotor set for two different carrier frequencies (F1 and F2) and the created shared flow area at different time steps

In addition to the flow area created through each stator/rotor set, a shared flow area will be created at each time step during the operation of the two rotors at the same time, see the part C of Figure 8.3. Due to the created shared flow area during the operation of the two rotors, a third carrier frequency (F3) was generated. The third carrier frequency F3 is

equal to F2 – F1. According to the example presented in Figure 8.3, the third frequency in this case could be F3 = 5 Hz – 2 Hz = 3 Hz. The part D of Figure 8.3 shows the calculated free flow area in case of the frequency of 3 Hz. For each time step, the calculated flow area (part D) is equal to the resulted shared flow area (part C). This confirms that the third carrier frequency (F3) created through the shared flow area is equal to F2 – F1. Also, in case of the parallel connection and for the same reason, the created shared flow area, a third frequency (F3 = F2 – F1) is expected to be generated.

8.2 Mathematical model investigation of different approaches for the multi-frequency mud siren concept

The single mud siren has one stator and one rotor. The rotor can be rotated (or oscillated) against the stator making continuous changes in the open flow area, which leads to generate continuous pressure waves with a specific frequency. The developed mathematical model is focused only on the change in the pressure (ΔP) created by the moving of the rotor against the stator. The developed mathematical model was made based on many assumptions. It was assumed that the flow rate (Q) and the fluid density (ρ) are constant. The fluid compressibility was not taken into consideration. Accordingly, the change in pressure can be expressed by the Equation (14):

$$\Delta P = \frac{1}{2} * \rho * v^2 = \frac{1}{2} * \rho * \frac{Q^2}{TFA^2} = \frac{1}{2} * \rho * Q^2 * \frac{1}{TFA^2}$$

$$\Delta P = Constant * \frac{1}{TFA^2} = \frac{0.04716628}{TFA^2} \qquad (14)$$

For simplifying the calculations, the used flowing medium is considered as water having a constant density (ρ) of 998 kg/m^3. The water flows at a constant flow rate (Q) of 35 m^3/h. Thus, the change in the pressure during the rotor moving at a certain time depends only on the total flow area at that time. The total flow area (TFA) is defined as the flow area, in the rotor-cross-sectional area, that is open at a certain time and the water can flow through it. The simulated multi-frequency mud siren uses multiple stators and rotors. Different approaches for the setup of the multi-frequency mud siren are considered by the mathematical investigations.

8.2.1 Multi-frequency mud siren with stators and rotors in a row

It is assumed that each of the stator and the rotor discs is a half circle and they are equal in the area. There is a clearance between the pipe wall and the outside of the stator/rotor. The area of this clearance is called clearance flow area (CFA), see Figure 8.4. The rotor will be rotated against the stator with a specific rotational speed or frequency.

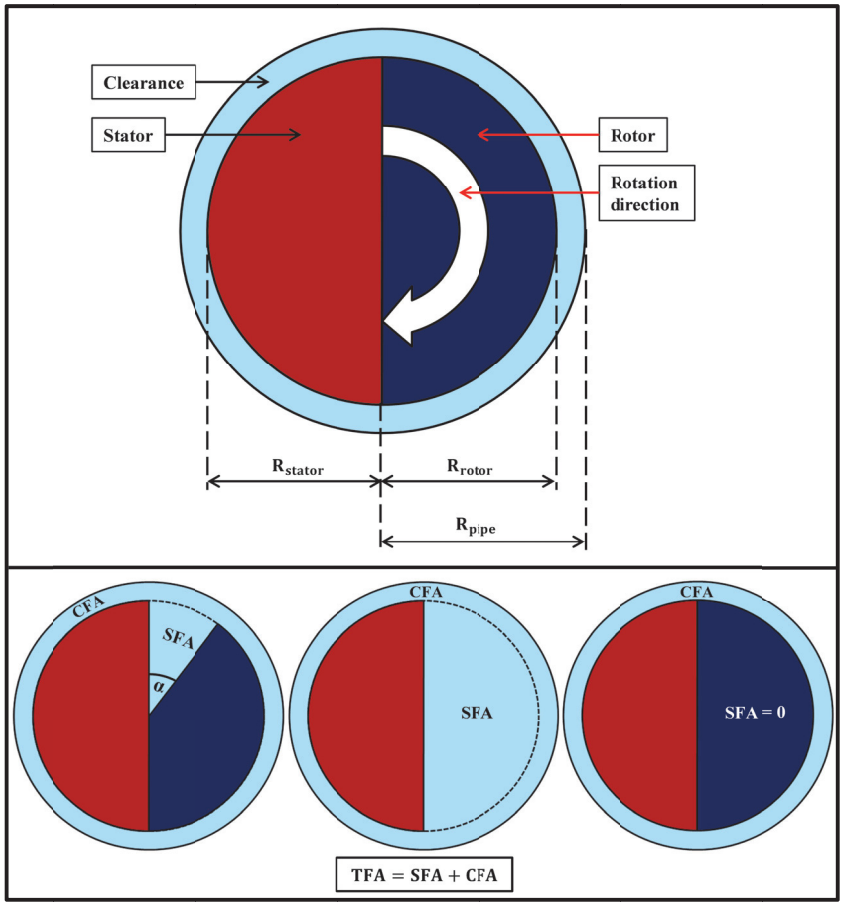

Figure 8.4: Illustration of the used stator and rotor in the mathematical model

In each time step, the rotor covers a certain area. This area can be expressed by the circular angle (α). Corresponding to the circular angle (α) at which the rotor has moved or rotated a free flow area through the stator and rotor discs will exist. This area is called section flow area of the siren (SFA). Thus, the total flow area during the rotor moving at a certain time (i) is:

$$TFA_i = SFA_i + CFA \tag{15}$$

The section flow area through the rotor at a certain time step (SFAi) is calculated using the Equation (16) depending on the circular angle at that time step (α_i):

$$SFA_i = \pi * {R_{rotor}}^2 * \frac{\alpha_i}{360} \tag{16}$$

The circular angle at a certain time step (i) can be calculated from the Equation (17) depending on the carrier frequency to be generated (F):

$$\alpha_i = 360 * i * F \tag{17}$$

According to this approach, the multi-frequency mud siren consists of two stator/rotor sets in a row. Each rotor has to be operated with a specific rotational speed in order to generate one carrier frequency. There are two different rotational speeds, also two different circular angels. Thus, there are two values for SFA at each time step, see the existing SFA1 and SFA2 in Figure 8.5. But only one value of them could be taken into the consideration by calculating the resulting change in the pressure, since the two rotors are in a row.

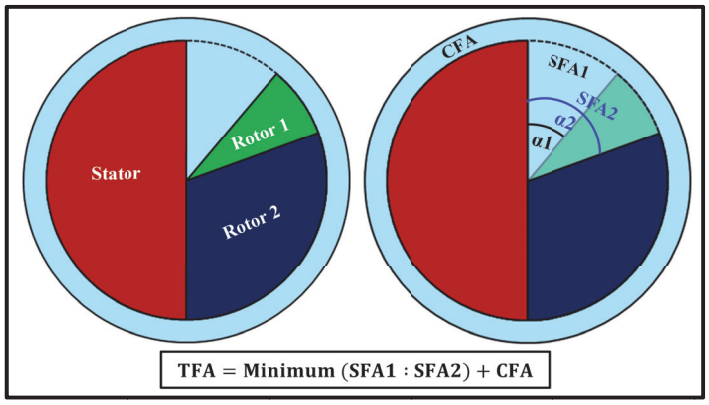

Figure 8.5: Created SFA1 and SFA2 by the use of two stator/rotor sets in a row

It is assumed that the resulting change in the pressure corresponds to the minimum SFA of the two rotors at each time step, because the amount of the water that can flow through the two rotors is limited by the smallest SFA of the two rotors.

Calculation example: In the following calculation example it was assumed that:

$R_{rotor} = R_{stator} = 40$ mm and $R_{pipe} = 46{,}5$ mm

One rotor must generate the frequency of 39 Hz and the other one must generate the frequency of 15 Hz. The calculations are made using a time step of 0.001 s. The calculated change in the pressure is presented in Figure 8.6 (upper section) as a pressure signal in time domain. The calculation with all details is available in the provided DVD, the corresponding file is saved under the name (15+39Hz_row-connection.xls).

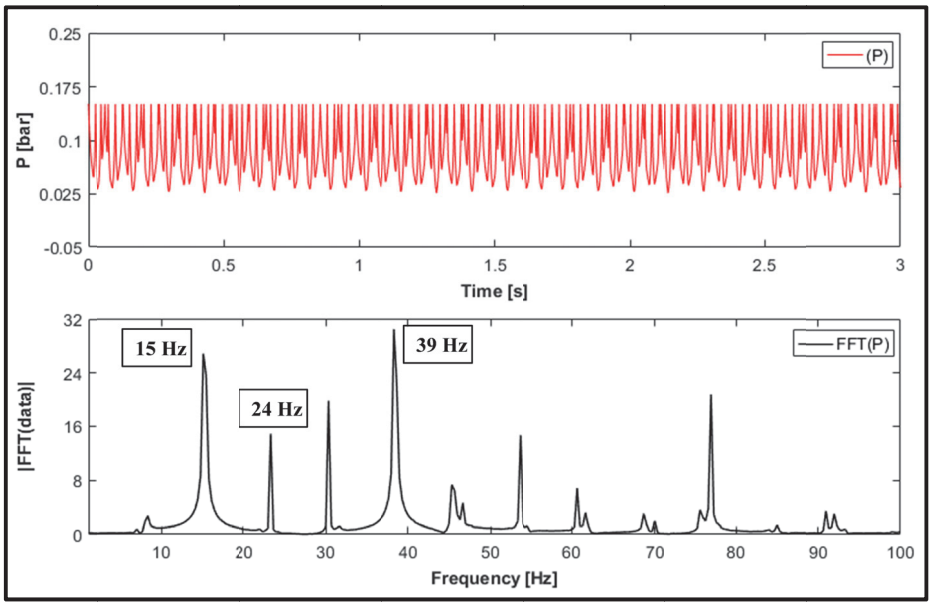

Figure 8.6: Two-frequency pressure signal calculated using two sets of stator/rotor in a row (upper section) and its frequency analysis (lower section)

The frequency analysis of the resulting pressure signal is presented in the lower section of the Figure 8.6. It shows that the two desired carrier frequencies (F1 = 15 and F2 = 39 Hz) could be generated at the same time. However, additional frequency (F3 = F2- F1 = 24 Hz) could be noticed. This will be considered as an interference and unwanted frequency.

8.2.2 Multi-frequency mud siren with parallel connection of stators and rotors

This section describes another configuration of stators and rotors for a multi-frequency mud siren. In this case, two stators and two rotors are located inside a pipe, but they are connected with each other in parallel. The first stator/rotor set is located in the center of the pipe sectional area, while the second stator/rotor set is located around the first set in the same pipe sectional area. Figure 8.7 shows the geometry and the dimensions of the two stator/rotor sets. The dimensions of the two stator/rotor sets are set so that the

maximum flow section area through each rotor (SFA) is the same. There is a space between the two stator/rotor sets as well as between the second stator/rotor set and the internal pipe wall.

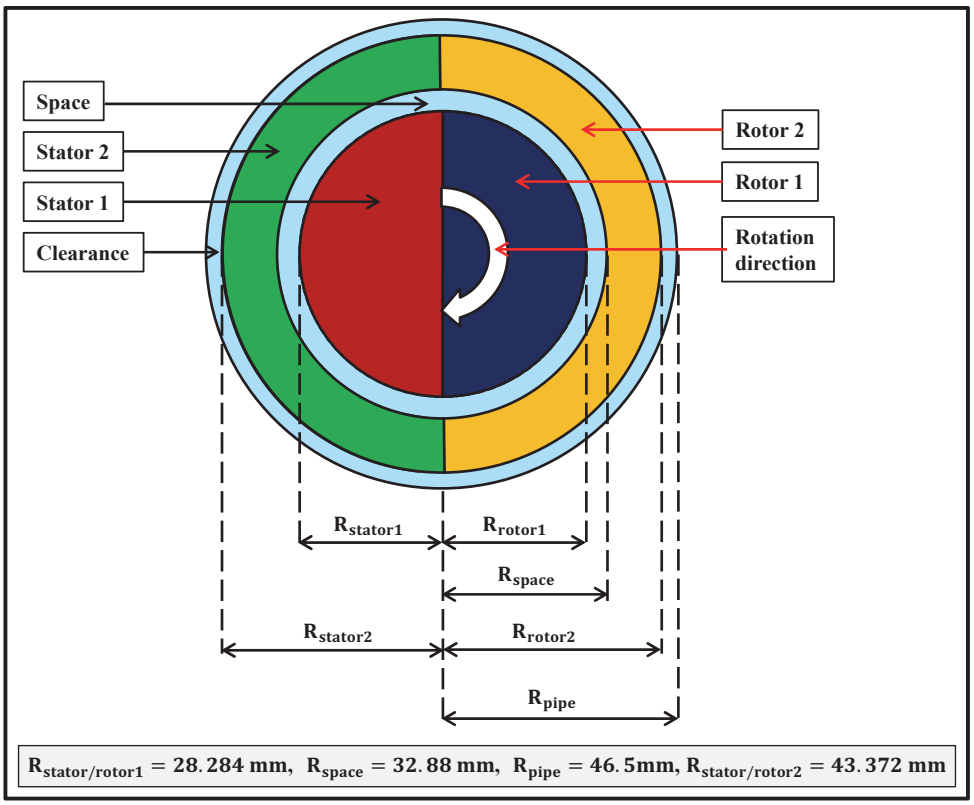

Figure 8.7: Geometry and dimensions of the two stator/rotor sets in case of parallel connection

The flow area in the space between the two sets is called space flow area (SPFA), while the flow area in the space between the second set and the internal pipe wall is called clearance flow area (CFA). Figure 8.8 shows flow areas at different cases. The water with its flow rate (Q) will flow across the two rotors and through the clearance and space flow area. Thus, the total flow area (TFAi) at each time step (i) can be calculated from Equation (18):

$$TFA_i = SFA1_i + SFA2_i + SPFA + CFA \qquad (18)$$

Thereafter, the calculated total flow area at each time step is set into the Equation (14) in order to calculate the resulting change in the pressure at that calculation step. Based on the Equations (18 and 14) and on the dimensions presented in Figure 8.7, the two-

frequency pressure signal (15 and 39 Hz) was calculated. Figure 8.9 presents the resulting pressure signal (upper section) and its frequency analysis (lower section).

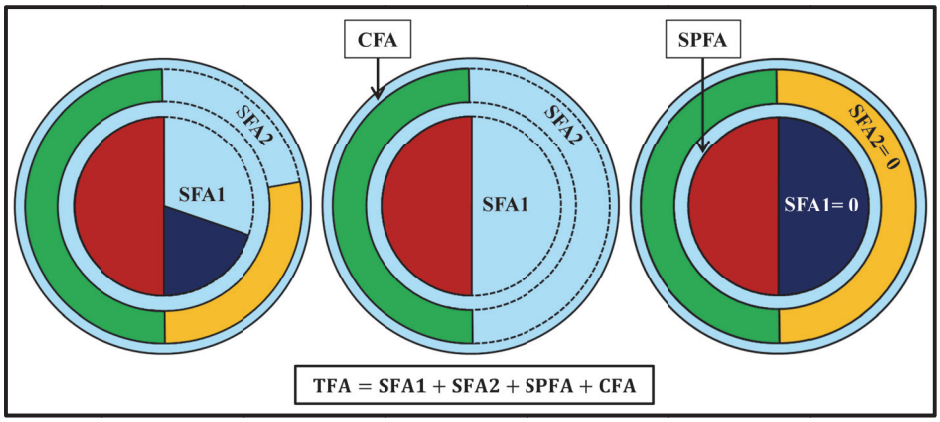

Figure 8.8: Flow areas at different cases for multi-frequency mud siren with parallel connection of two stator/rotor sets

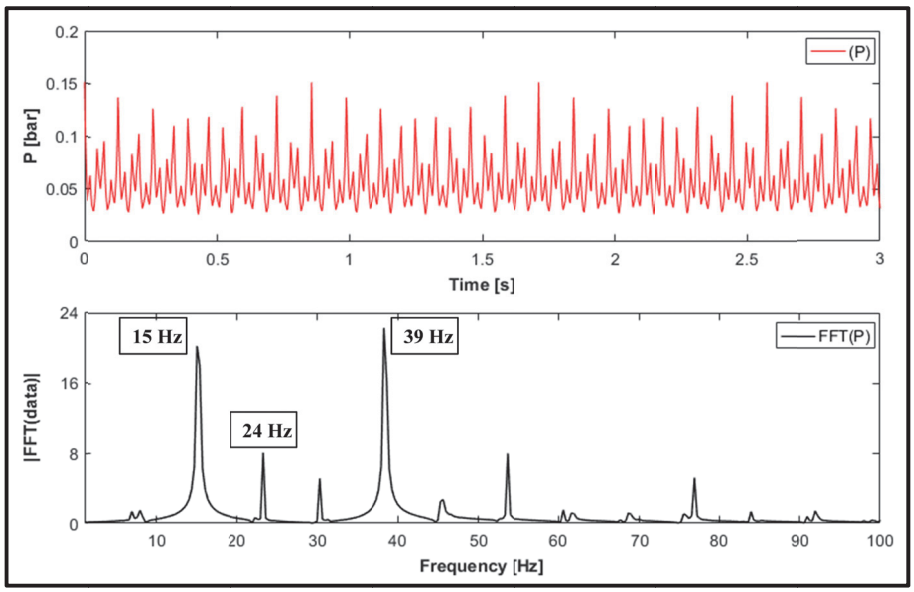

Figure 8.9: Two-frequency pressure signal calculated using the approach of multi-frequency mud siren with two sets of stator/rotor in parallel connection (upper section) and its frequency analysis (lower section)

Figure 8.9 shows that the generated pressure signal and its carrier frequencies (15 and 39 Hz) have lower amplitudes compared to those calculated using the last approach (multi-frequency mud siren with two sets of stator/rotor in a row). Moreover, in addition to the two desired carrier frequencies an interference frequency (F3 = 39 – 15 = 24 Hz) will also be generated in this case. The calculation file is available in the provided DVD and saved under the name (15+39Hz_parallel-connection.xls).

8.3 Numerical model investigation of multi-frequency mud siren with two sets of stator/rotor in a row

According to the results of the mathematical model investigations, the approach "multi-frequency mud siren with two sets of stator/rotor in a row" was the best regarding the source amplitude of the generated pressure signal and its carrier frequencies as well. Therefore, the approach of multi-frequency mud siren with two sets of stator/rotor in a row will be further investigated. For performing such investigations at the test facility, two sets of stator/rotor (or two mud sirens) are required. Unfortunately, there is only one stator/rotor set (one mud siren) available for the use at the test facility of the Institute of Drilling Engineering and Fluid Mining. Therefore, the approach "multi-frequency mud siren with two sets of stator/rotor in a row" will be investigated during the present research work using a numerical simulation model.

As mentioned in Chapter 6, a basic numerical simulation model for the test facility and for the laboratory mud siren was created in ANSYS CFX during a previous research work. The ANSYS CFX model depends on solving a set of equations which are described in (6.3). For hydraulic data transmission it is very necessary to consider the compressibility of the flowing medium (water). This can be achieved by using the Equation (19) according to (Ismaier and Schlücker, 2009) and (Yan et al., 2010). The water density will be calculated depending on the reference density (ρ_0), reference pressure (P_0), absolute pressure (P_a) and the wave speed (c):

$$\rho = \rho_0 + \frac{(P_a - P_0)}{c^2} \tag{19}$$

The used wave speed in the executed numerical simulation is 462 m/s. The most of the pipe sections of the test facility lie horizontally. There is a pipe section that lies vertically and connects the pump and the horizontally pipe section. The hydrostatic pressure of this vertical section must be taken into the consideration. Therefore, the gravitational acceleration was activated in the ANSYS model, and the magnitude was defined for each direction. For x- and y-axes the gravity magnitude was set to zero while in z-axis it was set to 9.8 m/s^2. A variable, called absolute pressure, will include the contribution of the hydrostatic pressure.

The existing ANSYS CFX model was updated, changed and extended, so that a 3D numerical simulation for data transmission using two mud sirens in a row can be run. Each mud siren simulates a set of stator/rotor, see Figure 8.10.

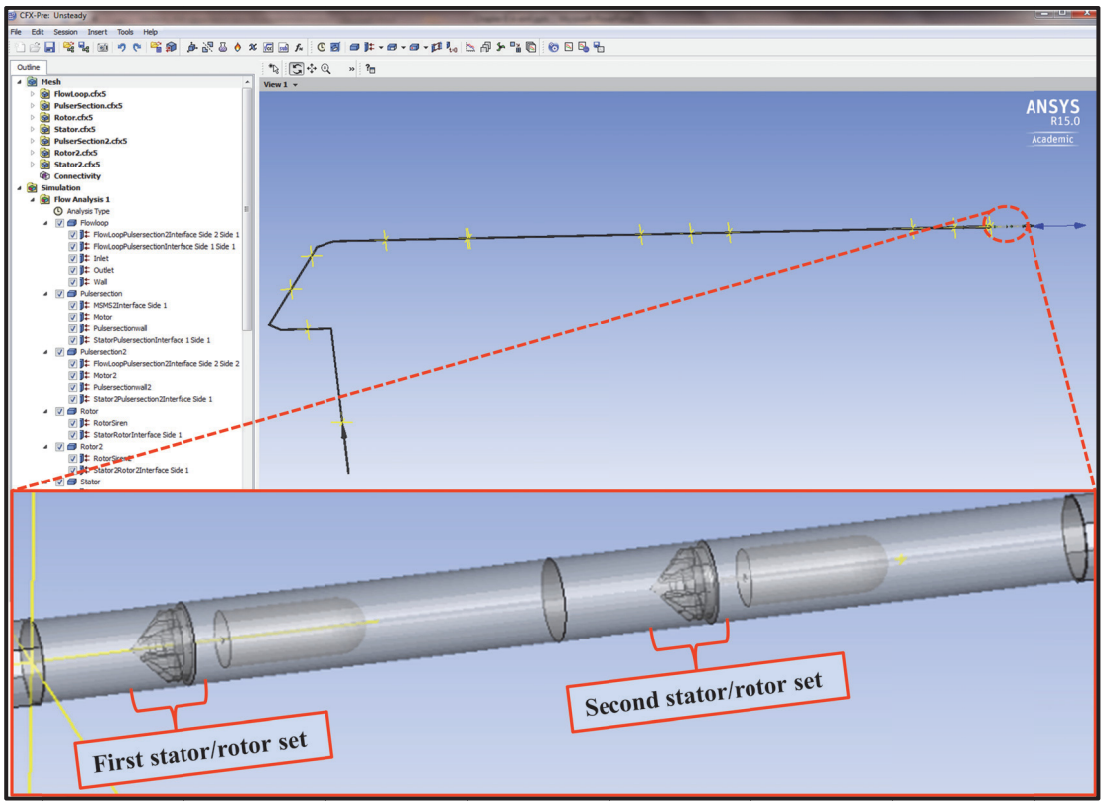

Figure 8.10: ANSYS CFX model for the pipe system of the IBF test facility with two sets of stator/rotor (two mud sirens) in a row

Steady-state and unsteady-state simulations were run. With the steady-state run, the two sets of rotors were still turned off and no pressure waves were generated. In the unsteady-state runs, one or both rotors were turned on with a specific rotational speed depending on which frequency or couple of frequencies was to be generated. The inlet boundary condition for steady-state simulations was set as a constant mass rate (9.845 kg/s), which corresponds to a flow rate (Q) of 35.513 m^3/h. This value of the flow rate was selected in order to maintain the comparability between the current numerical model and the first simulation model developed by Namuq et al. (2012). The outlet boundary condition was set as an opening constant pressure (1.122 bar). Depending on the steady state results, the inlet boundary condition for unsteady state was set to a constant total pressure (2.236

bar), and the outlet boundary condition was set as an opening constant Cartesian velocity components (U= 0, V= 4.01338, and W= 0 m/s). The simulation model has many monitoring points corresponding to the positions of the measuring sensors at the test facility (P1, P2, P3 and P4). The simulation model for all cases investigated during this work can be found in the provided DVD.

8.3.1 Numerical simulations for data transmission with a multi-frequency mud siren using two carrier frequencies

In the case of simultaneous generating two carrier frequencies using the multi-frequency mud siren, two bits per time slot can be transmitted. The transmission options using a multi-frequency mud siren with two carrier frequencies (15 and 39 Hz) are represented in Table 8.1.

Table 8.1: Transmission options with a multi-frequency mud siren using two carrier frequencies (15 and 39 Hz)

First carrier frequency (15 Hz)	Second carrier frequency (39 Hz)	Symbol
off	off	0 0
on	off	1 0
off	on	0 1
on	on	1 1

The four transmission options were investigated using the numerical simulation model. For transmitting the symbol (0 0) the two rotors were turned off. The second rotor was still turned off while the first rotor was turned on and the carrier frequency of 15 Hz was generated representing the transmission symbol (1 0). For transmitting the symbol (0 1) the first rotor was turned off and the second rotor was turned on to generate the carrier frequency of 39 Hz. For generating the two carrier frequencies, 15 and 39 Hz, at the same time, the two rotors were turned on. In this case the symbol (1 1) was transmitted. The right part of Figure 8.11 shows the simulation results for the pressure signals for the four transmission options using a transmission time slot of 0.7 s. The represented signals were predicted at the monitoring point (P1), the distance between the monitoring point (P1) and the interface of the first stator/rotor is 34.522 m. The resulting signals were analyzed

in the frequency domain. The frequency analysis is represented in the left part of Figure 8.11.

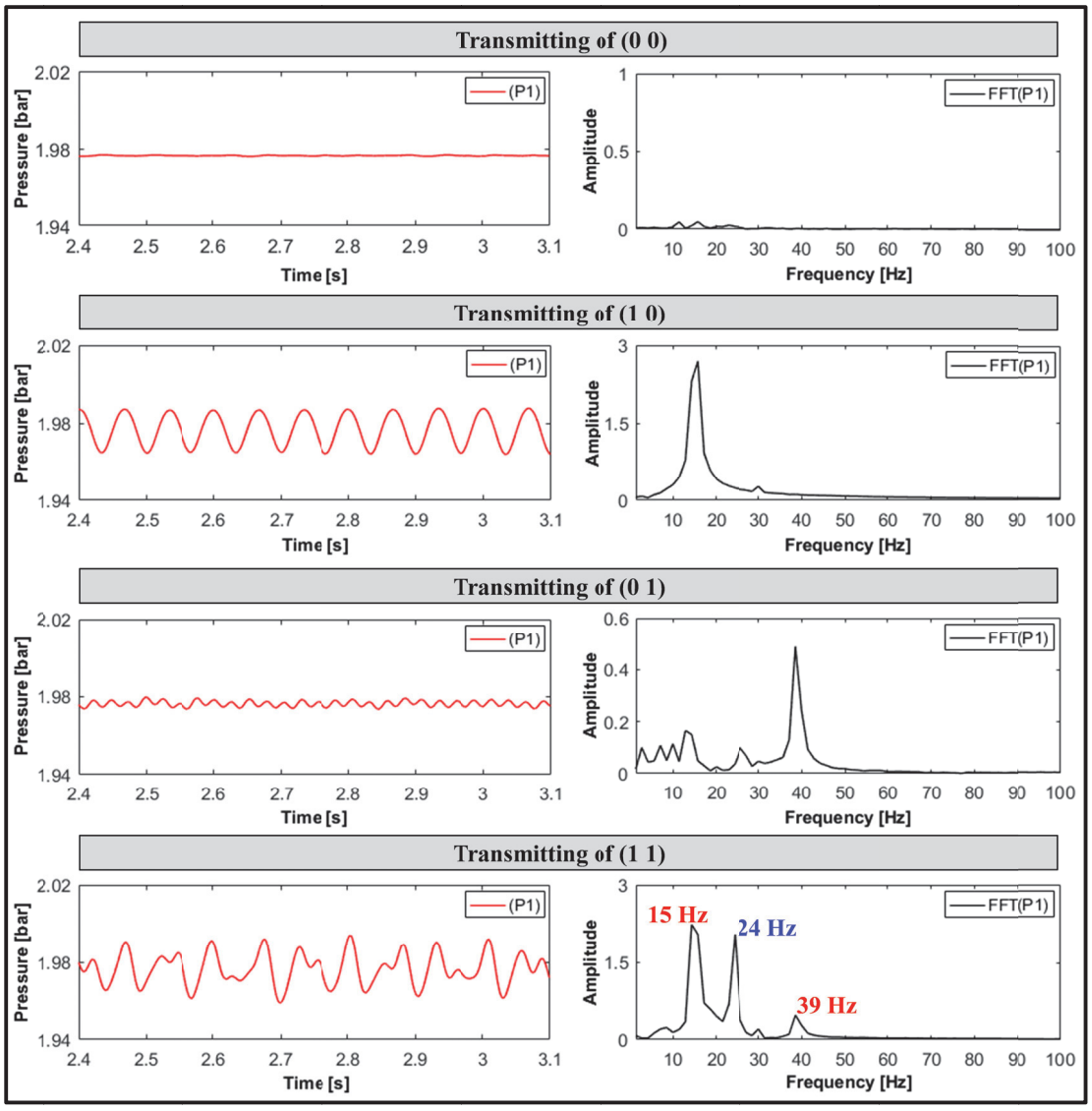

Figure 8.11: Predicted pressure signals (left) and frequency analysis (right) of two sirens in a row

The simulation results show that when only one rotor was working at the time, the corresponding carrier frequency (15 Hz or 39 Hz) was successfully transmitted. When both rotors were working at the same time, two dominant carrier frequencies (at 15 Hz and 24 Hz) were predicted at the receiver (monitoring point P1). Similar to the mathematical model results, the multi-frequency mud siren induced the two individual frequencies (F1 and F2) in addition to the third frequency (F3 = F2 – F1). In this case, the

deep frequency (15 Hz) and the deviation of both frequencies (39 Hz – 15 Hz = 24 Hz) were transmitted and predicted as dominant frequencies while the frequency of 39 Hz had a lower amplitude in comparison to the other two frequencies.

8.3.2 Evaluation of the simulation results

Firstly, the generated 24 Hz will be considered as an interference frequency. In order to make sure that the last simulation result was correct, the simulation model was exactly checked. The next step was to repeat the transmitting of (1 1) using other mesh sizes, also with a finer and much finer grid. The mesh refinement was performed in two stages. The mesh resulting from the first refinement stage is called fine Mesh, while the mesh resulting from the second refinement stage is called very fine Mesh. More refinement is not possible using the available academic version. Table 8.2 presents the different mesh sizes; here the mesh used for running the first simulation (results in Figure 8.11) is called Mesh.

Table 8.2: Total number of nodes for different mesh cases

Mesh name	Mesh size (total number of nodes)
Mesh	367091
Fine Mesh	419427
Very fine Mesh	511899

The simulation run for the transmission option (1 1) was repeated with different mesh sizes. The used transmission time slot was increased to 2 s in order to make a more exact analysis for the measured frequencies, also to measure the frequencies with higher amplitudes. The simulation results with their analysis in the frequency domain are presented in Figure 8.12. The frequency analysis shows that the results with different mesh sizes are identical with each other completely.

The pressure signal was also predicted at the monitoring point (P3) which is much closer to the interface of the first stator/rotor set. The distance between them is only 0.512 m. The predicted signal at (P3) and its frequency analysis are shown in Figure 8.13. It can be

found that the interference frequency of 24 Hz is generated at the same time with the other induced frequencies (15 and 39 Hz).

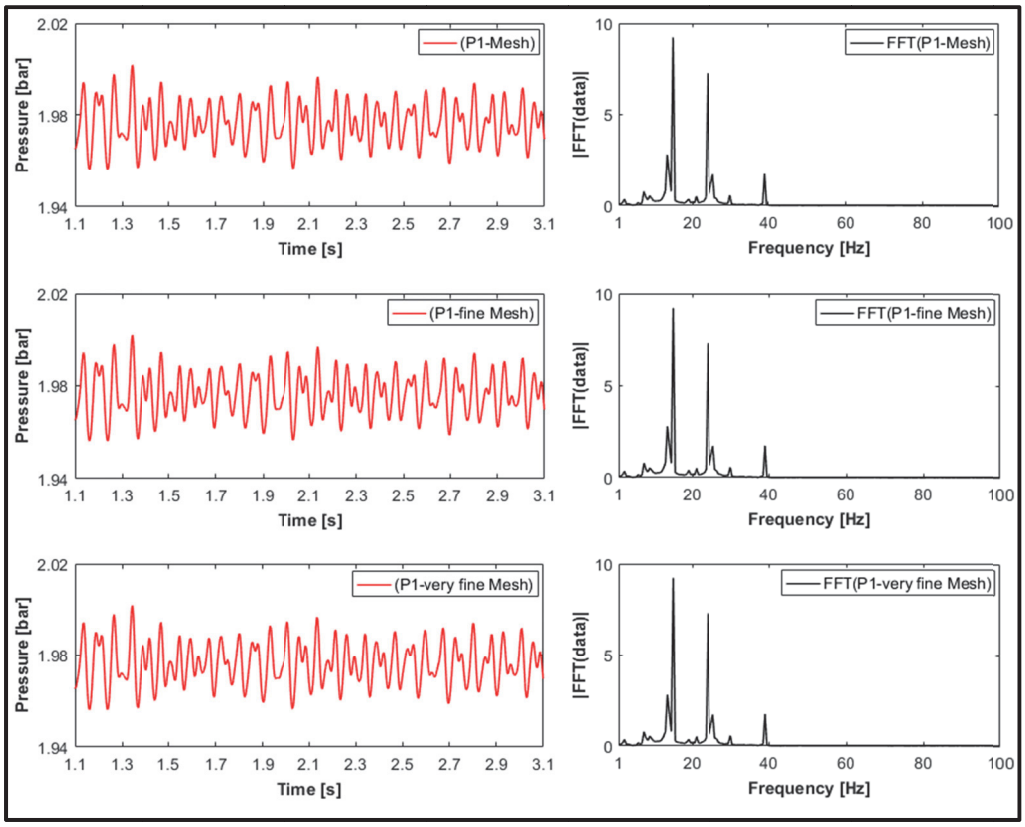

Figure 8.12: Predicted pressure signals (left) and frequency analysis (right) of two sirens in a row for different mesh sizes

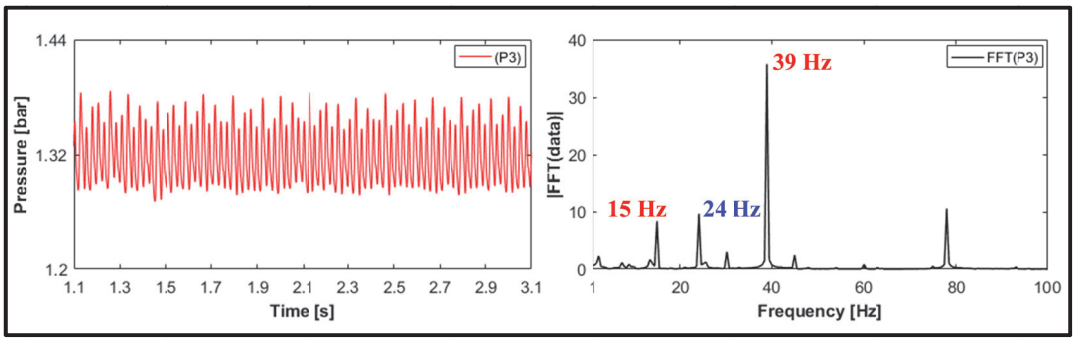

Figure 8.13: Pressure signal predicted at the monitoring point P3 (left) and its frequency analysis (right)

Simulation runs with different carrier frequency sets were made. For instance, a simulation was run to generate the two carrier frequencies (15 and 41 Hz). This run has also shown an unwanted third frequency (interference frequency 26 Hz). The simulation

result is presented in the Appendix. All simulation runs are available in the provided DVD. The simulation results confirm the results obtained by the mathematical model for a multi-frequency mud siren with two sets of stator/rotor in a row. The two desired frequencies (F1 and F2) and a third frequency (F3 = F2 - F1) will be generated.

Based on the simulation and mathematical investigation results of the concept "multi-frequency mud siren using two carrier frequencies", the transmission concept must be updated to be usable with a third frequency. For example, Table 8.3 gives a new code concept for transmitting two bits per time slot using three frequencies. Another solution could be the development of a method to compensate the third frequency (interface frequency) or any other unwanted frequencies. In other words, in order to detect successfully only the desired carrier frequencies with reasonable amplitudes (see Chapter 10).

Table 8.3: Code concept for transmission of two bits per time slot using three frequencies

Rotor 1	Rotor 2	15 Hz	39 Hz	24 Hz	Code
off	off	-	-	-	0 0
on	off	+	-	-	1 0
off	on	-	+	-	0 1
on	on	+	+	+	1 1

8.3.3 Increasing the transmission reach of the mud siren for deep drilling operations

The main disadvantage of the mud siren is the low transmission reach compared to the pressure pulser. The main cause is the high attenuation of the mud siren signal. In order to extend the transmission reach of the mud siren, the intensity of the mud siren signal must be increased, so that the SNR at the receiver end is high enough for a successful detection of the mud siren signal. Increasing the intensity of the mud siren signal can be achieved by taking the advantages of the use of two sets of stator/rotor. The two stator/rotor sets can be adjusted so that the two rotors have the same phase and work at the same rotational speed and to generate the same carrier frequency. In this case, the

intensity of the measured signal and its one carrier frequency at the main receiver is much higher than in the case where only one rotor is turned on. For instance, two simulation runs were made to generate the carrier frequency of 18 Hz. In the first run only the first rotor was turned on, while both rotors were turned on in the second simulation run. Figure 8.14 presents the simulation results of the pressure signals (left) and the frequency analysis of the resulting signals (right). In both time and frequency domains, the resulting signal from the transmission case (18 + 18 Hz) shows a higher intensity than the signal resulting from the transmission case (18 + 0 Hz). An increase in the signal intensity of approximately 40 % was achieved.

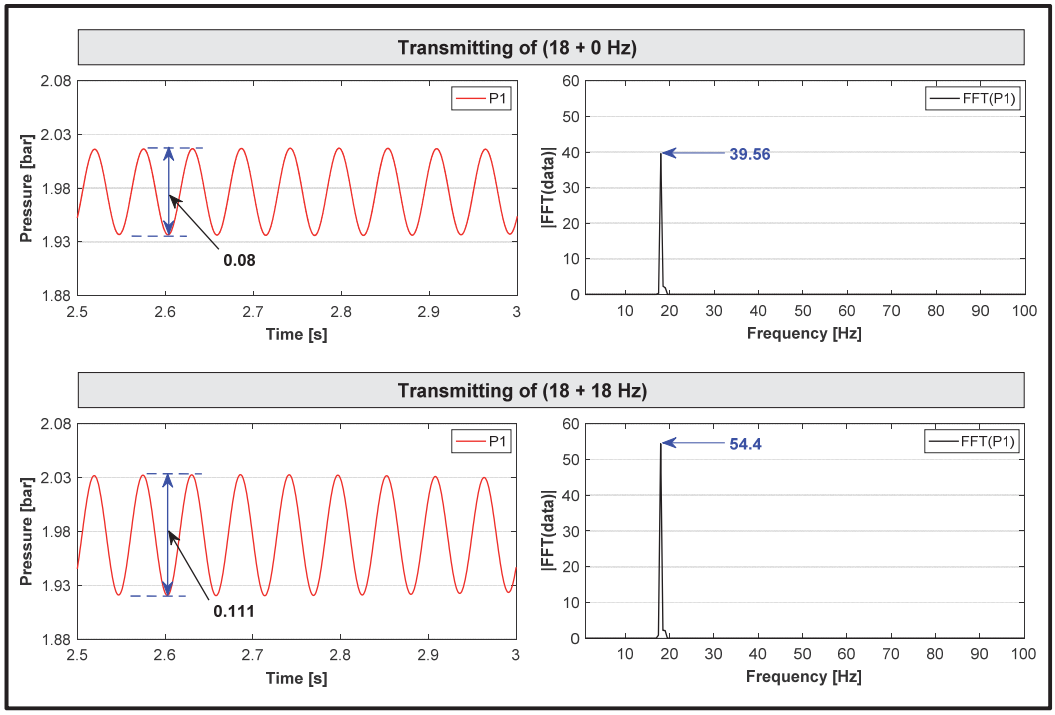

Figure 8.14: Predicted pressure signals (left) and frequency analysis (right) for transmission cases (18 + 0 Hz) and (18 +18 Hz)

However, simulation results are not sufficient to give an exact evaluation of the investigated concept. It should be verified by making laboratory investigations which demand in turn construction and building of the suitable prototype for each concept or approach.

CHAPTER 9 Laboratory Investigations of Multi-Carrier Hydraulic Data Transmission Using an Experimental Multi-Frequency Generator

To date, the passband date transmission in boreholes is performed using the conventional mud siren. The used mud siren is able to generate only one carrier frequency within each time slot. Using multi-carrier frequencies for transmitting the data in passband could significantly increase the hydraulic data transmission rate in boreholes. Such a concept is very new and not be applied to date for data transmission in boreholes. Initial investigations are therefore required. As presented in Chapter 8, using two mud sirens in a row for simultaneous generating of two carrier frequencies could not work without problems. Therefore, a new transmitter tool with the capability to generate a multi-carrier signal was required for performing the aimed investigations.

In addition to the multi-carrier transmitting, new ideas for improving the hydraulic data transmission in boreholes were to be investigated in the context of the present work. Chirp Spread Spectrum (CSS) is one of the latest radio technologies and allows a data transmission with a high robustness against noise and interferences (described in 3.3, Chapter 3). It was very interesting to investigate the data transmission in boreholes using the CSS, since the hydraulic noise and interferences significantly affect the telemetry signal. The available mud siren prototype is also unable to generate such CSS signals.

To date, the used rotating and oscillating mud sirens transmit the data in boreholes in passband by generating coded sinusoidal pressure waves. Therefore, it should be investigated whether different wave forms could be better and more suitable for the passband data transmission in boreholes. For instance, the main disadvantage of the pressure waves generated by mud sirens is their lower transmission reaches in comparison to the pressure waves of generated by the pressure pulsers. In the context of the present research work, investigations had to be executed to find out whether other wave forms have a higher transmission reach than the sine wave. Sawtooth, triangle, rectangle and sine wave forms were to be investigated and compared with each other. Figure 9.1 shows the wave forms in time domain (left part) and their frequency spectra

(right part) according to (Smith, 1999). The frequency spectrum of the sine wave has only the main frequency, called fundamental frequency. For triangle and rectangle waves, the fundamental frequency with only the harmonics having odd numbers is presented in the frequency spectrum. In contrast, the fundamental frequency with its entire harmonics is shown in the frequency spectrum of the sawtooth wave. This must be taken into the consideration by evaluation of the transmission test signals. Generating pressure signals with different wave forms is also impossible with the available mud siren prototype.

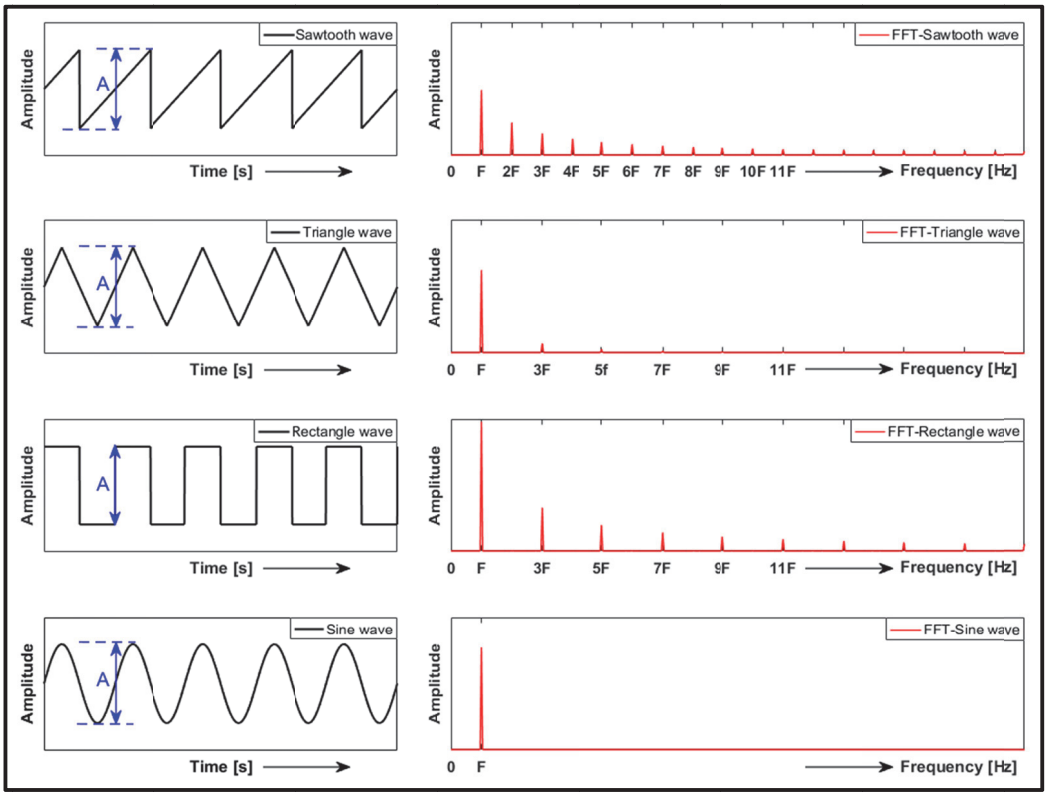

Figure 9.1: Wave forms in time domain (left) with their frequency spectra (right)

In order to perform the investigations of the new ideas and approaches mentioned above, an experimental multi-frequency generator prototype was built and used for executing different transmission tests at the IBF test facility, see Figure 9.2. The construction and testing of the new experimental multi-frequency generator prototype was performed during a student master thesis (Ehras, 2016) supervised in the context of the present research work. Two special powerful audio speakers with Kevlar membranes are used and screwed back-to-back in a plexiglas cylinder. They are connected in parallel with a

180° change in phase. The outside areas of the kevlar membranes are covered with a thin rubber coat to ensure an impregnation against the flowing water inside the pipeline of the flow loop. The inner volume between the two speakers must be filled with a non-conductive and incompressible medium. It was filled with silicone oil, because it does not contain organic elements and is chemically inert, neutral and non-toxic. Thus, only the dynamic force of the flowing water acts on the membrane. The two loudspeakers are both controlled and actuated in a phase-twisted manner so that they always move in the same direction. Thus, the pressure inside the cylinder by knocking out the first membrane is compensated by a retraction of the second membrane and vice versa.

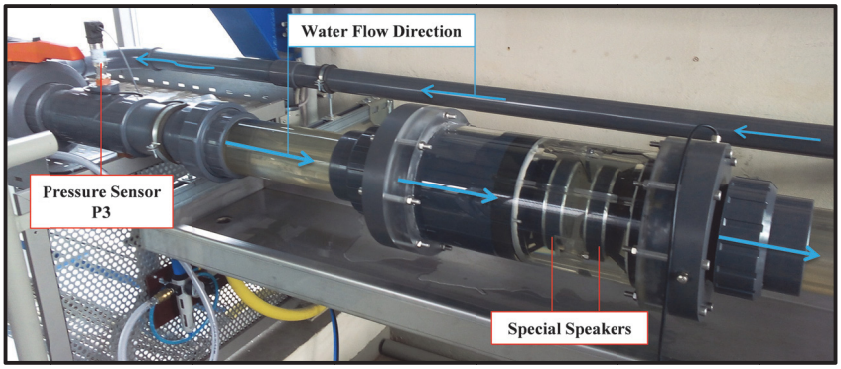

Figure 9.2: Laboratory multi-frequency generator at the IBF test facility

The speaker system is connected to an audio amplifier which is supplied with test signals from the operating software via the control system of the flow loop. A power of up to 100 W can be delivered. However, the loudspeaker was manufactured for music reproduction in the air but not in or under the water medium, which has a 1000 times the density of air. More details of the design and construction of the used experimental multi-frequency generator prototype can be found in the Appendix.

9.1 Laboratory multi-carrier frequency transmission tests

All the following transmission tests were executed at a flow rate of 20.1 m^3/h. The used sampling rate for recording the test signals was set either to 1000 Hz or 2000 Hz. In order to make all the measured transmission test signals comparable with each other, the rotary encoder of the audio amplifier was set to a fixed value of 65 clicks for all the signals presented in this section. The experimental multi-frequency generator had to be used at

the test facility after extension. The stop and passbands represented in Figure 8.1 were measured for the test facility before extension, and they could differ after the extension. Therefore, in order to select the best carrier frequencies to be used for transmitting the data in the following transmission tests, it was necessary to measure the transmission function of the pipeline channel after extension. For this purpose, the multi-frequency generator was installed at the first transmitter position, and a sweep signal from 1 up to 100 Hz was sent. The transmitting duration for each carrier frequency within the sweep was set to two seconds. Figure 9.3 presents the STFT analysis of the sweep signal measured at the maximum distance to the transmitter (at P1).

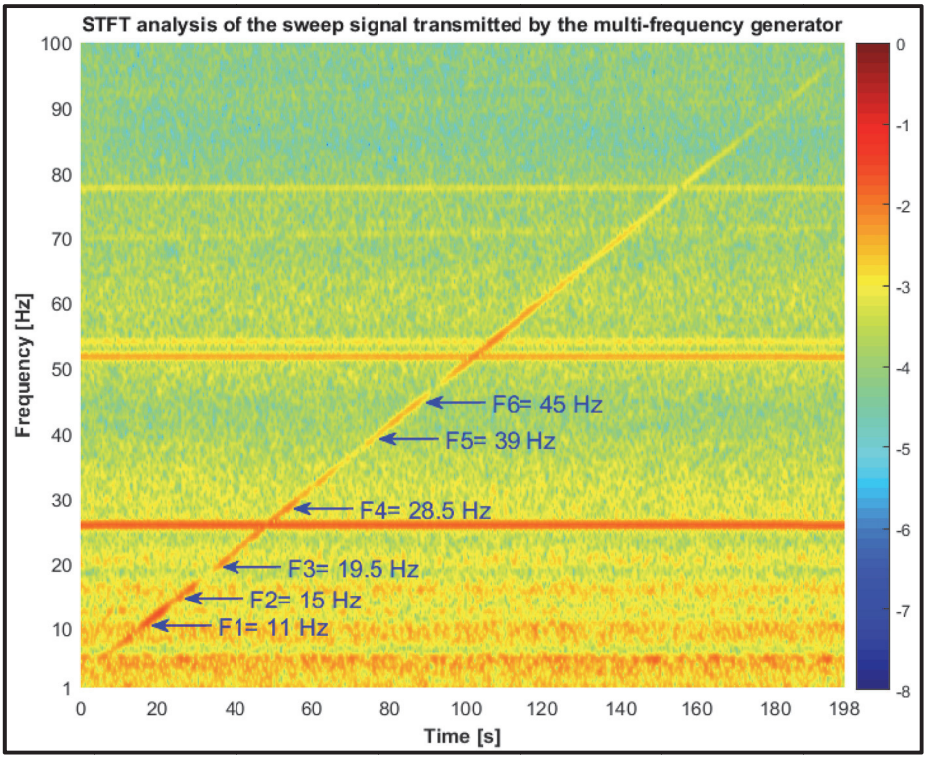

Figure 9.3: STFT analysis of the sweep signal sent from the first transmitter position and measured at P1 (Sweep 1 – 100 Hz, audio amplifier = 65 clicks, sampling rate = 1000 Hz, flow rate = 20.1 m^3/h), (modified), (Ehras, 2016)

The Red-colored areas indicate higher amplitudes. The horizontal red stripe at 26 Hz refers to the pump frequency, where its first and second harmonics are seen at 52 and 78 Hz, respectively. The sweep is represented as a diagonal line from 1 to 100 Hz. Compared to the passbands presented in Figure 8.1, the new analysis results showed some differences. For instance, the frequency bands, from 20 to 30 Hz and from 49 to 53

Hz, could be very suitable for transmitting the data. These bands were considered as stopbands by the first transmission function measurement (before extension). Depending on the new analysis result, several carrier frequencies were selected from the available passbands. For the first transmission test a set of six frequencies, called set 1, is selected so that the frequencies lie with some distance to each other. These frequencies are: 11, 15, 19.5, 28.5, 39 and 45 Hz. For a transmission test with carrier frequencies that are as close to each other as possible, a set of three frequencies of 11, 13 and 15 Hz are selected and called set 2.

Both multi-frequency sets (1 and 2) were modulated using OOK code modulation and transmitted using a time slot of 2 seconds for each symbol. In the transmitting case using set 1, 64 different symbols can be modulated and 6 bits can be transmitted via each transmission symbol. In the case of set 2, 8 different symbols having three bits can be modulated. For instance, Table 9.1 illustrates the modulated transmission symbols for the transmission set 2. A list of the modulated transmission symbols that can be transmitted with set 1 can be found in the Appendix.

Table 9.1: Transmission options for set 2 using three carrier frequencies (11, 13 and 15 Hz)

Symbol		3 Carrier Frequencies		
Number	**Bits**	**11 Hz**	**13 Hz**	**15 Hz**
1	0 0 1	off	off	on
2	0 1 0	off	on	off
3	0 1 1	off	on	on
4	1 0 0	on	off	off
5	1 0 1	on	off	on
6	1 1 0	on	on	off
7	1 1 1	on	on	on
8	0 0 0	off	off	off

Figure 9.4 shows the STFT analysis of the transmitted multi-frequency signal set 1 measured very close to the transmitter, also at P3. The six carrier frequencies gradually change their states (on or off) so that all the 64 possible frequency combinations were

sent. The individual time slots are marked and it is easy to recognize which state the carrier frequencies have in each time slot.

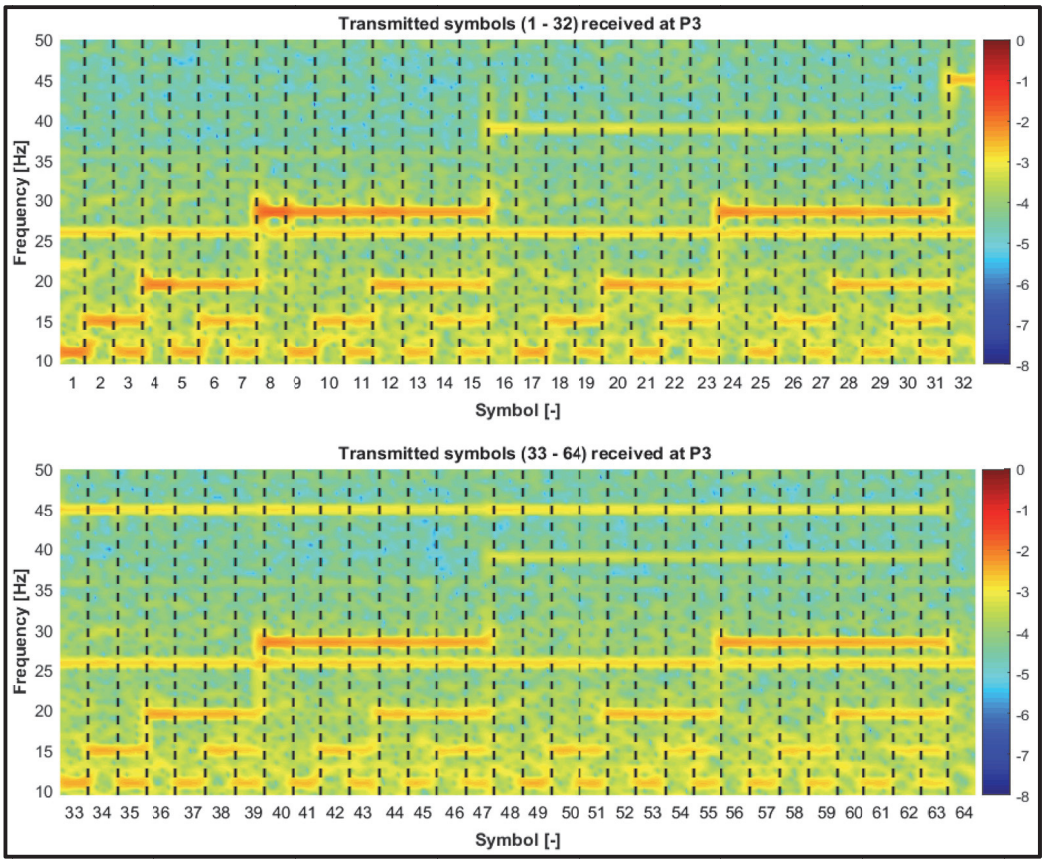

Figure 9.4: STFT analysis of the transmitted multi-frequency signal (set 1) sent from the first transmitter position and measured at P3 (time slot = 2 s, code modulation = OOK, carrier frequencies = 11, 15, 19.5, 28.5, 39 and 45 Hz, audio amplifier = 65 clicks, sampling rate = 2000 Hz, flow rate = 20.1 m^3/h)

The orange stripes represent the frequencies with the higher amplitudes. The measured amplitudes corresponding to the symbols (1, 2, 4, 8, 16 and 32) are higher than those in the adjacent symbols. In the mentioned symbols only one carrier frequency was sent. The more frequencies are transmitted in a symbol, the weaker the measured signal becomes. The symbol 63, where all the six carrier frequencies were sent, has the weakest amplitude compared to the other symbols. Similarly, the symbols having five carrier frequencies (like 61 and 62) were received with lower amplitudes than those symbols with a lower number of carrier frequencies. This is because for the parallel generation of multiple carrier frequencies, the power of the used loudspeaker is distributed over the individual frequencies. It means the full power of the loudspeaker can be used for transmitting a

symbol having only one carrier frequency, while the used power for transmitting a symbol with six carrier frequencies is reduced to only one sixth of the loudspeaker power. Figure 9.5 shows the STFT analysis of the multi-carrier signal set 1 measured at P1 (at maximum distance to the transmitter).

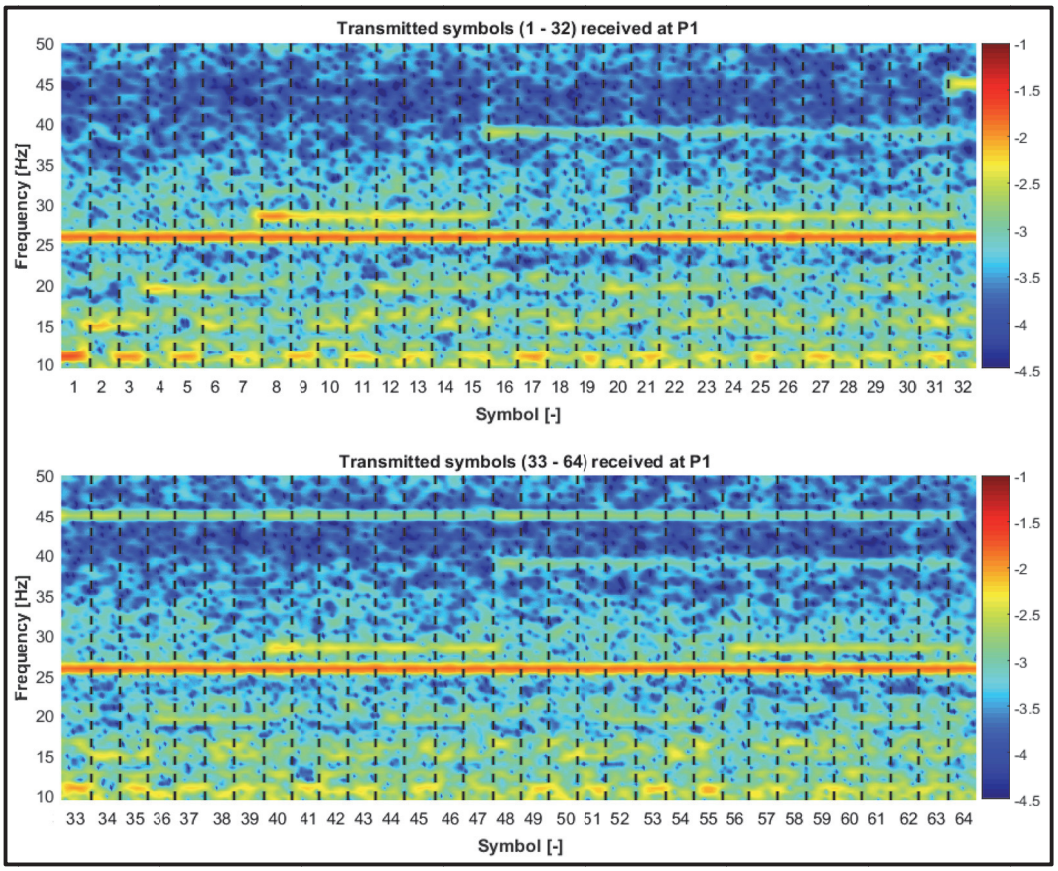

Figure 9.5: STFT analysis of the transmitted multi-frequency signal (set 1) sent from the first transmitter position and measured at P1 (time slot = 2 s, code modulation = OOK, carrier frequencies = 11, 15, 19.5, 28.5, 39 and 45 Hz, audio amplifier = 65 clicks, sampling rate = 2000 Hz, flow rate = 20.1 m^3/h)

With increasing distance from the transmitter towards the pump the signal strength decreases as expected. At the same time the hydraulic noise increases as the distance to the pump decreases so that the individual states are hardly recognizable at the maximum distance to the transmitter. In contrast, in the case of the transmitting test with only three carrier frequencies (set 2), all the transmitted symbols could be successfully received and decoded as shown in Figure 9.6, because all the used carrier frequencies have higher amplitudes. It was possible to distinguish whether the respective frequencies are active or not. It can be seen, however, that at the transitions areas of the adjacent time slots or

symbols additional frequencies were generated. For transmitting the symbol 2, for example, the generator must stop transmitting the frequency of 11 Hz and start with generating the frequency 13 Hz. This shifting from 11 to 13 Hz took a certain time by the generator, and during this shifting time the frequencies between 11 and 13 Hz were generated.

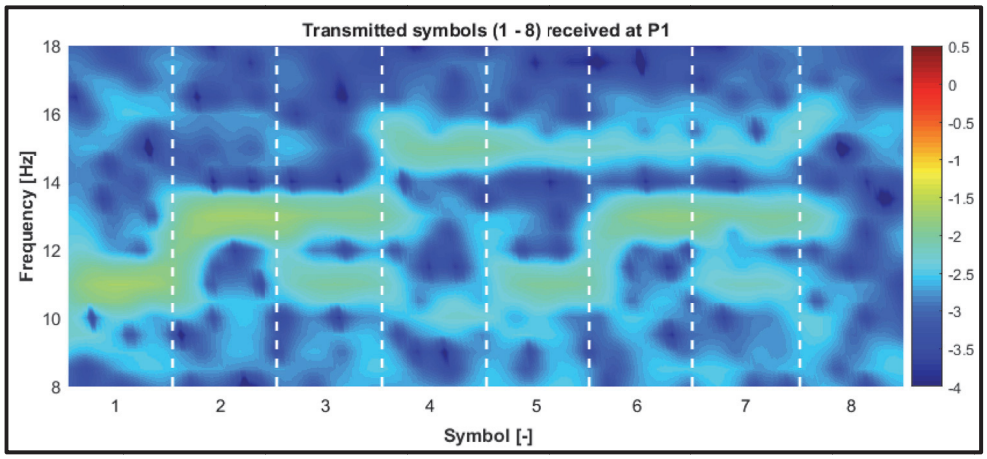

Figure 9.6: STFT analysis of the transmitted multi-frequency signal (set 2) sent from the first transmitter position and measured at P1 (time slot = 2 s, code modulation = OOK, carrier frequencies = 11, 13 and 15 Hz, audio amplifier = 65 clicks, sampling rate = 2000 Hz, flow rate = 20.1 m^3/h)

The signals measured during the transmission tests (set 1 and set 2) were presented here without filtering or any other signal processing procedure. The presented signals clearly show that the generation of a hydraulic multi-carrier signal is possible in principle with the experimental multi-frequency generator. However, it seems possible to transmit the data via the hydraulic mud channel over several carrier frequencies. On the other hand, the presented examples show that the use of the concept of multi-frequency for data transmission in boreholes in the field still requires considerable development and optimization work both on the transmitter end (stronger signals) and on the receiver end (signal processing). The shifting effect of the generator at the transitions between two adjacent symbols can be eliminated, for example, by using a suitable pass filter for removing all the unwanted frequencies from the measured signal. The main problem was that the states of the carrier waves were hardly recognizable at some frequencies in the individual time slots, for instance the frequencies of 11 and 15 Hz by transmission test, set 1. This issue was also encountered in the transmission test set 2, where only three

carrier frequencies were sent. For example, it was here possible but not easy to recognize the frequency of 15 Hz in the symbols 6 and 7 in comparison to the other two frequencies. This does not mean, however, that the hardly recognizable frequencies were very bad or unsuitable for transmitting the signal. But the six carrier frequencies clearly differ with their amplitudes or intensity as they arrive at the receiver. And, accordingly, it is not practicable to evaluate all the frequencies with the same strength scale in the used analysis tool, here STFT analysis. Each measured carrier frequency has its strength that differs from the others, and needs to be evaluated with a certain and suitable strength scale which might not be suitable for other frequencies. Noise cancellation will further improve the evaluation process.

As an example, Figure 9.7 presents the first 32 symbols received during the transmission test set 1. Here, a pass filter was applied to remove the hydraulic noise from the measured signal. The measured carrier frequencies of 11 and 15 Hz were separately analyzed and evaluated. For this analysis, different strength scales were used. The top part shows the evaluation of the carrier frequency of 11 Hz, while the lower part represents the evaluation of the carrier frequency of 15 Hz. It can clearly be seen that the different states of the both frequencies could be successfully recognized over all the received symbols.

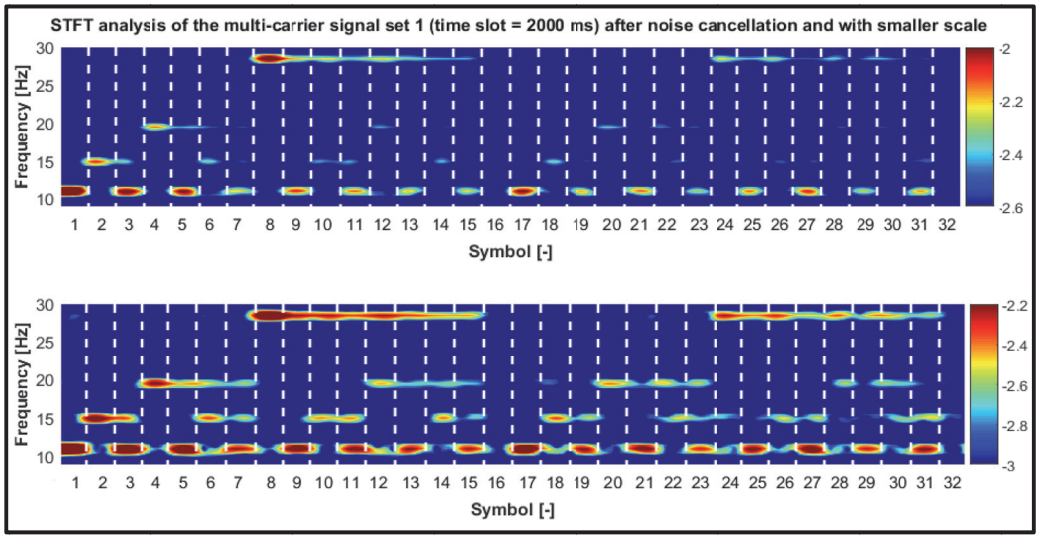

Figure 9.7: STFT analysis after noise cancellation and with smaller scales for the first 32 symbols received during the transmission test set 1 (signal sent from the first transmitter position and measured at P1, time slot = 2 s, code modulation = OOK, carrier frequencies = 11, 15, 19.5, 28.5, 39 and 45 Hz, audio amplifier = 65 clicks, sampling rate = 2000 Hz, flow rate = 20.1 m^3/h)

By developing an approach for multi-carrier frequency data transmission in boreholes, the worst-case scenario must be also taken into consideration. The worst-case scenario could happen, if one carrier frequency, at least, for any reason could not be successfully received and evaluated. This will strongly affect the data decoding at the receiver end. In the worst case, the data decoding could be totally failed out. For instance, in the transmission test using set 1 presented above, the 64 transmission symbols were modulated depending on the states (on/off) of six different carrier frequencies simultaneously. Assuming that the carrier frequency of 11 Hz could never be received and extracted from the measured signal at the receiver end, this will lead to decoding error in all the 64 transmission symbols. Actually, it is possible that more than one frequency could be not received.

The aim was to speed up the transmitting of the downhole telemetry data frame. In the transmission tests mentioned above, multi-carrier frequencies were used simultaneously to modulate and transmit each individual word of the data frame. Here, the transmission time for each individual word was reduced, several symbols can be modulated and multiple bits can be loaded in each symbol. But in order to avoid the worst-case scenario, when at least one frequency could not be received and, accordingly, the whole data frame could be failed out, another modulation method should be applied.

Such a transmitting method is already applied in the wireless communication and networks; it is called the frequency division multiplexing (FDM). Here, many signals can be transmitted at the same time if each signal is modulated onto a different carrier frequency. The carrier frequencies must be sufficiently separated in order to avoid overlapping of the signals (Stallings, 2005).

Thus, instead of transmitting each one word over several multi-carrier frequencies at the same time, each available individual carrier frequency could be used for modulating and transmitting of only one individual word. Here, the number of the transmission times within each data frame is reduced. Hence, only the two simple transmission symbols can be modulated, each one is loaded with only one bit (0 or 1). Assuming that six carrier frequencies, as in the transmission test set 1, could be used for transmitting the data

frame, then six different words could be transmitted simultaneously. Here, if one carrier frequency could not be received, then only one word has decoding errors and could be failed out, but not the whole data frame as in the first modulation option. The described modulation and transmitting method using FDM will increase the robustness of the multi-carrier transmission system to be developed. An example for transmitting a telemetry data frame based on FDM method and using six carrier frequencies, for instance, is given in Figure 9.8.

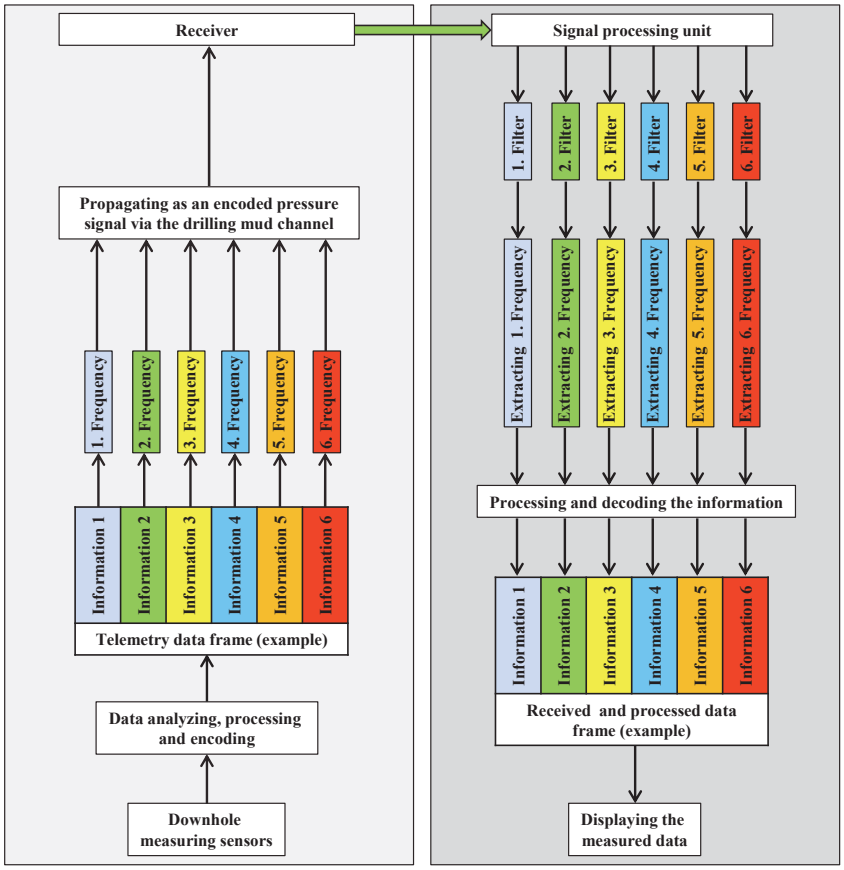

Figure 9.8: Example of a robust FDM method for transmitting the telemetry data frame over several carrier frequencies in boreholes

9.2 Investigation of the Wavelet analysis suitability for the detection of multi-frequency signal transmitted in boreholes

With the aim to improve the signal detection at the receiver end and to find out the best tools for processing multi-frequency signals transmitted via the hydraulic channel, a lot development work had to be done at the receiver end. One of the development works was

to investigate whether the evaluating the measured multi-frequency signals using Wavelet analysis could provide better results compared with the standard analysis tool (Fourier analysis). The signals measured during the transmission tests (set 1 and 2) were used for investigating the suitability of the Wavelet analysis.

First of all, it was very clear that the two measured signals could not be evaluated using the Wavelet analysis without filtering the hydraulic noise and all the other unwanted frequency components that do not belong to the generated signal. The Wavelet analysis for both signals without noise filtering can be found in the Appendix. In contrast, the STFT analysis without noise cancellation can provide a good view of the available frequency components in the considered signal. In the next step, the noise had to be filtered from the measured signal and then the Wavelet analysis was applied. Here, the Morelet wave was used as a waveform for executing the Wavelet analysis. Accordingly, the resulting Wavelet scales corresponding to the frequencies of 11, 13, 15, 19.5, 28.5, 39 and 45 Hz are 147.7, 125, 108, 83, 57, 41.7 and 36, respectively. The Wavelet analysis for the signal measured during the transmission test set 1 is presented in Figure 9.9.

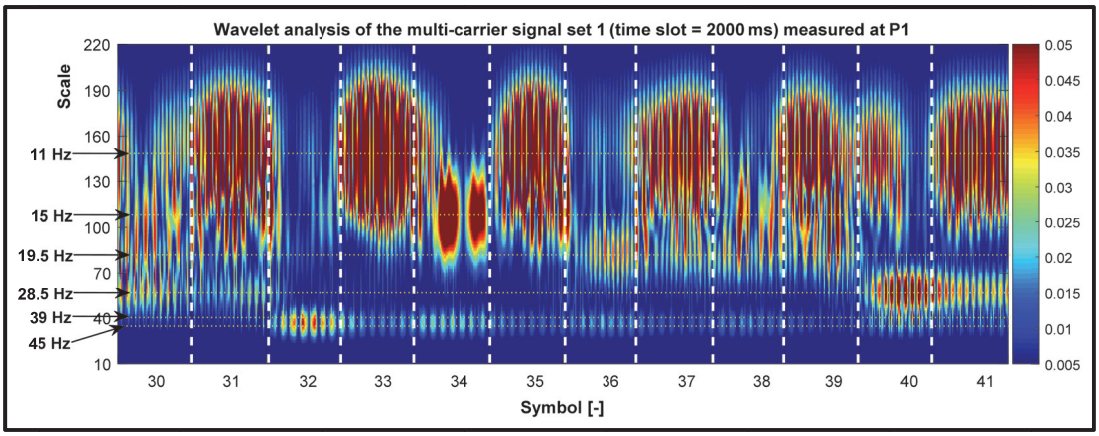

Figure 9.9: Wavelet analysis of the transmitted multi-frequency signal (set 1) after noise cancellation (signal sent from the first transmitter position and measured at P1, time slot = 2 s, code modulation = OOK, carrier frequencies = 11, 15, 19.5, 28.5, 39 and 45 Hz, audio amplifier = 65 clicks, sampling rate = 2000 Hz, flow rate = 20.1 m^3/h)

In order to make a focus on the analysis quality, only 10 received transmission symbols with different carrier frequency combinations were considered. The Wavelet scales corresponding to the investigated carrier frequencies are marked with horizontal lines. A view of the frequency components available in the considered signal can be given. The

transmitted and measured frequencies are represented as colored bands, where the dark red refers to the higher amplitudes. Similar to the STFT analysis, analyzing a multi-frequency signal using the same signal strength scale (also in one diagram) can make the frequencies detection more difficult. The difficulty increases with the Wavelet analysis, because in Wavelet analysis the color bands representing lower frequencies are stretched over a wide range. For instance, the color band for the frequency of 11 Hz was stretched and has reached in most cases the representing band of the frequency of 15 Hz. The color bands representing the higher frequencies are compressed and do not spread over a wide area of the diagram.

But on other hand, the higher frequencies are located very close to each other. For instance, the frequency of 45 Hz was always sent during the transmission symbols (32, 34 and 40). In the mentioned symbols the frequency 39 Hz was not transmitted. Due to the small distance between the representing locations of the two frequencies, the color band for the frequency of 45 Hz has also covered the location of the frequency of 39 Hz. This can lead to detection errors in all the mentioned symbols. Transmission symbols having fewer carrier frequencies that are not close to each other could be clearly visible, as in the case of symbols (33, 34 and 36).

Once the transmitted frequencies are located close to each other on the Wavelet diagram, recognizing the correct state of the frequencies within the transmission symbol becomes more difficult. This problem can be encountered even in transmitting cases using a lesser number of carrier frequencies. Figure 9.10 presents the Wavelet analysis of the transmission test using set 2, where only three carrier frequencies but close to each other were used. The transmission symbol 5 gives a good example of the mentioned problem. Here, only the frequencies of 11 and 15 Hz were transmitted, but the color bands presented in the diagram look as if the frequency of 13 Hz was transmitted too. The color band representing the frequency of 11 Hz is stretched over a wide range. A successful evaluation of the measured transmission signals using Wavelet analysis requires, therefore, the separate analysis of each individual carrier frequency. In the STFT analysis it was sufficient to filter the interfering noise and to set the used scale of the signal strength suitable to the considered frequency.

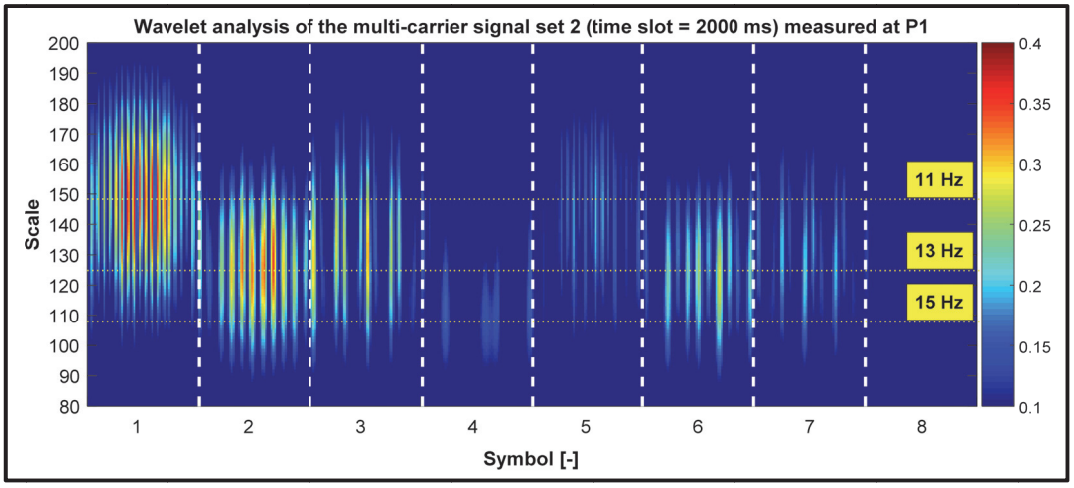

Figure 9.10: Wavelet analysis of the transmitted multi-frequency signal (set 2) after noise cancellation (signal sent from the first transmitter position and measured at P1, time slot = 2 s, code modulation = OOK, carrier frequencies = 11, 13 and 15 Hz, audio amplifier = 65 clicks, sampling rate = 2000 Hz, flow rate = 20.1 m^3/h)

Due to the representing specifications of the Wavelet analysis, also stretched bands for low frequencies and compressed bands but very close together for higher frequencies, the Wavelet analysis must be repeated many times. The number of the repeated Wavelet analyses depends on the number of the carrier frequencies used during the transmission test. Within each Wavelet analysis step, only one carrier frequency has to be evaluated.

For evaluating the carrier frequency of 11 Hz, for instance, a suitable pass filter must be applied. The applied filter must remove all the other used carrier frequencies in addition to the interfering noise. Thereafter, the strength scale of the Wavelet analysis can be set to be suitable for evaluating the investigated frequency of 11 Hz. This procedure must be repeated for evaluating each carrier frequency received during the transmission test set 1. For this purpose, a special program code was written in MATLAB in order to perform such multi-step Wavelet analysis of the received multi-frequency signal. The analysis results of the transmitted multi-frequency signal set 1 are represented in Figure 9.11.

In such a way, all the received carrier frequencies can be successfully evaluated and their information can be extracted. This leads to the same conclusion found by evaluating the measured signal using the STFT analysis. Once several carrier frequencies can be used for transmitting the downhole data frame, each available individual carrier frequency must be used for modulating and transmitting of only one individual data.

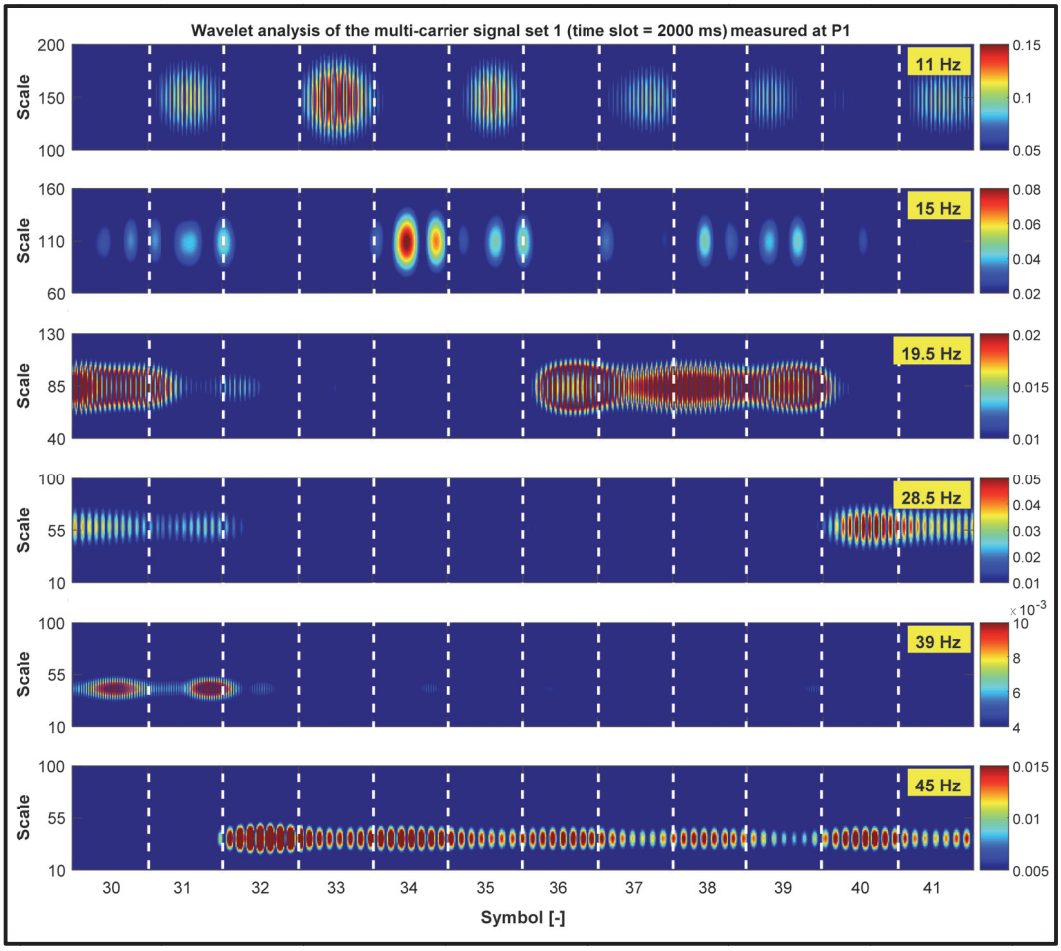

Figure 9.11: Multi-step Wavelet analysis of the transmitted multi-frequency signal (set 1) sent from the first transmitter position and measured at P1 (time slot = 2 s, code modulation = OOK, carrier frequencies = 11, 15, 19.5, 28.5, 39 and 45 Hz, audio amplifier = 65 clicks, sampling rate = 2000 Hz, flow rate = 20.1 m^3/h)

Depending on the last analysis results, it could be said that the STFT analysis could provide a view of the frequency components contained in the measured signal even if the interfering noise is not filtered. Moreover, it could be used to evaluate the carrier frequencies in some cases without the need for noise cancellation. In contrast, analyzing the received signals using the Wavelet analysis could not be performed without noise cancellation. The Wavelet analysis might be a very suitable way for dealing with single-carrier signal. The better the specific signal characteristics to be detected (amplitude, frequency, and waveform) are known, the more efficiently the Wavelet algorithm can search for it. This makes it possible to detect weak pressure signals measured with strong interfering noise. This could also make Wavelet advantageous, if other waveforms, for instance triangle or rectangle waves) would be used for data transmission in boreholes.

9.3 Initial investigations of hydraulic data transmission using chirp modulation and different pressure wave forms

The developed experimental multi-frequency generator has opened a window to study how it could seem, if totally different new ideas would be applied for first time for the hydraulic data transmission in boreholes. With the experimental multi-frequency generator, data transmission tests using one of the latest radio technologies, chirp modulation or chirp spread spectrum (CSS), were executed and evaluated. Furthermore, many transmission tests using different wave forms for the generated pressure waves were performed and analyzed. The results of the initial laboratory investigations of the two ideas are presented in the next section.

9.3.1 Data transmission using chirp modulation (Chirp Spread Spectrum, CSS)

A transmission CSS signal was modulated to send 16 different up and down short frequency chirps. Accordingly, 16 different symbols could be represented and four bits could be loaded in each transmission symbol. Each short chirp had a length of three seconds and had to sweep up or down for 5 Hz. A list of the modulated transmission symbols can be found in the Appendix. The STFT analysis of the CSS signal measured at P1 (very close to the pump) is presented in Figure 9.12.

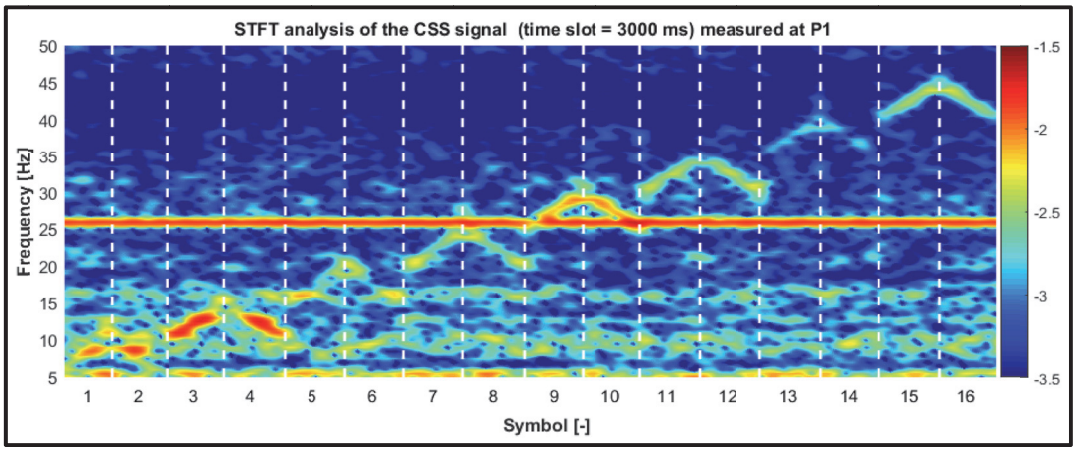

Figure 9.12: STFT analysis of the CSS signal sent from the first transmitter position and measured at P1 (time slot = 3 s, code modulation = chirp modulation, frequency chirps = 5-10, 10-15, 15-20, 20-25, 25-30, 30-35, 35-40 and 40-45 Hz, audio amplifier = 65 clicks, sampling rate = 2000 Hz, flow rate = 20.1 m^3/h)

The more chirps can be distributed in the frequency spectrum, the higher is the data rate. The transmission example presented in Figure 9.12 shows that 16 chirps could be

distributed over the used transmission band and recognized at the receiver end. But the chirp modulation could not contribute alone to increasing the hydraulic data rates, because each chirp requires a certain spreading time to be recognizable. In the presented example three seconds were required for generating a short chirp representing a symbol with four bits. This can be expressed as a data rate of 1.333 bit/s, which is much lower than the data rate of the single frequency mud siren. The main advantage of chirp modulation application in radio technologies was to make the transmission process highly robust against the strong interfering noise.

Depending on the presented transmission test, it could be said that the chirp modulation was successfully applied to transmit the data even in the most noisy frequency range of the transmission band, also in the frequency window where the noise of the mud pump is dominant. This can be clearly recognized in the transmission symbols (7, 8, 9 and 10) in Figure 9.12. To date, transmitting the data via mud pulse telemetry using the conventional modulation techniques in the frequency range, where the noise of the mud pump is dominant, is not possible. This advantage of chirp modulation could be used in turn for increasing the data rate, where chirp modulation could be used for transmitting only two symbols (having one bit) or four symbols (having two bits) in the most noisy frequency range of the transmission band. At the same time, the used multi-frequency generator could transmit other data over several carrier frequencies (in other frequency ranges) using at least one of the conventional code modulations (like OOK).

9.3.2 Data transmission using different wave forms

For each wave form, pressure waves at a carrier frequency of 20 Hz were generated using the experimental multi-frequency generator. The signals with a duration of 10 s were sent from the transmitter position 3 and measured at P1. They were evaluated in time and frequency domains and compared with each other. A pass filter was applied to remove the hydraulic noise from the measured signals. Since each one of the investigated wave forms has its own harmonics and differs from the other waves, the applied pass filter was to be adapted according to the harmonic series of each wave type. Figure 9.13 and Figure

9.14 show the evaluation of the measured signal after filtration in the time and frequency domains, respectively.

It was found that the rectangle wave has the highest measured amplitude in both time and frequency domains. According to the measured values in time domain, it could have a transmission reach of 33% higher than the reach achieved by using the standard sine wave. This could be explained by the area existing under the wave curve which, in turn, corresponds to the energy amount contained in this area for each used wave form. Assuming that the symbol (1) having a fixed duration or time slot (T) and a constant amplitude (A) would be transmitted with the mentioned wave forms. As shown in Figure 9.15, for the same transmission parameters (F, T and A), the energy amount contained in the area existing under the wave curve for the rectangle wave form is the highest. And therefore, it could enable transmitting the data over longer distances.

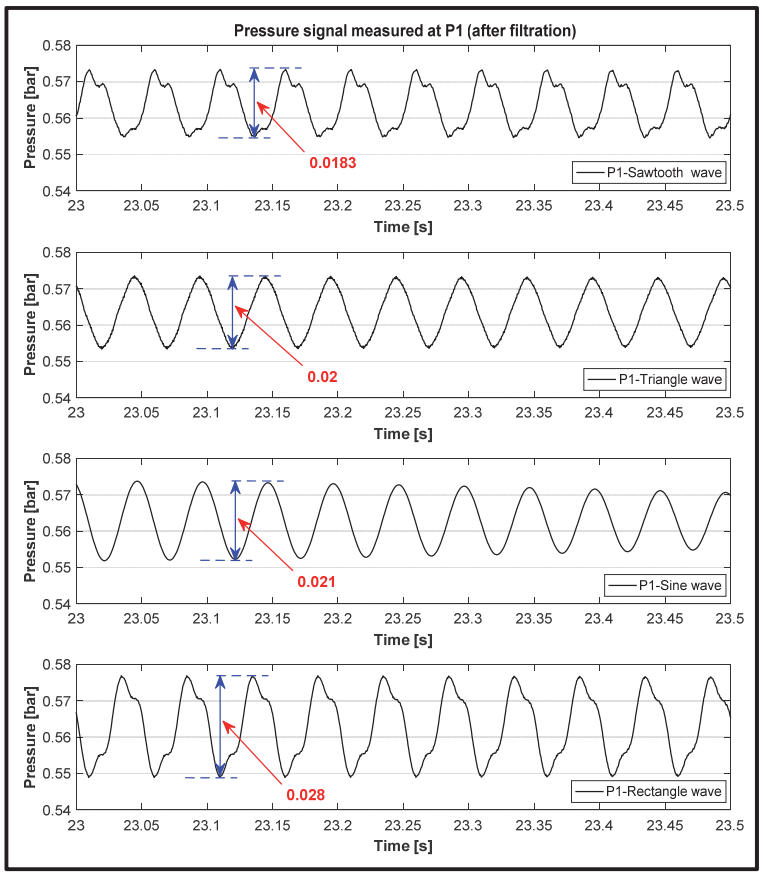

Figure 9.13: Pressure signals with different wave forms after filtration sent from the third transmitter position and measured at P1 (transmission time = 10 s, carrier frequency = 20 Hz, audio amplifier = 90 clicks, sampling rate = 2000 Hz, flow rate = 20.1 m^3/h)

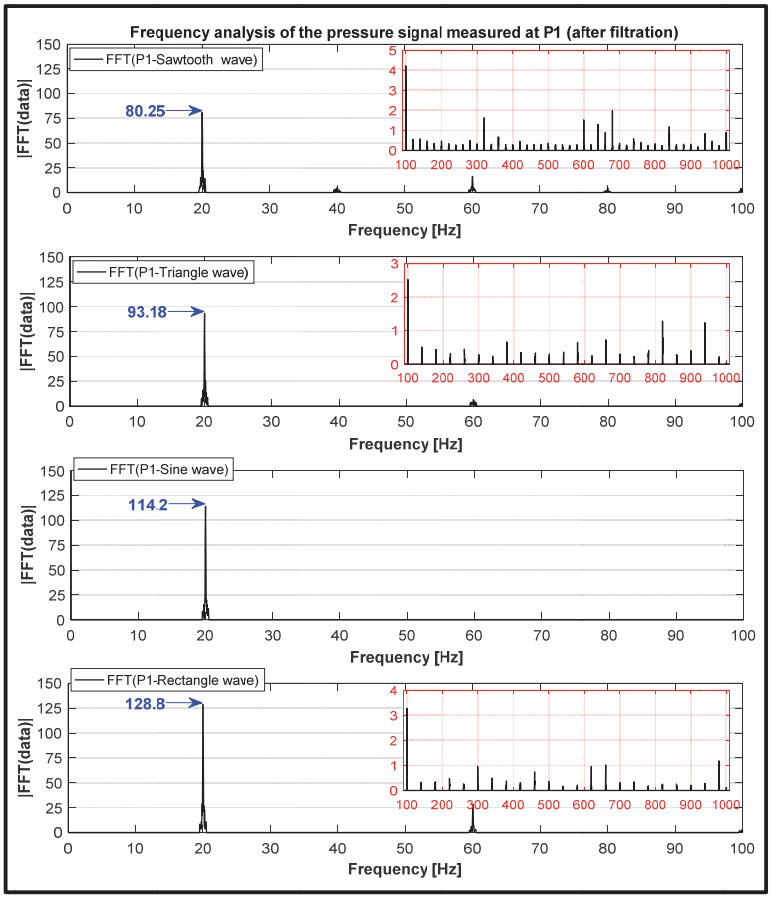

Figure 9.14: Frequency analysis of the measured signals with different wave forms after filtration

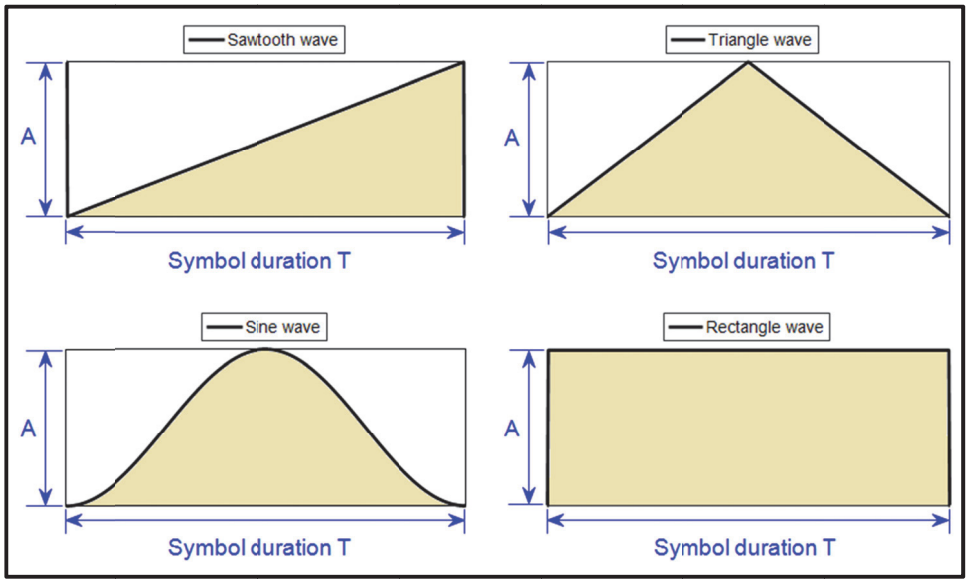

Figure 9.15: Energy amount contained within the area existing under the wave curve for different wave forms by transmitting the same symbol at the same transmission parameters (F, T and A)

CHAPTER 10 Investigation of the Use of a Multi-Sensor Receiver for Improving the Hydraulic Data Transmission in Boreholes

The receiver position has a great influence on the received telemetry signal. The measured signal amplitude and, accordingly, the resulting pass and stopbands at a certain time are related to the considered receiver position. The propagated carrier wave has minimum pressure amplitudes at some certain positions (pressure nodes) and maximum pressure amplitudes at other certain positions (pressure antinodes). To date, the telemetry signal is measured at the surface using one or two receiver sensors. Overcoming the transmission limitations represented in the resulting stopbands and improving the detection of pressure carrier waves at the surface could be achieved by using a multi-sensor receiver. Depending on the transmitter and receiver configuration, two transmission cases were investigated. In the first case, the use of a single transmitter and multiple receiver elements (SIMO) was investigated. In the second case, the simultaneous use of multiple transmitter and receiver elements (MIMO) was investigated. The use of a multi-sensor receiver was investigated numerically with the available ANSYS CFX model and laboratory by means of the experimental multi-frequency generator. The investigation results are presented in the next sections.

10.1 Numerical model investigation of the use of a multi-sensor receiver

10.1.1 Data transmission using single-input and multiple-output (SIMO)

The available ANSYS CFX simulation model with one transmitter (single mud siren) was updated. To follow the carrier wave generated by the single mud siren and propagating towards the main receiver P1 and to find out the best measuring positions for a successful signal receiving and detection, several monitoring points were installed along the pipeline. As shown in Figure 10.1, 18 monitoring points are set between P3 and P2 (P2-1 to P2-18). Similarly, 14 monitoring points are set between P2 and P1 (P1-1 to P1-14). The distance between each two adjacent monitoring points is 1 m. The transmission function for the test facility pipeline with a single transmitter is represented in Figure 8.1.

It shows, for instance, that the carrier frequencies of 49 and 53 Hz were measured at P1 with lower amplitudes and, consequently, are located in a stopband. These two carrier frequencies were selected to be numerically investigated using a multi-sensor receiver.

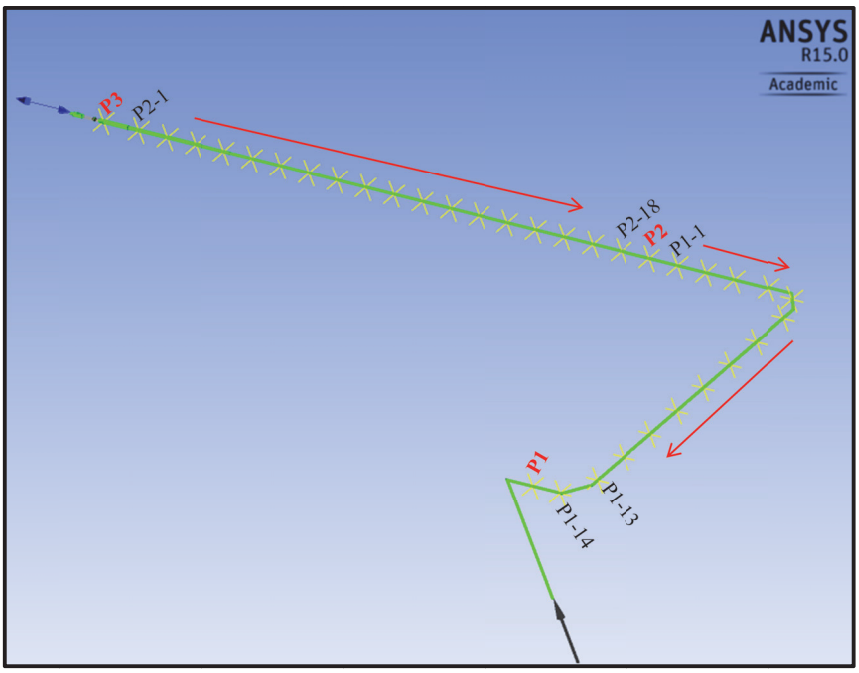

Figure 10.1: ANSYS CFX numerical model for the test facility with a single transmitter and several monitoring points

Steady-state and unsteady-state simulations were run. With the steady-state run, the mud siren was turned off. The inlet boundary condition for steady-state simulation was set as a constant mass rate (8.428 kg/s) which corresponds to a flow rate (Q) of 30.4 m^3/h. The outlet boundary condition was set as an opening constant pressure (0.817 bar). In unsteady-state runs, the single mud siren was turned on with a specific rotational speed depending on which frequency was to be generated (49 or 53 Hz). Depending on the steady-state results, the inlet boundary condition for unsteady-state was set to a constant total pressure (1.562 bar), and the outlet boundary condition was set as an opening constant Cartesian velocity components (U= 0, V= 3.327 m/s, and W= 0 m/s).

Simulation runs were executed to investigate the carrier frequencies of 49 and 53 Hz. The pressure signal for each carrier frequency predicted at the installed monitoring points was analyzed in the frequency domain. For instance, Figure 10.2 shows the predicted amplitudes in the frequency domain of the pressure wave generated with a carrier

frequency of 49 Hz at the considered monitoring points. The carrier wave was predicted at P1 with a much lower amplitude. But as expected, the same carrier wave could be predicted with higher or much higher amplitudes at other monitoring points. Such positons are also very close to P1. For instance, the predicted amplitude at the monitoring point P1-13, exactly at a distance of 2 m from P1, was 15 times larger than the amplitude predicted at P1.

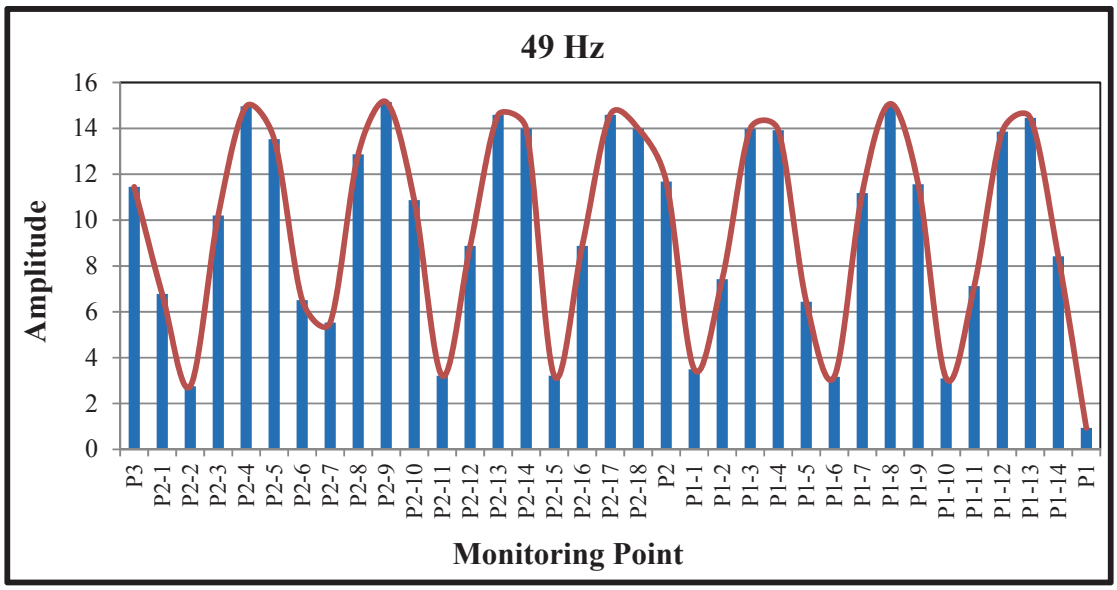

Figure 10.2: Predicted amplitudes in the frequency domain of the pressure wave with a carrier frequency of 49 Hz at several monitoring points

By using a receiver unit consisting of just the main receiver sensor P1, the carrier frequency of 49 Hz was located in a stopband and could not be used for data transmission. Once another receiver located at a distance of 1 m (P1-14) or 2 m (P1-13) from the main receiver P1 (or more receivers) would be used, the 49 Hz carrier wave could be successfully measured and detected. Accordingly, the carrier frequency of 49 Hz could be used for transmitting the data. This was not possible in the case of the single main receiver P1.

The investigation of the pressure wave generated with the carrier frequency of 53 Hz has shown the same results, see Appendix. The simulation results confirmed the theoretical description of the pressure nodes and antinodes for a carrier wave propagated inside a pipeline illustrated in Figure 5.4.

10.1.2 Data transmission using multiple-input and multiple-output (MIMO)

The investigation of the simultaneous use of two transmitters (two mud sirens or two stator/rotor sets) for increasing the data rate was presented in (8.3.1). The generated signals were predicted using only the main receiver P1. This case is known in wireless communication as MISO (multiple-input and single-output). It was found that the generation of two carrier frequencies at the same time is very complex. The two transmitters were operated to generate two frequencies (15 and 39 Hz), but at the main receiver a different couple of dominant frequencies was detected (15 and 24 Hz). The carrier frequency of 39 Hz was predicted with a much lower amplitude compared to the 15 and 24 Hz. This was a main challenge for the use of the concept of the multiple sirens for simultaneous generating of several carrier frequencies.

A solution should be found in order to compensate the interface or any unwanted frequency and successfully detecting and extracting only the induced carrier frequencies. The use of a receiver unit with multiple sensors could enable a successful detection of the two desired frequencies. For all the simulation runs represented in Chapter 8, a few monitoring points in addition to P1, P2, P3 and P4 were installed along the pipeline and used to maintain the comparability between the current numerical model and the first simulation model developed by Namuq et al. (2012), see the yellow cross points in Figure 8.10. One of these monitoring points was located at a distance of 4.039 m from P1. Figure 10.3 presents the frequency analysis of the pressure signal predicted at P1 (upper section) and at a monitoring point at a distance of 4.039 m from P1 (lower section).

The results show that the two induced carrier frequencies (15 and 39 Hz) could be successfully detected and the interface frequency (24 Hz) could be neglected with its minimum amplitude, when the measuring point is shifted for 4.039 m from P1. Thus, the use of a multi-sensor receiver can effectively help to overcome the challenges encountered by the data transmission using a multi-frequency mud siren, where the generated and desired carrier frequencies could be received with amplitudes sufficient to be recognized and detected. Consequently, the use of the multi-frequency mud siren in a combination with a multi-sensor receiver could increase the hydraulic data transmission rates in boreholes.

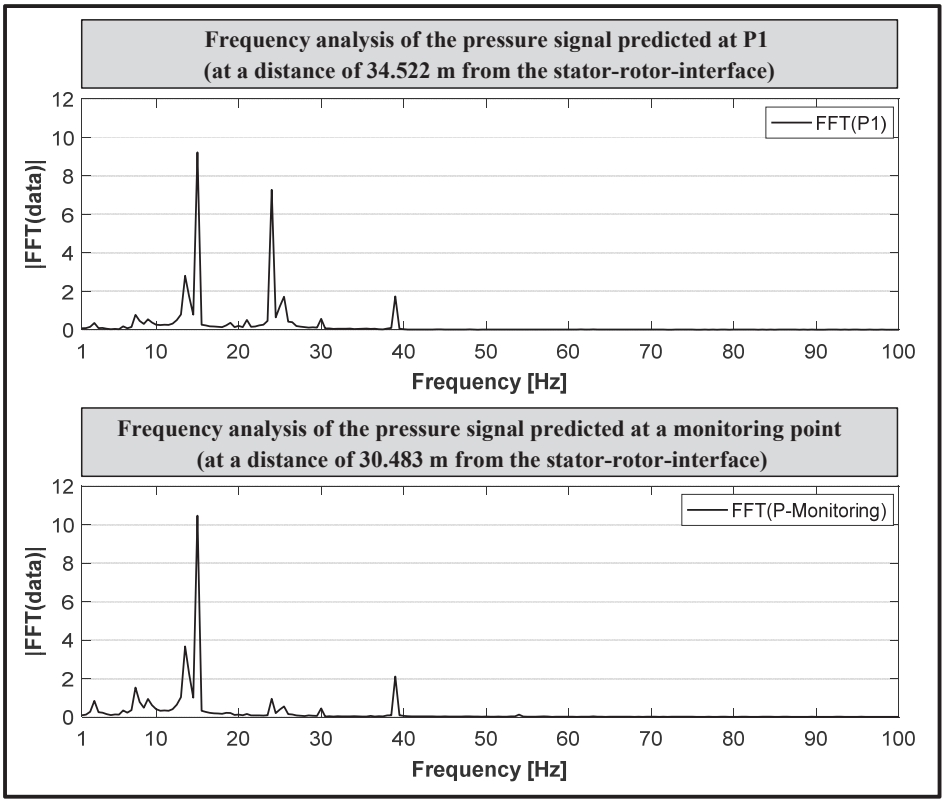

Figure 10.3: Frequency analysis of the pressure signal generated using two sirens connected in series and predicted at P1 (upper section) and at a monitoring point at a distance of 4.039 m from P1 (lower section)

10.2 Laboratory investigations of the use of a multi-sensor receiver

The experimental multi-frequency generator was used for the laboratory investigations of the use of a multi-sensor receiver. In this case, sweeps were sent from all the four transmitter positions. The generated wave will encounter many reflectors along the pipeline of the test facility. The first dogleg (kink) in the pipeline behind the pressure sensor P2 was considered as the first reflector. For simplification, only the propagation way between the membrane and the first reflector was considered during the investigations. Sending the sweeps from all the four transmitter positions could allow shifting the distance between the membrane and the reflector within a range of 3 m and, accordingly, to vary the existing pressure nodes and antinodes of the investigated carrier wave.

Figure 10.4 shows the frequency spectra of the sweeps sent from all four positions and received at the pressure sensor P3. It could be noticed that the sweeps sent from all the

four transmitter positions and measured at P3 have shown an approximately equal strength in the low frequency range up to approximately 20 Hz. At higher frequencies, the measured sweeps significantly differ in some cases.

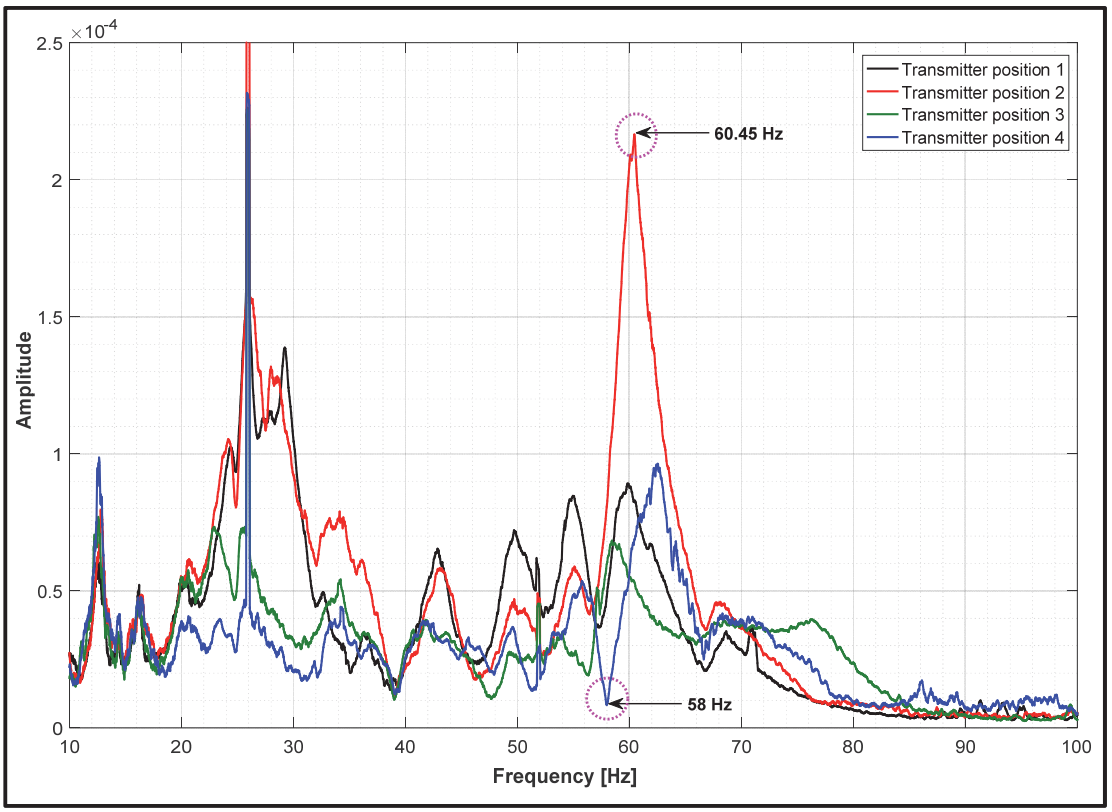

Figure 10.4: Frequency spectra of sweeps sent from all four transmitter positions and received at P3, (modified), (Ehras, 2016)

A focus was given to the waves with carrier frequencies of 58 and 60.45 Hz, since the carrier frequency of 58 Hz sent from transmitter position 4 was measured with its maximum amplitude and the carrier frequency of 60.45 Hz sent from transmitter position 2 was measured at its minimum amplitude at P3. For a propagation speed of 462 m/s, the resulting wave lengths of the carrier frequencies of 58 and 60.45 Hz are 7.966 and 7.643 m, respectively. The calculated positions of the pressure nodes and antinodes for the carrier wave with the frequency of 58 Hz sent from the transmitter position 4 and for the carrier wave with the frequency of 60.45 Hz sent from the transmitter position 2 are represented in Figure 10.5.

The distance from the membrane built in position 4 to the pressure sensor P3 is exactly 4 m. The first pressure node for the 58 Hz carrier wave is located at a distance of 3.983 m from the membrane. Thus, the pressure sensor P3 is located at a pressure node for the 58 Hz carrier wave, see the top section of Figure 10.5. Therefore, it was measured with its minimum amplitude as shown in Figure 10.4. The pressure sensor P3 is located at a distance of 2 m from the membrane built in position 2. The 60.45 Hz carrier wave sent from position 2 shows a first pressure antinode at a distance of 1.911 m from the membrane. This means that the pressure sensor P3 is approximately located at the first pressure antinode for the 60.45 Hz carrier wave, see the lower section of Figure 10.5. Therefore, it was measured with its maximum amplitude as shown in Figure 10.4.

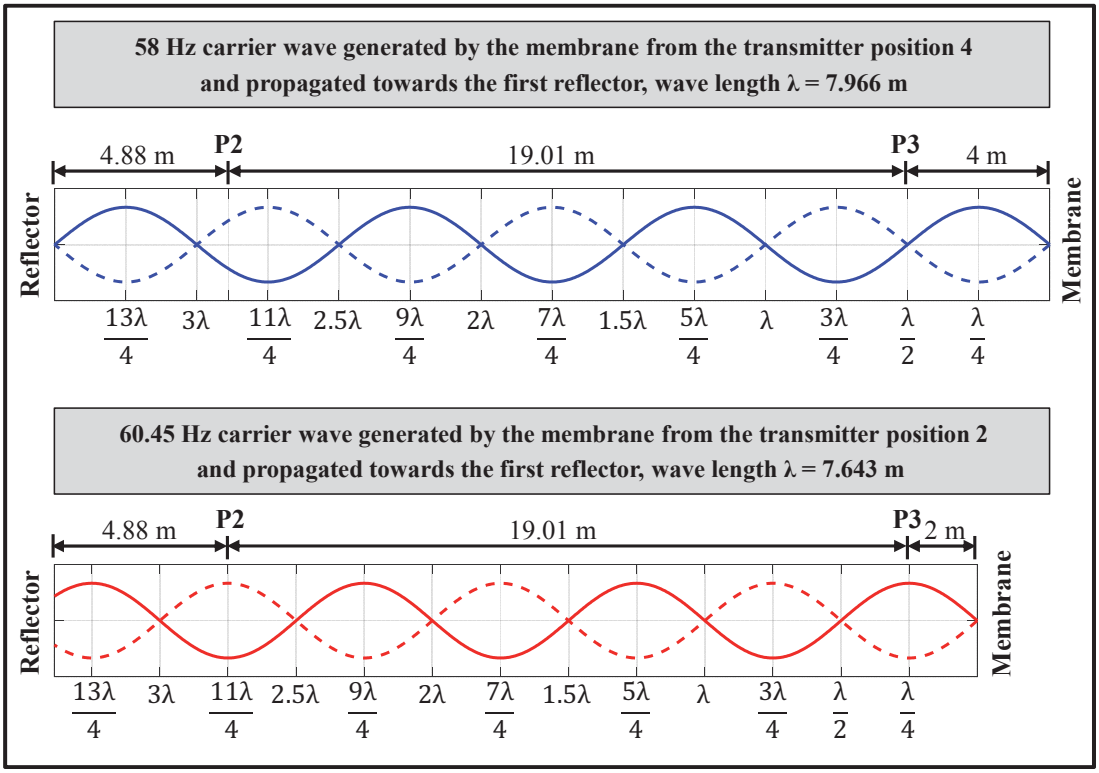

Figure 10.5: Calculated pressure nodes and antinodes for the 58 and 60.45 Hz carrier pressure waves sent from the transmitter positions 4 and 2, respectively

The calculated pressure nodes and antinodes represented in Figure 10.5 show that the pressure sensor P2 is located at a position between the sixth pressure antinode and sixth pressure node in case of the 58 Hz carrier wave sent from transmitter position 4. In case of 60.45 Hz carrier wave sent from transmitter position 2, the pressure sensor P2 is

approximately located at the sixth pressure antinode. Therefore, it was expected that the 58 Hz carrier wave sent from transmitter position 4 could be measured at P2 with a higher amplitude and the 60.45 Hz carrier wave sent from transmitter position 2 could be measured with its maximum amplitude. The frequency spectra of the sweeps measured at the pressure sensor P2 are represented in Figure 10.6. They show a slight deviation from the prediction presented in Figure 10.5.

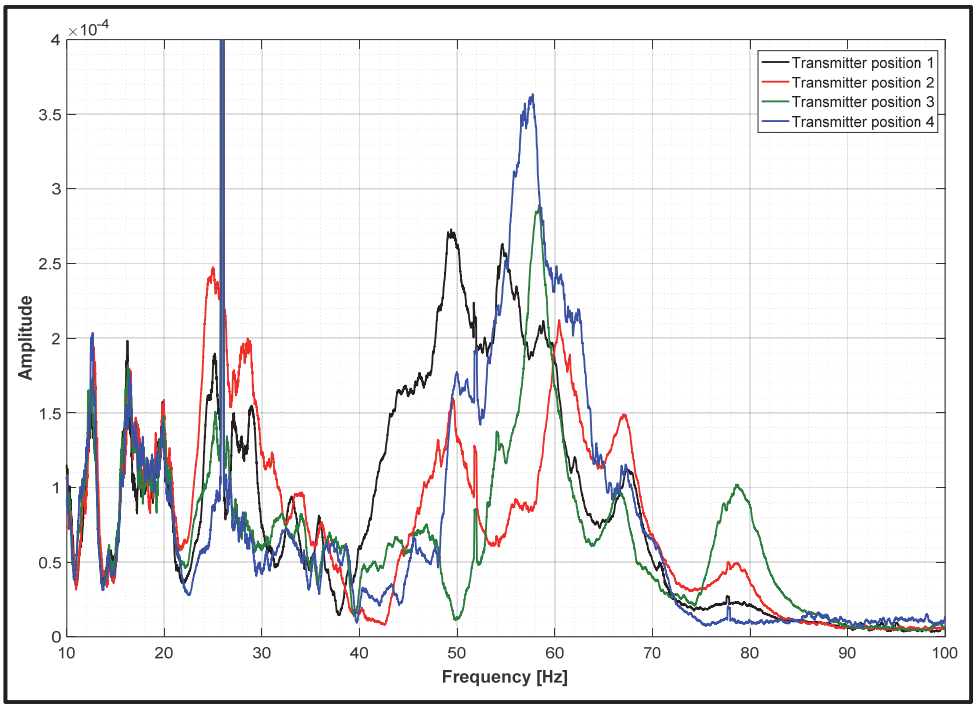

Figure 10.6: Frequency spectra of sweeps sent from all four transmitter positions and received at P2, (modified), (Ehras, 2016)

Actually, the 58 Hz carrier wave sent from transmitter position 4 was measured at its maximum, and the 60.45 Hz carrier wave sent from transmitter position 2 was measured at a higher amplitude. The reasons for such a slight deviation could be that the constructive overlapping was different for the two investigated carrier waves. It could be that the propagation velocity of the wave inside the pipe is not constant at 462 m/s, since the pipeline has not only one internal diameter. The carrier wave will encounter many reflectors along its propagation way from the membrane towards the pump. However, only the first reflector behind the pressure sensor P2 was considered for creating the prediction of pressure nodes and antinodes represented in Figure 10.5.

The sweeps sent from all the four transmitter positions were also measured at the pressure sensor P4 which is located directly behind the transmitter section. The frequency spectra of the sweeps measured at the pressure sensor P4 are represented in Figure 10.7. In comparison to the sweep spectra measured at the other two pressure sensors (P3 and P2), it could be found that the generated waves were measured with much higher amplitudes. The pressure sensor P4 is directly located in front of the dogleg (kink) that connects between the transmitter section and the backflow pipeline. This dogleg behaves as a reflector. This in turn confirms that pressure antinodes are created close to the reflectors through the wave reflections.

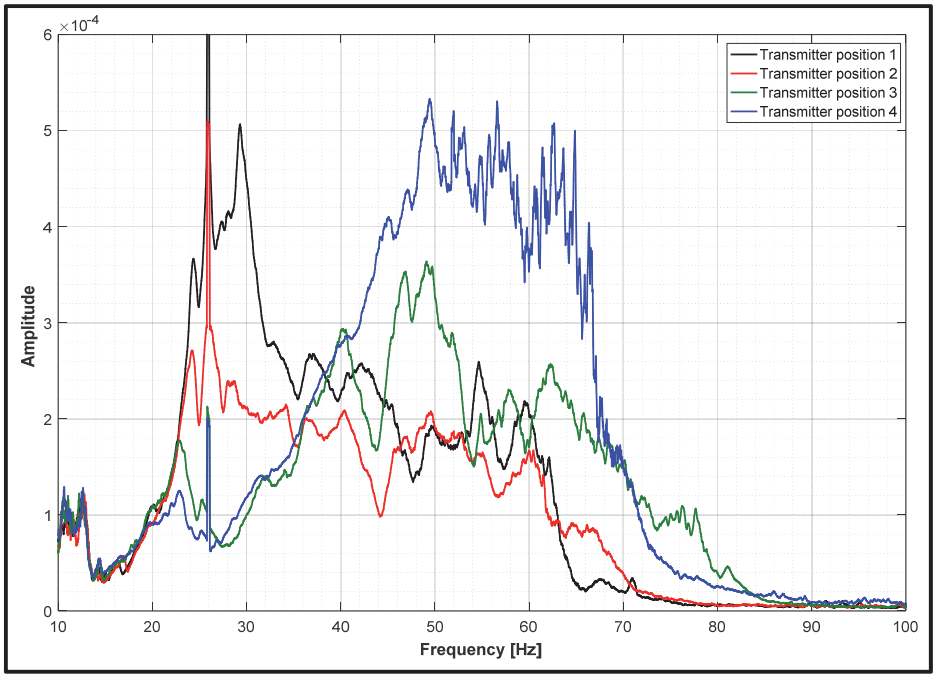

Figure 10.7: Frequency spectra of sweeps sent from all four transmitter positions and received at P4, (modified), (Ehras, 2016)

10.3 Evaluating the use of a multi-sensor receiver for improving the hydraulic data transmission in boreholes

The effect of the measuring position on the transmitted carrier signal and the use of a multi-sensor receiver as well were numerically and laboratively investigated. Different scenarios were applied and tested during the investigations. The investigations have demonstrated the great effect of the measuring position on the carrier signal transmitted

and propagated in a pipeline. The relationship between the measuring position and the positions of the pressure nodes and antinodes of the carrier wave determines whether the carrier wave could be measured with a higher/maximum or minimum amplitude. Therefore, the use of a single-sensor receiver in practice cannot successfully detect all the transmission carrier waves which have different configurations of pressure nodes and antinodes.

The undetected or with minimum amplitudes measured carrier waves will be located in stopbands and cannot be used for transmitting the data. This does not mean, however, that those carrier waves are always located in stopbands. The existing stopbands are related to the used single-sensor receiver. Once another measuring sensor is used, different pass and stopbands can exist. A carrier wave with a certain frequency can be located in a stopband at a measuring sensor (I) but in a passband at another measuring sensor (II). For instance, the single carrier signals, 49 Hz and 53 Hz, were located in stopbands based on the measurement using only P1. Thanks to the use of the multi-sensor receiver, they could be measured with higher amplitudes and used for transmitting the data.

Thus, the transmission limitation represented in the stopbands could be overcome by the use of multiple measuring sensors. This will increase the number of the carrier frequencies that are available to be used for data transmission. As a result, the capacity of the transmission system can be increased. It could also contribute to the increase of the data rates through the successful detection of the received signals.

Detection of the two-frequency signal generated by the multi-frequency mud siren was very difficult by using a single-sensor receiver. Thanks to the use of the multi-sensor receiver, the two induced carrier frequencies could be successfully predicted and detected as shown in the transmission example (15 and 39 Hz). This could help to make the concept of multi-frequency mud siren usable in the practice. The investigations have also shown that the carrier waves could be predicted with a much higher amplitude when the measuring sensor is located very close to a reflector. For instance, Figure 10.2 has shown much higher amplitudes at the monitoring positions (P1-3, P1-4, P1-12 and P1-13),

which are located very close to reflectors. This issue was also confirmed through the laboratory investigation. Figure 10.7 has shown that the sweeps sent from all the four transmitter positions and measured at P4 were measured with higher amplitudes than at other pressure sensors (P2 and P3). The pressure sensor P4 is located much closer to a reflector. It could be claimed that pressure antinodes are created close to the reflectors through the wave reflections. It could be useful, therefore, to install one sensor at least near to an available reflector.

The use of the multi-sensors receiver seems to be very promising for increasing the efficiency of the data transmission in boreholes. In practice, however, the standpipe connecting between the mud pumps and the drill string may not be suitable to install multiple pressure sensors. Instead, the top section of the drill string below the blowout preventer (BOP) could be used for installing such multiple pressure sensors. Assuming that carrier frequencies between 10 and 40 Hz are used for transmitting the data, and the generated pressure waves travel to the surface at a velocity of about 1300 m/s, then the top 50-100 m of the drill string below the blowout preventer could be used for installing the multiple pressure sensors. The data collected by these sensors could be retransmitted to the main receiver unit at the surface using electromagnetic waves, see Figure 10.8. For instance, at each measuring position a small unit including the pressure sensor plus an electromagnetic transmitter may be used.

With the progress of the drilling operation, new drill pipes should be screwed onto the drill string. The drill pipes containing the multiple sensors should be tripped out of the borehole before screwing the new drill pipes. The drill pipes containing the multiple sensors will be screwed onto the top of the new drill pipes and run back into the boreholes. This process including tripping out of the drill pipes having multiple sensors, screwing of new drill pipes and finally running back the drill pipe with multiple sensors into the borehole, will take a lot of nonproductive time and, accordingly, additional drilling costs which must be avoided. In order to make the new approach suitable for the use in practice, the drill pipes containing the multiple sensors should be used as usual drill pipes and should not be tripped out before adding new drill pipes. The successful detection of the signal at the surface becomes more challenging with the increased

drilling depths. The large amount of data is required in drilling operations at depths of, may be, up to 3.000 m. Therefore, the drill pipes containing such multiple sensors could be used, for instance, only when the drilling depth is up to 3.000 m. The electromagnetic waves could be successfully transmitted and received over a distance of a 1.000 m. Once the drilling pipes containing the multiple sensors are away from the surface, may be more than 1.000 m, then this set of drill pipes should not be used any longer as a multiple receiver. Instead, a new set of drill pipes with multiple sensors could be screwed to the top of the drill string below the BOP and used for receiving the signals.

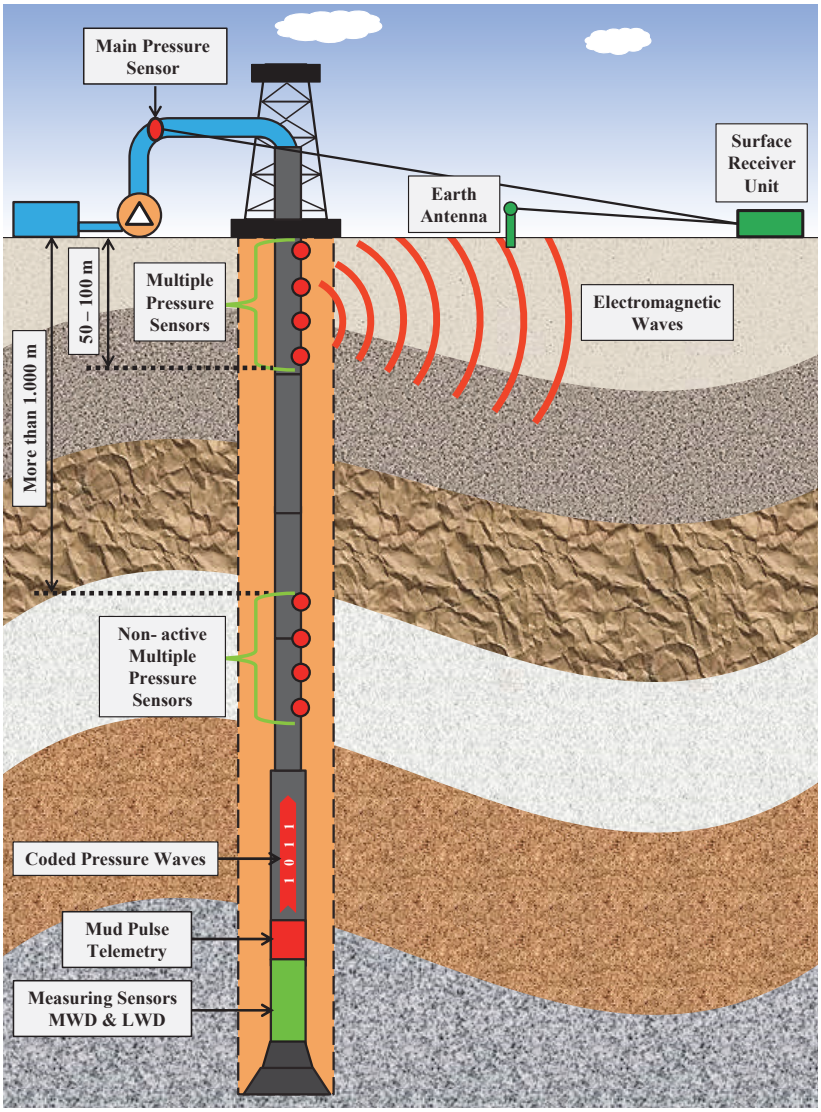

Figure 10.8: Mud pulse telemetry with multiple pressure sensors receiver unit

CHAPTER 11 Conclusion and Outlook

11.1 Conclusion

Cost-effective drilling operations with high safety and precise placement of the last borehole section into the reservoir require transmitting the processed geological and directional data from the bottom of the borehole towards the surface with higher rates in real time. The mostly used system for data transmission in boreholes is the mud pulse telemetry. The main disadvantage of the mud pulse telemetry is its low data rates. Improvement of the data transmission rate was the main target of the present research work. Alternative methods for speeding up the data transmission of the mud pulse telemetry were to be developed and investigated.

The mud pulse telemetry system, like any transmission system, consists of transmitter end, transmission channel and receiver end. The drilling mud inside the drill string is used as a transmission channel. The drilling mud specifications and the drill string dimensions are identified within the context of the drilling program, and thus, they could not be changed during the drilling process for purposes such as a better data transmission. Therefore, the development work during the present research work has focused only on the transmitter and receiver ends.

Several new approaches regarding the transmitter end were developed. In the first approach, a hybrid mud pulse telemetry was developed and tested. The hybrid mud pulse telemetry uses two different transmitter devices, such as a mud siren and a pressure pulser, for transmitting the data at the same time. The hybrid mud pulse telemetry works at two different time slots. Each component of the hybrid mud pulse telemetry system (mud siren and pressure pulser) works at its own workable transmission time slot. Two different combinations, the combination of the mud siren with the positive pressure pulser and the combination of the mud siren with the negative pressure pulser, were successfully investigated and tested. Hence, the hybrid mud pulse telemetry was tested using different combinations of code modulations. All the transmission signals could be successfully received and decoded. The laboratory investigations have confirmed the

functionality of the hybrid mud pulse telemetry system (see Chapter 7). Assuming that the mud siren and the pressure pulser are operated in practice at time slots of 0.1 and 0.5 s, respectively, an increase in the data transmission rate of 20% can be achieved. The achieved increase is not much higher to boost the downhole data transmission into a new age. But on the other side, the achieved increase in the data rate does not require a lot of changes in the downhole tools, since all the mechanical/hardware components for such a system are already available and used but in a separate way. An approach for using the hybrid mud pulse telemetry in practice is described in Chapter 7. The most particularly interesting data during the drilling process can be transmitted to the surface in a faster sequence using the mud siren while the less important ones can be transmitted using the pressure pulser (see Figure 7.7).

In the second approach a great focus was made on the multi-frequency mud siren. The capability of the multi-frequency mud siren to simultaneously generate two carrier frequencies was investigated. For this purpose, a multi-frequency mud siren consisting of two sets of stator/rotor was investigated based on mathematical and numerical models. Several configurations of stators/rotors, such as a row connection and a parallel connection, were taken into consideration. The investigation results have shown a third carrier frequency in addition to the two induced carrier frequencies. The third frequency was identified as an interference frequency. Using the additional received carrier frequency for encoding the data would allow to employ the multi-frequency mud siren for transmitting the data. A data encoding concept for transmitting two bits per time slot using three frequencies is described in Chapter 8 (see Table 8.3). Thus, the data transmission rate can be doubled by using a two-frequency mud siren.

The mud siren is faster than the pressure pulser but it has a lower transmission reach compared to the pressure pulser. It was found during the investigations using two sets of stator/rotor that the intensity of the transmission signal, and thus the transmission reach, could be increased. Here, the two rotors should be operated at the same rotational speed to generate the same carrier frequency. It should be taken into consideration that the two rotors must be operated at the same phase. With a transmission example, an extension in the transmission reach of approximately 40 % was achieved, see Chapter 8.

Using multi-carrier frequencies for transmitting the data in boreholes can significantly increase transmission rates of the mud pulse telemetry. Generating multi-carrier signal using a multi-frequency mud siren is a very complicated issue, as shown in Chapter 8. In order to further investigate the data transmission using multi-carrier frequencies, an experimental multi-frequency generator prototype was built for the use at the IBF test facility. Several transmission tests were executed using the experimental multi-frequency generator. The test results have shown that it seems possible to transmit the data via the hydraulic mud channel over several carrier frequencies. Up to six frequencies, and consequently up to six bits/symbol, could be transmitted. However, considerable further development and optimization work both on the transmitter end (stronger signals) and on the receiver end (signal processing) is required to develop a sound concept for practical use. The evaluation of the received signals has shown that modulating and transmitting of one word over several carrier frequencies at the same time could have errors. Decoding of the transmitted symbols could be failed out when one of the several carrier frequencies could not be successfully received. For a robust multi-carrier data transmission in boreholes, each available individual carrier frequency should be used for modulating and transmitting of only one individual word of the telemetry data frame. This method is one of the wireless communication techniques and called as frequency division multiplexing. An example for transmitting a telemetry data frame in boreholes using six carrier frequencies is illustrated in Figure 9.8 (see Chapter 9).

One of the biggest challenges regarding data transmission in boreholes using the mud pulse telemetry is the dominant noise of the mud pumps. Transmission tests using the chirp modulation, one of the latest radio technologies, were performed. The executed transmission tests have shown that applying the chirp modulation could enable transmitting the data even in the frequency range where the noise of the mud pumps is dominant.

In the context of the present research work, transmission tests were executed using sawtooth, triangle, rectangle and sine waves to find out which wave form could be used for performing data transmission with a higher reach. The experimental multi-frequency generator was used for executing the transmission tests. The transmission test results

have shown that the rectangle wave has the highest measured amplitude in both time and frequency domains. The energy amount contained in the area existing under the wave curve for the rectangle wave form is higher than by all other wave forms, therefore it could be used for transmitting the data over longer distances. Based on the transmission tests in Chapter 9, rectangle waves could be used to achieve transmission reaches of approximately 33% higher than those achieved by using the sine wave.

At the receiver end, development work was made to improve the signal detection and to insure that the receiver end is capable to successfully receive and process multi-frequency signals. All the measured multi-frequency signals were evaluated and analyzed using the Fourier and Wavelet tools for signal analysis. In contrast to the Fourier analysis, the Wavelet analysis could not provide a good evaluation of the measured multi-frequency signal without filtering the hydraulic noise and all the other unwanted frequency components that do not belong to the generated signal. For both signal analysis tools, the investigation results have shown that analyzing a multi-frequency signal using the same signal strength scale can make the frequencies detection more difficult. It becomes more challenging by using the Wavelet analysis, since the color bands representing lower frequencies in the Wavelet analysis are stretched over a wide range.

For a successful evaluation and analyzing of the measured multi-frequency signals, a certain series of processing steps was required. This includes filtration of the hydraulic noise from the measured signal and the analysis of each individual carrier frequency with a suitable signal strength scale. The need for a separately evaluation for each measured carrier frequency at the receiver end lends itself very well to the suggested method for decoding and transmitting the data over several carrier frequencies at the transmitter end based on frequency division multiplexing, see Figure 9.8.

The effect of the receiver position on the signal detection was investigated numerically and laboratively. The investigation results have demonstrated the great effect of the measuring position on the carrier signal propagated in a pipeline. The carrier wave could be measured with a higher/maximum or minimum amplitude at the receiver end depending on the relationship between the measuring position and the positions of the

pressure nodes and antinodes of the carrier wave (see Figure 10.4 and Figure 10.5). The use of a multi-sensor receiver could increase the efficiency of the receiver unit and its capability for successful signal detection. A carrier wave with a certain frequency can be located in a stopband at a certain measuring sensor but in a passband at another measuring sensor (see Figure 10.2). Moreover, the use of a multi-sensor receiver could allow a successful detection of the multi-frequency signal generated by the multi-frequency mud siren (see Figure 10.3). This was not possible by using only a single-sensor receiver. Due to the promising results, an innovative approach for installing a receiver unit with multiple pressure sensors at the drilling rig is drafted and explained in Chapter 10 (see Figure 10.8).

Based on the results of the present research work, it could be said that a two-frequency mud siren could be used in a combination with a pressure pulser to increase the data rate. An increase in the data transmission rate of more than the double could be achieved.

11.2 Outlook

Transmitting the data in boreholes in passband via multi-carrier frequencies could be very promising. However, there is still a need for further research and developments in order to make the multi-frequency transmission usable in the field. The results of the present research work can be used as a basis for the next research and development works.

A laboratory prototype for a multi-frequency mud siren should be built. The construction and design of the laboratory prototype must be so flexible, that different configurations of stator/rotor sets can be installed and testes. Such configurations could be, for instance, one stator and two rotors in a row connection, two sets of stator/rotor in a row connection and two sets of stator/rotor in a parallel connection. Hence, the construction and design of the stator/rotor lobes must be flexible, so that the multi-frequency mud siren could also be investigated by using different wave forms.

Several receiver sensors, for instance with 1 m distance between each other, could be installed at the pipeline section between P1 and P2, in order to study the propagation behavior of the generated multi-frequency signal. The mathematical model developed

during the present research work could be extended to be able to calculate and predict the generated multi-frequency signal after its propagation along the pipeline of the test facility. The extended mathematical model should take the fluid compressibility into consideration by calculating the generated and transmitted signal. The test facility with its suggested multiple-sensor receiver (between P1 and P2) could be used to validate the results of the extended mathematical model.

Finally, a prototype for a multi-frequency mud siren for field tests could be built based on the gained experience and research results.

References

Ali et al., 2008
Ali, T.H.; Sas, M.; Hood, J.A.; Lemke, S.R.; Srinivasan, A.; McKay, J; Fereday, K.S.; Mondragon, C.; Townsend, S.C.; Edwards, S.T.; Hernandez, M. and Reeves, M.: High Speed Telemetry Drill Pipe Network Optimizes Drilling Dynamics and Wellbore Placement, prepared for presentation at the 2008 IADC/SPE Drilling Conference held in Orlando, Florida, USA, 4–6 March 2008, IADC/SPE 112636

Berger, 1999
Berger, P.E.; Helgesen, T.B. and Kismul, J.K.: FE-MWD Logging in a Different Environment Induced by Drilling with a Rotary Steerable System, prepared for presentation at the 1999 SPE Annual Technical Conference and Exhibition held in Houston, Texas, 3-6 October 1999, SPE 56451

Berro et al., 2016
Berro, M. J.; Reich, M.; Gutierrez Estevez, M. A.; Krüger, U.; Krüger, K.; Giese, R.; Eggemann, K. and Zandi-Nia, A.: Robust Unidirectional OFDM-Communication System: Integration in a Drill String and Measurements of the Autarkic System, OIL GAS European Magazine 4/2016, OG 183-189

Berro[a] and Reich, 2015
Berro, M. J. and Reich, M.: Signal Transmission in Boreholes and its Processing in MATLAB, prepared for presentation at the 17th annual conference of the International Association for Mathematical Geosciences held in Freiberg, Germany, 5-13 September 2015, IAMG 2015, ISBN 978-3-00-050337-5

Berro[b] and Reich, 2015
Berro, M. J. and Reich, M.: Innovative Concepts to Increase the Data Rate of Downhole Hydraulic Data Transmission Systems, OIL GAS European Magazine 1/2015, OG 1-5

Calderoni et al., 1998
Calderoni, A.; Oppelt, J.; Ligrone, A.; Trampini, A. and Gauld, S.: Automated Steering Systems Applied to Complex Horizontal Well in South Italy, prepared for presentation at the 1998 SPE International Conference on Horizontal Well Technology held in Calgary, Alberta, Canada, 1–4 November 1998, SPE 50379

Caruzo et al., 2012
Caruzo, A.; Hutin, H.; Reyes, S.; Tweel, A. and Temple, P.: Advanced Design and Execution Techniques for Delivering High Data Rate MWD Telemetry for Ultradeep Wells, prepared for presentation at the Arctic Technology Conference held in Houston, Texas, USA, 3-5 December 2012, OTC 23749

Chen et al., 2015
Chen, J.; Li, S.; MacMillan, C. and Wood, D.: Long Range Electromagnetic Telemetry Using an Innovative Casing Antenna System, prepared for presentation at the Annual Technical Conference and Exhibition held in Houston, Texas, USA, 28-30 September 2015, SPE-174821-MS

Chin, 1996
Chin, W. C.: Measurement-While-Drilling, United States Patent, Patent Number: 5,583,827, Date of Patent: Dec. 10, 1996, downloaded on 23 September 2015, http://www.google.de/patents/US5583827

Chin and Ritter, 1998
Chin, W. C. and Ritter, T. E.: Turbo Siren Signal Generator for Measurement While Drilling Systems, United States Patent, Patent Number: 5,740,126, Date of Patent: Apr. 14, 1998, downloaded on 25 November 2015, http://www.google.com/patents/US5740126

Cooper and Santos, 2015
Cooper, P. and Santos, L. S. B.: New Mud-Pulse Telemetry System Delivers Improved Drilling Dynamics and Formation Evaluation Data, prepared for presentation at the SPE Russian Petroleum Technology Conference held in Moscow, Russia, 26–28 October 2015, SPE-176543-MS

Das, 2010
Das, A.: Digital Communication Principles and System Modelling, Springer-Verlag Berlin Heidelberg 2010, ISBN 978-3-642-12742-7

Das, 2012
Das, A.: Signal Conditioning An Introduction to Continuous Wave Communication and Signal Processing, Springer-Verlag Berlin Heidelberg 2012, ISBN 978-3-642-28274-4

Devereux, 2012
Devereux, S.: Drilling Technology in Nontechnical Language, Second Edition, PennWell Corporation, 2012, ISBN: 978-1-59370-264-9

Edward et al., 2013
Edwards, S. T.; Coley, C. J.; Whitley, N. A.; Keck, R. G.; Ramnath, V.; Foster, T.; Coghill, K. and Honey, M.: A Summary Of Wired Drill Pipe Field Trials And Deployments In Bp, prepared for presentation at the SPE/IADC Drilling Conference and Exhibition held in Amsterdam, The Netherlands, 5–7 March 2013, SPE/IADC 163560

Ehras, 2016
Ehras, J.: Student Master Thesis 2016 „Investigation of a Novel Signal Generator (Multi-Frequency Generator) to Speed up the Hydraulic Data Transmission in Borehole“, supervised by Dipl.-Ing. Mouhammed Jandal Berro

Ehrenfried, 2004
Ehrenfried, K.: Strömungsakustik, Skript zur Vorlesung, Berlin, Mensch-und-Buch-Verl., 2004, ISBN: 3898206998

Emmerich[a] et al., 2016
Emmerich, W.; Akimov, O.; Ben Brahim, I. and Greten, A.: Field Performance of Automated High-Speed Mud Pulse Telemetry System, prepared for presentation at the IADC/SPE Drilling Conference and Exhibition held in Fort Worth, Texas, USA, 1–3 March 2016, IADC/SPE-178871-MS

Emmerich[b] et al., 2016
Emmerich, W.; Ben Brahim, I.; Akimov, O. and Greten, A.: Improved High-Speed Mud Pulse Telemetry Performance Under Harsh Conditions, prepared for presentation at the Offshore Technology Conference Asia held in Kuala Lumpur, Malaysia, 22–25 March 2016, OTC-26765-MS

Emmerich[c] et al., 2016
Emmerich, W.; Greten, A.; Ben Brahim, I. and Akimov, O.: Evolution in Reliability of High-Speed Mud Pulse Telemetry, prepared for presentation at the Offshore Technology Conference held in Houston, Texas, USA, 2–5 May 2016, OTC-26886-MS

Foster, 1965
Foster, L. E.: Telemetry Systems, New York, Wiley, John Wiley & Sons, Inc., 1965

Freyer, 2009
Freyer, U.: Nachrichtentechnik-Übertragungstechnik Grundlagen, Komponenten, Verfahren und Systeme der Telekommunikationstechnik, 6., neu bearbeitete Auflage, Carl Hanser Verlag München, 2009, ISBN: 9783446414624

Garg, 2007
Garg, V. K.: Wireless Communications and Networking, Elsevier Inc., 2007, ISBN: 978-0-12-373580-5

Gravley, 1983
Gravley, W.: Review of Downhole Measurement-While-Drilling Systems, Journal of Petroleum Technology, 1983, P. 1439-1445, SPE 10036

Hansen and White, 1991
Hansen, R. R. and White, J.: Features of Logging-While-Drilling (LWD) in Horizontal Wells, prepared for presentation at the SPE/IADC Drilling Conference held in Amsterdam, Netherlands, March 11-13, 1991, SPE/IADC 21989

Hutin et al., 2001
Hutin, R.; Tennent, R. W.; Kashikar, S. V.: New mud pulse telemetry techniques for deepwater applications and improved real-time data capabilities, presented at the SPE/IADC Drilling Conference held in Amsterdam, the Netherlands, 27 February – 1 March 2001, SPE/IADC 67762

Hutin et al., 2010
Hutin, R.; Mehta, S; Battentier, A.; Yu, H.: Multi-stage modulator, European Patent Application, EP 2 230 379 A2, Application number: 10156119.9, Date of filing 10.03.2010, downloaded on 12 January 2016, https://data.epo.org/publication-server/rest/v1.0/publication-dates/20100922/patents/EP2230379NWA2/document.html

Ismaier, 2009
Ismaier, A.; Schlücker, E.: Fluid dynamic interaction between water hammer and centrifugal pumps. Elsevier, Journal of Nuclear Engineering and Design, 239, December 2009, Nr. 12, P. 3151-3154

Janwadker, 2010
Janwadker, S.; Klotz, C.; Welch, B. and Finegean, S.: Electromagnetic MWD Technology Improves Drilling Performance in Fayetteville Shale of North America, prepared for presentation at the 2010 IADC/SPE Drilling Conference and Exhibition held in New Orleans, Louisiana, USA, 2–4 February 2010, IADC/SPE 128905

Klotz[a] et al., 2008
Klotz, C.; Wasserman, I.; Hahn, D.: Highly flexible mud-pulse telemetry: A new system, prepared for presentation at the Indian Oil and Gas Technical Conference and Exhibition held in Mumbai, India, 4-6 March 2008, SPE 113258

Klotz[b] et al., 2008
Klotz, C.; Bond, P.; Wasserman, I.; Priegnitz, S.: A new mud pulse telemetry system for enhanced MWD/LWD applications, prepared for presentation at the IADC/SPE Drilling Conference held in Orlando, Florida, USA, 4-6 March 2008, IADC/SPE 112683

Lehr, 2005
Lehr, J.: Rotational Pulsation System and Method for Communicating United States Patent Application Publication, Pub. No.: US 2005/0117453 A1, Pub. Date: Jun. 2, 2005, downloaded on 18 December 2015, https://www.google.com.ar/patents/US20050117453

Manual ANSYS CFX Introduction, 2006
ANSYS CFX Introduction, ANSYS CFX Release 11.0, December 2006

Manual ANSYS CFX-Solver Theory Guide, 2006
ANSYS CFX-Solver Theory Guide, ANSYS CFX Release 11.0, December 2006

Martin et al., 1994
Martin, C. A.; Philo, R. M.; Decker, D. P.; Burgess, T. M.: Innovative advances in MWD, prepared for presentation at the IADC/SPE Drilling Conference held in Dallas, Texas, 16-18 February 1994, IADC/SPE 27516

MATLAB R2016b
Software Documentation, Continuous Wavelet Transform and Scale-Based Analysis

Misiti et al., 2009
Misiti, M.; Misiti, Y. and Poggi, J.-M.: Wavelet Toolbox 4 User's Guide, The MathWorks, Inc., 1997–2009, downloaded on 20 June 2017, https://www.ltu.se/cms_fs/1.51590!/wavelet%20toolbox%204%20user's%20guide%20(larger%20selection).pdf

Namuq, 2010
Namuq, M. A. and Reich, M.: Laboratory Experiments on Pressure Wave Propagation in Drill Strings (Mud Pulse Telemetry), OIL GAS European Magazine 3/2010, OG 1-6

Namuq et al., 2012
Namuq, M. A.; Reich, M. and AL-Zoubi, A.: Numerical Simulation and Modeling of a Laboratory MWD Mud Siren Pressure Pulse Propagation in Fluid Filled Pipe, OIL GAS European Magazine 3/2012, OG 125-130

Neff et al., 2007
Neff, J. M. and Camwell, P. L.: Field-Test Results of an Acoustic MWD System, prepared for presentation at the SPE/IADC Drilling Conference held in Amsterdam, The Netherlands, 20-22 February 2007, SPE/IADC 105021

Nygaard et al., 2008
Nygaard, V.; Jahangir, M.; Gravem, T.; Nathan, E.; Evans, J.; Reeves, M.; Wolter, H. and Hovda, S.: A Step Change in Total System Approach Through Wired Drillpipe Technology, prepared for presentation at the IADC/SPE Drilling Conference held in Orlando, Florida, 4-6 March 2008, IADC/SPE 112742

Pixton et al., 2014
Pixton, D. S.; Shishavan, R. A.; Perez, H. D.; Hedengren, J. D. and Craig, A.: Addressing UBO and MPD Challenges with Wired Drill Pipe Telemetry, prepared for presentation at the SPE/IADC Managed Pressure Drilling and Underbalanced Operations Conference and Exhibition held in Madrid, Spain, 8-9 April 2014, SPE/IADC-168953-MS

Rath et al., 2010
Rath, S.; Mandadi, S.; Thamizhmani, V. and Samuel, R.: Amplifier/Booster Joint Positioning Framework Design for a High-Speed Wired Telemetry System in MWD/LWD Downhole Tool Environment, prepared for presentation at the SPE Annual Technical Conference and Exhibition held in Florence, Italy, 19–22 September 2010, SPE 134504

Reeves et al., 2011
Reeves, M. E.; Camwell, P. L. and McRory, J.: High Speed Acoustic Telemetry Network Enables Real-Time Along String Measurements, Greatly Reducing Drilling Risk, prepared for presentation at the SPE Annual Technical Conference and Exhibition held in Aberdeen, UK, 6–8 September 2011, SPE 145566

Reeves et al., 2006
Reeves, M.; Macpherson, J.; Zaeper, R.; Bert, D.; Shursen, J.; Armagost, K.; Pixton, D. and Hernandez, M.: High-Speed Drillstring Telemetry Network Enables New Real-Time Drilling and Measurement Technologies, prepared for presentation at the IADC/SPE Drilling Conference held in Miami, Florida, USA, 21–23 February 2006, IADC/SPE 99134

Reich, 2012
Reich, M.: Hunting Underground A high-tech search for oil, gas and geothermal energy, The ideal introduction to the fascinating world of deep drilling technology, add-books, Germany, 2012, ISBN-Nr.: 978-3-00-032008-8

Reich et al., 2012
Reich, M.; Namuq, M. and Fischer, N.: Effekte der hydraulischen Datenübertragung in Bohrlöchern hörbar (und sichtbar) gemacht, ERDÖL ERDGAS KOHLE 128. Jg. 2012, Heft 11, P. 448-453

Reyes et al., 2010
Reyes, S.; Hutin, R.; Tennent, R. W. and Reed, C. P.: Mud Pulse Telemetry Data Modulation Technique, United States Patent Application Publication, Pub. No.: US

2010/0195442 A1, Pub. Date: Aug. 5, 2010, downloaded on 02 February 2017, https://www.google.com/patents/US20100195442

Rodriguez et al., 2013
Rodriguez, A.; MacMillan, C.; Maranuk, C. and Watson, J.: Innovative Technology to Extend EM-M/LWD Drilling Depth, prepared for presentation at the SPE Annual Technical Conference and Exhibition held in New Orleans, Louisiana, USA, 30 September–2 October 2013, SPE 166190

Schnitger and Macpherson, 2009
Schnitger, J. and Macpherson, J.: Signal Attenuation for Electromagnetic Telemetry Systems, prepared for presentation at the SPE/IADC Drilling Conference held in Amsterdam, The Netherlands, 17-19 March 2009, SPE/IADC 118872

Schramm, 2018
Schramm, A.: Construction and work preparation at the central workshop of the Faculty 3 of the TU Bergakademie Freiberg, Institute of Drilling Engineering and Fluid Mining, Freiberg, Germany, technical drawing and construction of the developed laboratory multi-frequency generator, 29.01.2018

Shah et al., 2004
Shah, V.; Gardner, W.; Johnson, D.H. and Sinanovic, S.: Design Considerations for a New High Data Rate LWD Acoustic Telemetry System, prepared for presentation at the SPE Asia Pacific Oil and Gas Conference and Exhibition held in Perth, Australia, 18–20 October 2004, SPE 88636

Shearer, 2013
Shearer, E. S.: Pulse Signaling for Downhole Telemetry, United States Patent, Patent No.: US008350715B2, Date of Patent: Jan. 8, 2013, downloaded on 02 February 2017, https://www.google.com/patents/US8350715

Sheng, 2013
Sheng, J. J.: Enhanced Oil Recovery Field Case Studies, Gulf Professional Publishing, 2013, ISBN: 9780123865465

Smith, 1999
Smith, S. W.: The Scientist and Engineer's Guide to Digital Signal Processing, California Technical Publishing 1997-1999, ISBN 0-9660176-6-8, downloaded on 15 February 2018,
https://users.dimi.uniud.it/~antonio.dangelo/MMS/materials/Guide_to_Digital_Signal_Process.pdf

Sohmer and Reich, 2010
Sohmer, M. and Reich, M.: The Potential of Advanced "Look Ahead" Sensors in Complex Drilling BHAs, prepared for presentation at the Abu Dhabi International Petroleum Exhibition & Conference held in Abu Dhabi, UAE, 1–4 November 2010, SPE 137334

Stallings, 2005
Stallings, W.: Wireless communications and networks, Second Edition, Pearson Prentice Hall, 2005, ISBN: 0131967908

Taylor et al., 2010
Taylor, J.; Bouska, R. R.; McKenty, M.; Silva, R. and Prochaska, E.: Effect of Bicenter Bit-BHA Design on BHA Behavior, prepared for presentation at the SPE/IADC Drilling Conference and Exhibition held in New Orleans, USA, 2-4 February 2010, IADC/SPE-128203

Thuselt and Gennrich, 2013
Thuselt, F. and Gennrich, F. P.: Praktische Mathematik mit MATLAB, Scilab und Octave für Ingenieure und Naturwissenschaftler, Springer-Verlag Berlin Heidelberg 2013, ISBN 978-3-642-25825-1

Tollefsen et al., 2007
Tollefsen, E.; Weber, A.; Kramer, A.; Sirkin, G.; Hartman, D. and Grant, L.: Logging While Drilling Measurements: From Correlation to Evaluation, presented at the 2007 International Oil Conference and Exhibition in Mexico held in Veracruz, Mexico, 27-30 June 2007, SPE 108534

Wand et al., 2006
Wand, P.; Bible, M. and Silvester, I.: Risk-Based Reliability Engineering Enables Improved Rotary-Steerable-System Performance and Defines New Industry Performance Metrics, prepared for presentation at the IADC/SPE Drilling Conference and Exhibition held in Miami, Florida, USA, 21-23 February 2006, IADC/SPE 98150

Warren, 2006
Warren, T.: Steerable Motors Hold Out Against Rotary Steerables, prepared for presentation at the 2006 SPE Annual Technical Conference and Exhibition held in San Antonio, Texas, USA, 24–27 September 2006, SPE 104268

Wassermann et al., 2008
Wassermann, I.; Hahn, D.; Reckmann, H.; Nguyen, D. H. and Macpherson, J.: Mud-pulse telemetry sees step-change improvement with oscillating shear valves, Oil & Gas Journal/ June 23, 2008, P.39-47

Werner, 2010
Werner; M.: Nachrichtentechnik Eine Einführung für alle Studiengänge, Vieweg+Teubner Verlag | Springer Fachmedien Wiesbaden GmbH 2010, ISBN 978-3-8348-0905-6

Yan et al., 2010
Yan, J.; Koutnik, J.; Seidel, U. and Hübner, B.: Compressible simulation of rotor-stator interaction in pump-turbines, IOP Conf. Series: Earth and Environmental Science 12 (2010) 012008

Yoon and Cha, 2011
Yoon, C. and Cha, H.: Experimental analysis of IEEE 802.15.4a CSS ranging and its implications, Elsevier Journal 2011, Computer Communications 34 (2011) 1361–1374

List of Figures

List of Tables

List of Publications

1. **Berro, M. J.**; M. Reich, M.; Ehras, J.: Symphonie im Bohrloch – höherer Datenrate durch Einsatz einer Mehrklangsirene, Poster und Veröffentlichung im Tagungsband der DGMK/ÖGEW-Frühjahrstagung 2017, Fachbereich Aufsuchung und Gewinnung, Celle, Germany 5-6 April 2017
2. **Berro, M. J.**; Gutierrez Estevez, M. A.; Krüger, U.; Krüger, K.; Reich, M.; Jaksch, K.; Giese, R.; Eggemann, K.; Zandi-Nia, A.: Robust Unidirectional OFDM-Communication System: Integration in a Drill String and Measurements of the Autarkic System, Oil Gas European Magazine, December, 2016
3. **Berro, M. J.**; Reich, M.: Review of Commercial Telemetry Systems for Real Time Data Transmission in Boreholes, GSSPE Student Technical Conference STC 2016, November 03-04, 2016, Wietze, Germany
4. Ehras, J.; Reich, M.; **Berro, M. J.**: Faster Hydraulic Telemetry Using a Novel Model-Scale Multi-Frequency-Generator, Celle Drilling 2016, International Conference and Exhibition for Advanced Drilling Technology, September 12-13, 2016, Celle, Germany
5. Reich, M.; Lehmann, F.; Sohmer, M.; **Berro, M. J.**; Pfeifer, J; Mezzetti, M.; Kirsten, U.: Entwicklung von Bohrtechnologien für die petrothermale Tiefengeothermie, Beitrag auf dem Seiten 283 - 297 im Buch „Glanzlichter der Forschung“, Herausgeber Ulrich Groß, ISBN 978-3-944509-26-6, Chemnitzerverlag, 2016
6. **Berro, M. J.**; Gutierrez Estevez, M. A.; Krüger, U.; Krüger, K.; Reich, M.; Jaksch, K.; Giese, R.; Eggemann, K.; Zandi-Nia, A.: Robustes, unidirektionales OFDM-Kommunikationssystem: Integration in einen Bohrstrang und Messungen des autarken Systems, Vortrag und Veröffentlichung im Tagungsband der DGMK/ÖGEW-Frühjahrstagung 2016, Fachbereich Aufsuchung und Gewinnung Celle, Germany 21-22 April 2016
7. **Berro, M. J.**; Reich, M.: Signal Transmission in Boreholes and its Processing in MATLAB, Presentation and Proceedings of the 17th annual conference of the International Association for Mathematical Geosciences, IAMG 2015, September 5-13, 2015, Freiberg (Saxony) Germany, ISBN 978-3-00-050337-5

8. **Berro, M. J.**; Reich, M.: Innovative Concepts to Increase the Data Rate of Downhole Hydraulic Data Transmission Systems, Oil Gas European Magazine, Volume 41, III/2015
9. **Berro, M. J.**; Reich, M.: Entwicklung und Erprobung alternativer Verfahren zur Beschleunigung hydraulischer Datenübertragungssysteme der Tiefbohrtechnik, Postersession, Freiberger Forschungsforum, 66. Berg- und Hüttenmännischer Tag, Freiberg, 18-19 Juni 2015
10. **Berro, M. J.**; Reich, M.: Neue Konzepte zur Steigerung der Datenrate von hydraulischen Übertragungssystemen der Tiefbohrtechnik, Vortrag und Veröffentlichung im Tagungsband der DGMK/ÖGEW-Frühjahrstagung 2015, Fachbereich Aufsuchung und Gewinnung Celle, Germany, 22-23 April 2015
11. **Berro, M. J.**; Reich, M.: Improving the Efficiency of Mud Pulse Telemetry, Young Scientist conference, St. Petersburg, Russia, 22-24 April 2015

List of Patents

1. **Berro, M. J.**; Sohmer, M.; Reich, M.: Mud-Sirenen-Anordnungen und Verfahren zum Codieren und Übertragen von einer mehrere Bits aufweisenden Information, english: Mud Sirens Assemblies and Methods for Encoding and Transmitting of Multiple Bits, registered at German Patent and Trade Mark Office for a Patnet in 2015, Patent number **DE 10 2015 104 101 B4** (2016.10.06)
2. Sohmer, M.; Reich, M.; **Berro, M. J.**: Mud-Sirenen-Anordnung, english: Mud Sirens Assembly, registered at German Patent and Trade Mark Office for a Patent in 2015, **DE 10 2015 017 138 A1** 2016.10.20
3. **Berro, M. J.**; Ehras, J.; Börner, E.; Schramm, A.; Reich, M.: Telemetrievorrichtung, englisch: Telemetry Device, registered at German Patent and Trade Mark Office for a Patent in 2016, **DE 10 2016 102 315 A1** 2017.08.10
4. **Berro, M. J.**; Thinibel, S.; Reich, M.: Kommunikationsvorrichtung für ein Bohrgerät, english: Communication Device for a Drilling Rig, registered at German Patent and Trade Mark Office for a Patent in 2018, Reference number: 10 2018 102 093.7

Appendix- Chapter 7

Transmission test (2):

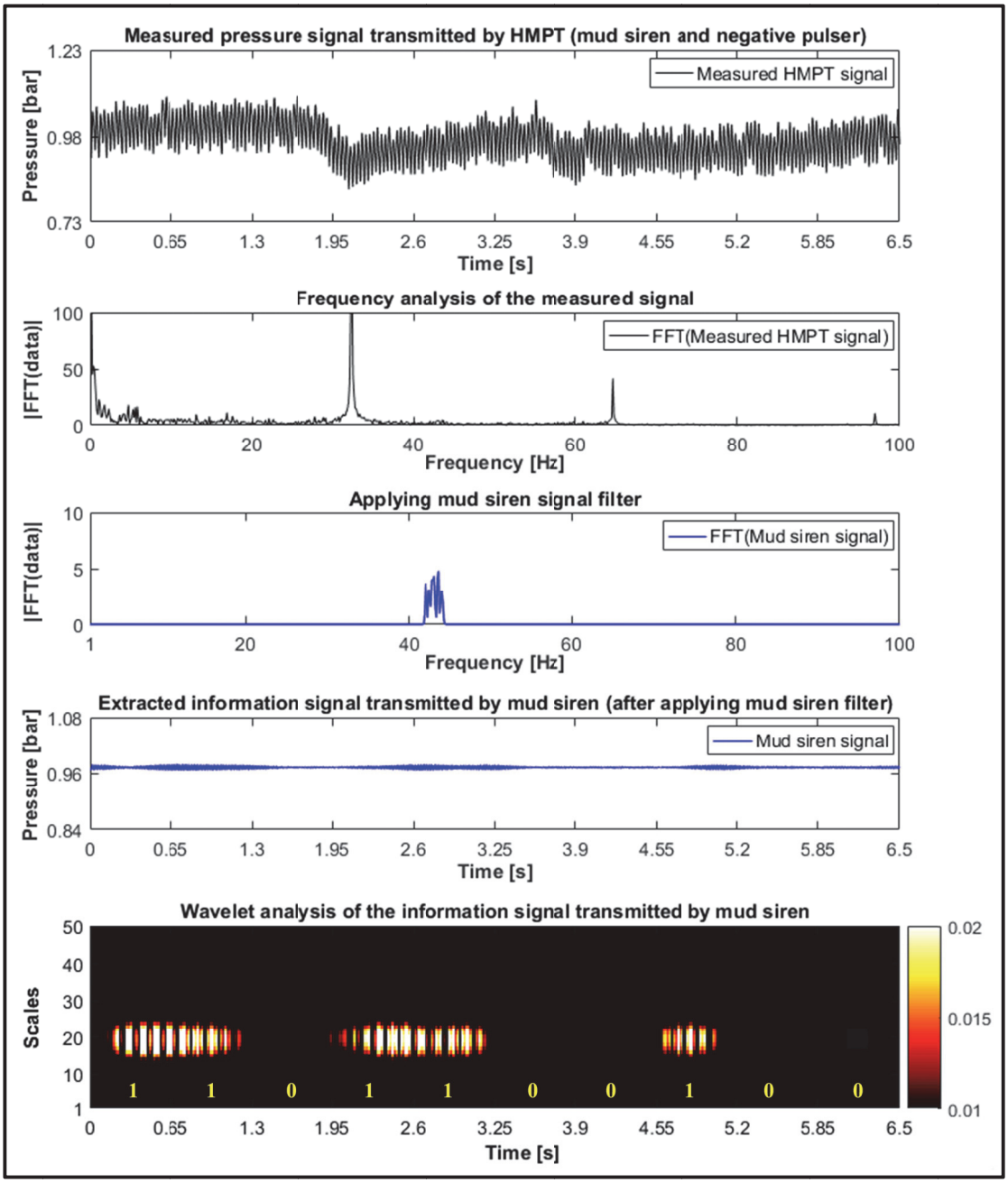

Figure 7.8: Extraction of the first data string (10-bits signal) transmitted in passband via the mud siren from the pressure signal received at the pressure sensor P1 and its evaluation using frequency and Wavelet analysis (time slot = 0.65 s, code modulation = OOK, carrier frequency = 43 Hz, sampling rate = 1000 Hz, average flow rate = 25.6 m^3/h)

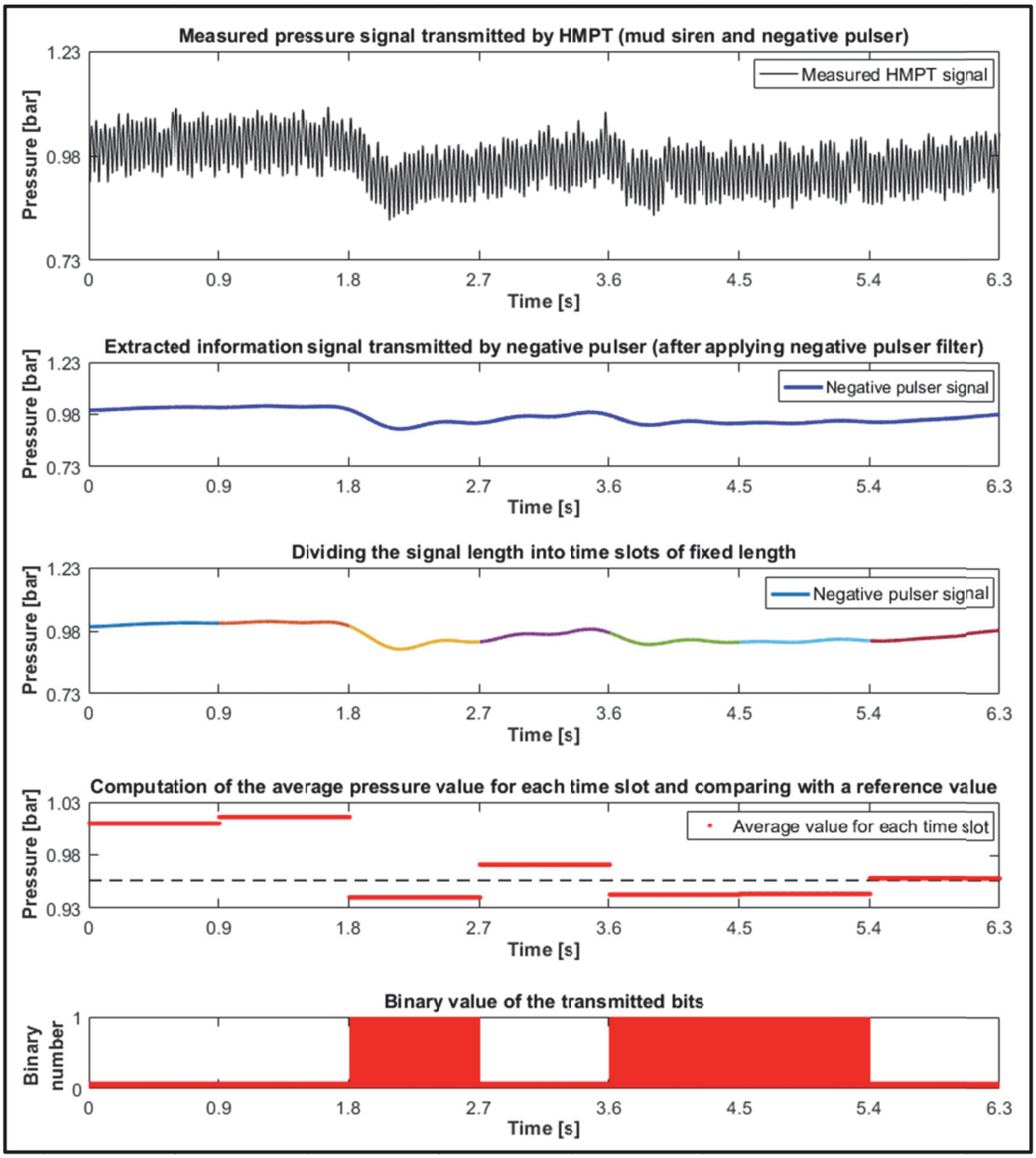

Figure 7.9: Extraction of the second data string (7-bits signal) transmitted in baseband via the negative pulser from the pressure signal received at the pressure sensor P1 and its evaluation using MATLAB (time slot = 0.9 s, code modulation = NRZ, sampling rate = 1000 Hz, average flow rate = 25.6 m^3/h, reference pressure value = 0.956 bars)

Appendix- Chapter 8

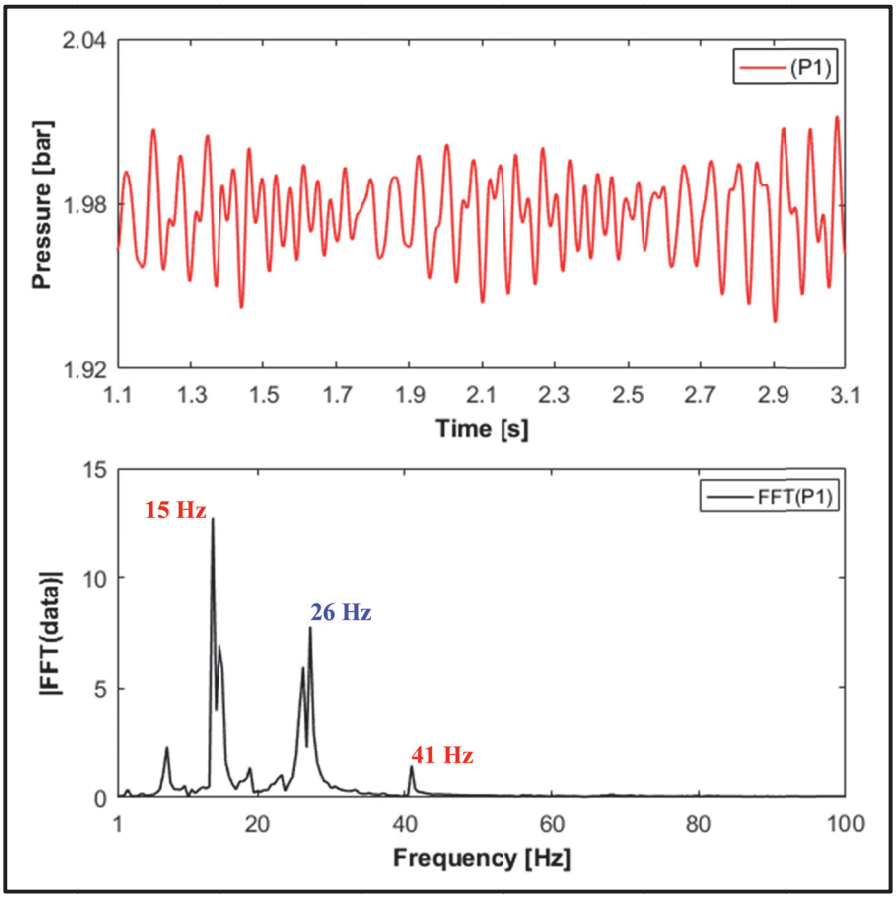

Figure 8.15: Predicted pressure signals (upper section) and frequency analysis (lower section) of two sirens in a row for transmission case (41 + 15 Hz)

Appendix- Chapter 9

The following figures represent the laboratory multi-frequency generator with its dimensions.

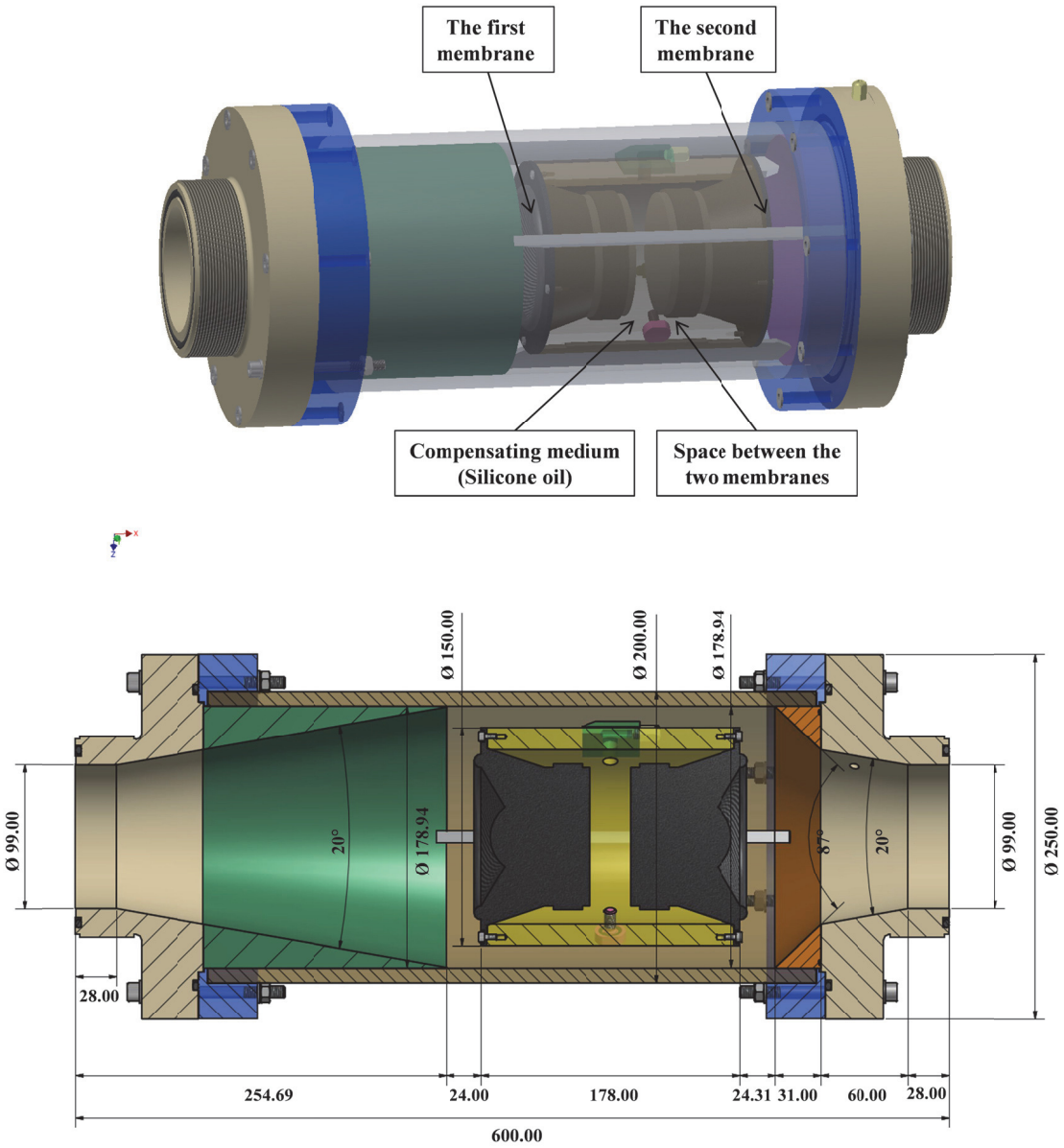

Figure 9.16: Laboratory multi-frequency generator, (modified), (Schramm, 2018)

Note:

- The symbol (Ø) represents the diameter
- All the dimensions represented in this figure are in mm

Table 9.2: Transmission options for set 1 using six carrier frequencies (11, 15, 19.5, 28.5, 39 and 45 Hz)

Symbol		6 Carrier Frequencies					
Number	**Bits**	**11 Hz**	**15 Hz**	**19.5 Hz**	**28.5 Hz**	**39 Hz**	**45 Hz**
1	1 0 0 0 0 0	on	off	off	off	off	off
2	0 1 0 0 0 0	off	on	off	off	off	off
3	1 1 0 0 0 0	on	on	off	off	off	off
4	0 0 1 0 0 0	off	off	on	off	off	off
5	1 0 1 0 0 0	on	off	on	off	off	off
6	0 1 1 0 0 0	off	on	on	off	off	off
7	1 1 1 0 0 0	on	on	on	off	off	off
8	0 0 0 1 0 0	off	off	off	on	off	off
9	1 0 0 1 0 0	on	off	off	on	off	off
10	0 1 0 1 0 0	off	on	off	on	off	off
11	1 1 0 1 0 0	on	on	off	on	off	off
12	0 0 1 1 0 0	off	off	on	on	off	off
13	1 0 1 1 0 0	on	off	on	on	off	off
14	0 1 1 1 0 0	off	on	on	on	off	off
15	1 1 1 1 0 0	on	on	on	on	off	off
16	0 0 0 0 1 0	off	off	off	off	on	off
17	1 0 0 0 1 0	on	off	off	off	on	off
18	0 1 0 0 1 0	off	on	off	off	on	off
19	1 1 0 0 1 0	on	on	off	off	on	off
20	0 0 1 0 1 0	off	off	on	off	on	off
21	1 0 1 0 1 0	on	off	on	off	on	off
22	0 1 1 0 1 0	off	on	on	off	on	off
23	1 1 1 0 1 0	on	on	on	off	on	off
24	0 0 0 1 1 0	off	off	off	on	on	off
25	1 0 0 1 1 0	on	off	off	on	on	off
26	0 1 0 1 1 0	off	on	off	on	on	off
27	1 1 0 1 1 0	on	on	off	on	on	off
28	0 0 1 1 1 0	off	off	on	on	on	off
29	1 0 1 1 1 0	on	off	on	on	on	off
30	0 1 1 1 1 0	off	on	on	on	on	off
31	1 1 1 1 1 0	on	on	on	on	on	off
32	0 0 0 0 0 1	off	off	off	off	off	on
33	1 0 0 0 0 1	on	off	off	off	off	on
34	0 1 0 0 0 1	off	on	off	off	off	on
35	1 1 0 0 0 1	on	on	off	off	off	on
36	0 0 1 0 0 1	off	off	on	off	off	on
37	1 0 1 0 0 1	on	off	on	off	off	on
38	0 1 1 0 0 1	off	on	on	off	off	on
39	1 1 1 0 0 1	on	on	on	off	off	on
40	0 0 0 1 0 1	off	off	off	on	off	on
41	1 0 0 1 0 1	on	off	off	on	off	on

42	0 1 0 1 0 1	off	on	off	on	off	on
43	1 1 0 1 0 1	on	on	off	on	off	on
44	0 0 1 1 0 1	off	off	on	on	off	on
45	1 0 1 1 0 1	on	off	on	on	off	on
46	0 1 1 1 0 1	off	on	on	on	off	on
47	1 1 1 1 0 1	on	on	on	on	off	on
48	0 0 0 0 1 1	off	off	off	off	on	on
49	1 0 0 0 1 1	on	off	off	off	on	on
50	0 1 0 0 1 1	off	on	off	off	on	on
51	1 1 0 0 1 1	on	on	off	off	on	on
52	0 0 1 0 1 1	off	off	on	off	on	on
53	1 0 1 0 1 1	on	off	on	off	on	on
54	0 1 1 0 1 1	off	on	on	off	on	on
55	1 1 1 0 1 1	on	on	on	off	on	on
56	0 0 0 1 1 1	off	off	off	on	on	on
57	1 0 0 1 1 1	on	off	off	on	on	on
58	0 1 0 1 1 1	off	on	off	on	on	on
59	1 1 0 1 1 1	on	on	off	on	on	on
60	0 0 1 1 1 1	off	off	on	on	on	on
61	1 0 1 1 1 1	on	off	on	on	on	on
62	0 1 1 1 1 1	off	on	on	on	on	on
63	1 1 1 1 1 1	on	on	on	on	on	on
64	0 0 0 0 0 0	off	off	off	off	off	off

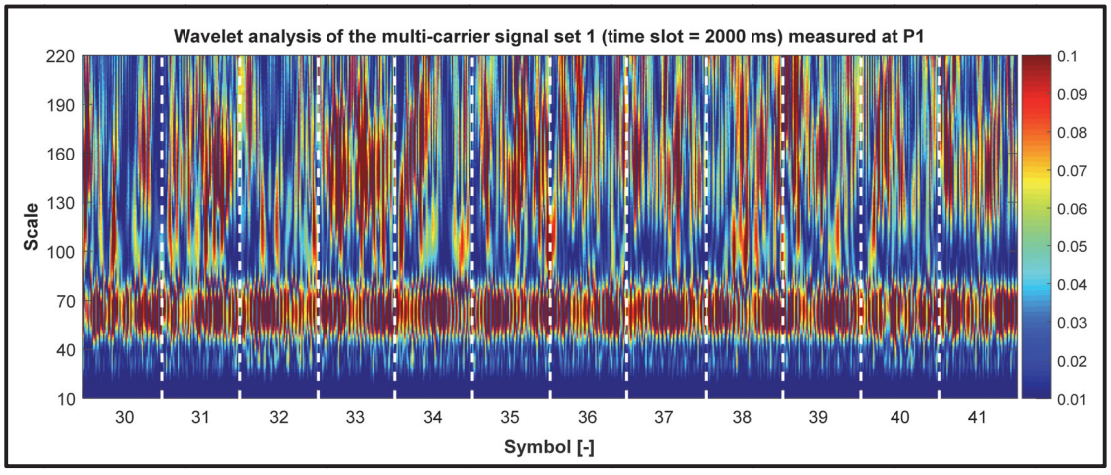

Figure 9.17: Wavelet analysis of the transmitted multi-frequency signal (set 1) sent from the first transmitter position and measured at P1 (without noise cancellation), (time slot = 2 s, code modulation = OOK, carrier frequencies = 11, 15, 19.5, 28.5, 39 and 45 Hz, audio amplifier = 65 clicks, sampling rate = 2000 Hz, flow rate = 20.1 m^3/h)

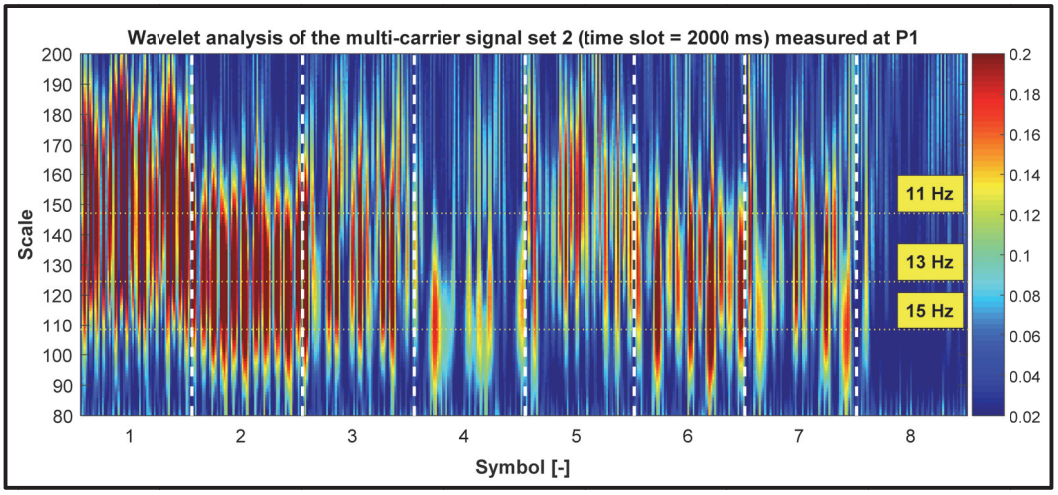

Figure 9.18: Wavelet analysis of the transmitted multi-frequency signal (set 2) sent from the first transmitter position and measured at P1 (without noise cancellation), (time slot = 2 s, code modulation = OOK, carrier frequencies = 11, 13 and 15 Hz, audio amplifier = 65 clicks, sampling rate = 2000 Hz, flow rate = 20.1 m^3/h)

Table 9.3: Transmission options for the transmission test using 16 modulated chirps

Symbol		Chirp direction	Frequency chirp [Hz]
Number	Bits		
1	0 0 0 0	up	5 - 10
2	1 0 0 0	down	10 - 5
3	0 1 0 0	up	10 - 15
4	0 0 1 0	down	15 - 10
5	0 0 0 1	up	15 - 20
6	1 1 0 0	down	20 - 15
7	1 0 1 0	up	20 - 25
8	1 0 0 1	down	25 - 20
9	0 1 1 0	up	25 - 30
10	0 1 0 1	down	30 - 25
11	0 0 1 1	up	30 - 35
12	1 1 1 0	down	35 - 30
13	1 0 1 1	up	35 - 40
14	1 1 0 1	down	40 - 35
15	1 1 1 0	up	40 - 45
16	1 1 1 1	down	45 - 40

Appendix- Chapter 10

Table 10.1: Distribution of the installed monitoring points

Monitoring Point	Distance from the stator-rotor-interface [m]
P1	**34.522**
P1-14	33.572
P1-13	32.522
P1-12	31.522
P1-11	30.522
P1-10	29.522
P1-9	28.522
P1-8	27.522
P1-7	26.522
P1-6	25.522
P1-5	24.522
P1-4	23.522
P1-3	22.522
P1-2	21.522
P1-1	20.522
P2	**19.522**
P2-18	18.522
P2-17	17.522
P2-16	16.522
P2-15	15.522
P2-14	14.522
P2-13	13.522
P2-12	12.522
P2-11	11.522
P2-10	10.522
P2-9	9.522
P2-8	8.522
P2-7	7.522
P2-6	6.522
P2-5	5.522
P2-4	4.522
P2-3	3.522
P2-2	2.522
P2-1	1.522
P3	**0.512**

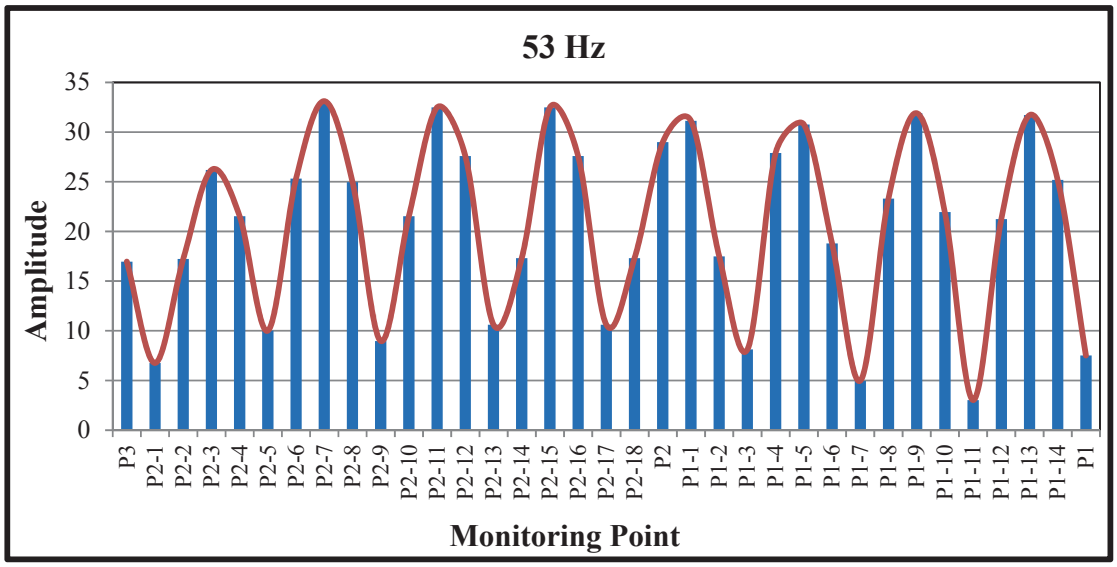

Figure 10.9: Predicted amplitudes in the frequency domain of the pressure wave with a carrier frequency of 53 Hz at several monitoring points